

# Grid Impact of Different Types of Heat Pumps

A Case Study on Transformer Overloading and Undervoltage Problems on a Dutch Low-Voltage Grid

R. Dijkman

Master thesis  
Sustainable Energy Technology  
April 14, 2025



# Grid Impact of Different Types of Heat Pumps

## A Case Study on Transformer Overloading and Undervoltage Problems on a Dutch Low-Voltage Grid

by

R. Dijkman

to obtain the degree of Master of Science  
at the Delft University of Technology,  
to be defended publicly on Monday April 14, 2025 at 11:00.

Student number:	4912233	
Project duration:	September 4, 2024 – April 14, 2025	
Supervisors:	Dr. S. H. Tindemans,	TU Delft
	Dr. ir. A. M. Van Voorden,	Stedin
	Ing. H. A. Fidler,	Stedin
Defence:	April 14, 2025 11:00	
Thesis committee:	Dr. S. H. Tindemans,	TU Delft
	Dr. ir. L. Ramírez Elizondo ,	TU Delft
	Dr. ir. A. M. Van Voorden,	Stedin

An electronic version of this thesis is available at <http://repository.tudelft.nl/>.

# Abstract

The Netherlands is committed to reducing carbon emissions in all sectors. This will cause the electricity production to be dominated by wind and solar power, and sectors such as mobility and industry will be heavily electrified. This poses significant challenges for the electricity grid. In addition, the government plans to phase out the use of natural gas in buildings by 2050. Local governments are now choosing alternative heating sources for specific neighbourhoods, and heat pumps are one of the options. As these use electricity for heating, it is important to consider their impact on the grid.

Therefore, this thesis analyses the impact of different types of heat pumps on a real Dutch low-voltage grid, focussing on transformer overload and voltage limit problems. A simulation model based on Powerfactory and Python is built, where different types of heat pumps are considered, including air- and ground-source heat pumps, as well as electric-resistive and natural gas hybrid heat pumps. Different control methods are also considered. In addition to heat pumps, public and private electric vehicle chargers and photovoltaic systems are also included in the model. Additionally, the effects of dynamic energy prices and domestic hot water production are investigated. The simulation is performed on an hourly basis using real data from the two coldest weeks of the winter of 2021.

The results show that air-source heat pumps have a significantly higher impact on transformer overload and voltage limit violations than ground-source heat pumps, and modulating heat pumps have a slightly lower impact on the grid than on-off controlled heat pumps. Gas-hybrid heat pumps are found to cause almost no grid problems on the low-voltage grid studied and have a significantly lower impact than the all-electric air-source heat pump. The presence of an electric-resistive backup heater in the heat pump significantly increases transformer overload and voltage limit problems. Scenarios for 2030 and 2050 show that problems are unlikely to occur in 2030, but the current grid will not be sufficient in 2050 if air-source heat pumps dominate the grid. More research is needed to determine whether the current grid is sufficient when ground-source heat pumps are dominant.

It was also found that dynamic energy prices will not be a problem for the grid at current rates of heat pump and home charging for electric vehicles. However, if every household has a heat pump, a penetration rate of 20% or more of dynamic energy contracts will substantially increase transformer overloads and voltage level violations. Finally, domestic hot water production does not significantly increase overloading and voltage limit problems.

In conclusion, heat pumps can cause significant problems for the low-voltage network. However, the impact can be reduced by choosing the right type of heat pump. It is recommended that future research considers cooling, heat and electricity storage, thermal ratings of transformers, and variable capacity tariffs.

Keywords: Heat Pumps, air-source heat pumps, ground-source heat pumps, hybrid heat pump, grid congestion, heat transition, domestic hot water, dynamic pricing, low-voltage grid, electric vehicles, flexible loads, simulation modelling, photovoltaic systems, renewable energy integration

# Preface

This thesis is written to conclude the Master's degree in Sustainable Energy Technology at the Delft University of Technology. The project is carried out in collaboration with the Intelligent Electrical Power Grids research group at the EEMCS faculty and the Dutch distribution operator Stedin.

The research done on this thesis feels like a fitting end to my university career, where I visited a lot of different aspects of engineering and natural sciences and focused for the last part on trying to fit renewable energy solutions into the world.

First and foremost, I would like to thank my daily supervisor at Stedin, Arjan van Voorden, for all the help and advice and for always being available when I needed help. Next, I would like to thank Simon Tindemans, my TU Delft supervisor, for our great discussions and quick responses, especially near the end. Of course, I cannot forget Henk Fidler, who helped me with great insight and connection inside and outside of Stedin. I could not have imagined better guidance for my thesis.

I would also like to thank all the nice people at Stedin for the support, especially Eveline Sahni for all the help and nice lunch walks, Paul Bierling for the help with PowerFactory and great discussions, and Titus Oosterkamp for all the helpful insights.

And, of course, I am very grateful for all the support that my family, friends, and girlfriend have given me throughout my whole adventure in Delft and beyond.

*R. Dijkman  
Rotterdam, April 2025*

# Acronyms

<b>ASHP</b>	Air Source Heat Pump
<b>COP</b>	Coefficient Of Performance
<b>DSO</b>	Distribution System Operator
<b>DHW</b>	Domestic Hot Water
<b>EV</b>	Electric Vehicle
<b>GO-e</b>	Gebouwde Omgeving Elektrificatie
<b>GSHP</b>	Ground Source Heat Pump
<b>LV</b>	Low-Voltage.
<b>PV</b>	Photo-Voltaic
<b>SAC</b>	Standard Annual Consumption
<b>TSO</b>	Transmission System Operator
<b>ZLT</b>	Zeer Lage temperatuur

# Contents

<b>Abstract</b>	<b>i</b>
<b>Preface</b>	<b>ii</b>
<b>Acronyms</b>	<b>iii</b>
<b>1 Introduction</b>	<b>1</b>
1.1 Prior Work . . . . .	2
1.2 Focus point . . . . .	3
1.3 Project Objective . . . . .	3
1.4 Research approach . . . . .	3
<b>2 Low-voltage Grid</b>	<b>5</b>
2.1 Grid constraints . . . . .	5
2.2 Chosen grid . . . . .	7
2.3 Powerfactory model . . . . .	8
<b>3 Dynamic Energy Pricing</b>	<b>10</b>
3.1 Influence on the consumer electricity consumption . . . . .	11
3.2 Determination of price . . . . .	11
<b>4 Household Electricity Consumption</b>	<b>13</b>
4.1 Non-flexible Consumption . . . . .	13
4.2 Electric Vehicle Home Charging model . . . . .	14
4.2.1 Charging optimisation for dynamic electricity pricing . . . . .	15
4.3 Electric Vehicle Public Charging model . . . . .	15
4.4 Solar Panels . . . . .	16
<b>5 Heat Pump Electricity Consumption</b>	<b>18</b>
5.1 Working principles . . . . .	18
5.2 Space Heating demand . . . . .	19
5.3 Domestic Hot Water production . . . . .	22
5.4 All-Electric Heat Pumps . . . . .	23
5.4.1 Air-Source Heat Pump . . . . .	23
5.4.2 Ground-source Heat Pump . . . . .	23
5.4.3 Control methods . . . . .	24
5.5 Hybrid Heat Pumps . . . . .	26

---

5.6	Dynamic energy price-based control . . . . .	28
5.7	Cooling . . . . .	32
<b>6</b>	<b>Results</b>	<b>33</b>
6.1	All-Electric Heat Pumps . . . . .	33
6.2	Hybrid Heat Pumps. . . . .	38
6.3	Influence of Dynamic Pricing. . . . .	41
6.4	Influence of Domestic Hot Water Production . . . . .	43
6.5	Scenarios . . . . .	45
6.5.1	Scenarios for 2030 . . . . .	45
6.5.2	Scenarios for 2050 . . . . .	48
<b>7</b>	<b>Discussion</b>	<b>54</b>
7.1	Voltage problems vs power limitations . . . . .	54
7.2	Socio-Economic Impact . . . . .	54
7.3	Limitations . . . . .	55
<b>8</b>	<b>Conclusion and Recommendations</b>	<b>57</b>
8.1	Conclusion . . . . .	57
8.2	Recommendations for future work. . . . .	58
8.3	Recommendations for distribution system operators and government . . . . .	59
	<b>Appendix</b>	<b>64</b>
A.1	Thermal house model parameters . . . . .	64
B.1	Power profiles . . . . .	65
B.2	Voltage profiles. . . . .	67
B.3	Overload energy plots . . . . .	69
B.4	Overload duration plots . . . . .	72

# 1

## Introduction

In recent decades, people have become increasingly aware of the effects of global warming. As a result, governments are making commitments to reduce the amount of carbon dioxide in the air and move towards a renewable energy system. This is also the case in the Netherlands, which aims to produce 70% of its electricity from renewable sources by 2030 [31]. It is estimated that onshore wind and solar production will produce 37 to 45 TWh in 2030 [40] and the government plans to increase offshore wind production to 49 TWh in the same year [31]. The government also wants to reduce carbon emissions from industry by replacing the natural gas currently used in industrial processes. This can be achieved by electrifying these processes or by replacing natural gas with green hydrogen produced from renewable energy. The mobility sector is also subject to electrification, for example newly sold cars should be electric by 2030 [31].

All this additional electricity will have to be transported through the Dutch electricity grid, which poses some considerable challenges. Increased electricity through the grid can lead to overloading of the components, which can cause them to fail. Another consequence of this additional load is that voltage limits will be exceeded at the household level, which can cause damage to electrical appliances. Grid operators are working hard to prepare the grid for this increased load as quickly as possible. This is quantified in 100,000 km of cables, +48,000 medium and low-voltage substations and 260-330 square kilometres of underground space needed for cables by 2050 while facing a shortage of 28,000 technicians by 2029 [34].

Simultaneously, the Dutch government is planning that by 2050, no more buildings will use natural gas. This means that 7 million homes and 1 million other buildings will have to find a new way to heat their homes and provide hot water [31]. Two main categories of alternative heating to natural gas are currently the most popular: high-temperature district heating and heat pumps. The first technology uses residual heat from an industrial process. This can come from, for example, burning waste or deep geothermal plants where limited electricity is needed at the household level. Heat pumps take heat from air, ground, or a water source and transport it inside, raising the temperature. This technology uses electricity to drive the process and is used at the household level. Uncertainty about the ability of the electricity grid to cope with the heat pump loads, together with the other household electricity demands mentioned above, has created a situation where local authorities, in general, do not have the perspective to take action to choose an alternative heating technology for a neighbourhood [32].

In the face of this grid challenge and to give local authorities the perspective to decide on an alternative heating solution, a better understanding of the real impact of all these low-carbon technologies on the grid can help understand the possibilities within the limited capacity of the current grid. Therefore, this thesis will analyse the impact of these low-carbon technologies on the low-voltage grid, focusing on different heat pump technologies in low-voltage grids.

This chapter first discusses previous work on the subject, from which a research gap will be deduced. The objective of the project is then explained in detail. Finally, the approach taken in this thesis is discussed.

## 1.1. Prior Work

Most studies of the impact of heat pumps on the electricity grid only consider air-source heat pumps (ASHPs), which extract heat from the outside air to heat the home. For example, in [1], the authors simulate the voltage of an 18-node low-voltage (LV) CIGRE test grid with air-source heat pumps, thermal and electric solar panels, and thermal energy storage. A thermal model of a house was used to obtain heat demand data. This study concluded that the voltage limits were exceeded if heat pumps were installed in all houses. When heat from solar collectors was added, the voltage limitations were just met. A combination of a heat pump with solar collectors and thermal storage could keep the voltage between the limits. In another study, six real low-voltage grids in the Netherlands are simulated. The houses are equipped with photovoltaic (PV) systems, electric vehicles (EV) and an air-source heat pump [13]. A thermal model of a house was used to determine the heat demand of the houses. They simulated different penetration rates for PV systems, EVs, and heat pumps and concluded that the transformer was overloaded in five of the six grids in winter. The lowest penetration rate where this happened was 6% in a suburban grid, which had an overload of almost 800% with 100% heat pump penetration.

In [33], a comparison is made between air-source heat pumps and ground-source heat pumps (GSHPs). Unlike ASHPs, GSHPs extract heat from the ground or use a low-temperature district heating network. The study is carried out on a suburban low-voltage test grid based on LV grids in the United Kingdom, and all heat pumps use a resistive electric auxiliary heater. They assume that 80% of the heat output is provided by the heat pump and the last 20% of the maximum heat output is provided by the auxiliary heater. It was found that at a heat pump penetration of 40 % and 50 %, respectively, the main feeder of the grid was overloaded with ASHPs and GSHPs. In addition, at penetration rates of 70 % for ASHPs and 90 % for GSHPs, voltage problems began to occur. When they changed the heat demand of the houses from 'modern' to 'old' and 'very old' insulation levels, the main feeder was overloaded at 20% and 15% ASHP penetration and 30% and 20% GSHP penetration. The researchers also simulated the use of gas boilers as backup heaters, which reduced the penetration rate when the main feeder was overloaded to 50% for ASHPs and 80% for GSHPs. Finally, they looked at what happened when they reduced the heat pump output to 60% of the maximum required output and found penetration thresholds of 5% for ASHPs and 10% for GSHPs. While these results are useful, this study was published in 2014, which means that the efficiencies of the simulated heat pumps were lower than they are today. In addition, the study only considered heat pumps with auxiliary heating, which is not always the case anymore today.

Dynamic electricity prices can also affect demand on the grid. Price differences during the day can cause some demand to be shifted to other times of the day. A study took this into account in a grid impact study on a low-voltage grid resembling a typical suburban low-voltage grid in Germany [46]. In this grid, households were placed where electric vehicles, PV systems, battery storage, heat pumps and home energy management systems are located. The household can choose between a fixed electricity tariff, two or three-tier time-of-use tariffs with two or three price levels within a day that are fixed throughout the year, or a tariff based on the day-ahead market as explained in chapter 3. The choice of tariff is modelled separately for each household, resulting in a mix of tariffs in the low-voltage grid. They simulated a scenario based on the current penetration of these technologies and three scenarios for 2035 with low, medium and high penetration of these technologies, both for a mix of tariffs and for all households with a static tariff. They found that a heterogeneous choice of tariffs can reduce peak loads on the low-voltage grid in all scenarios. In addition, voltage problems were reduced with a heterogeneous choice of tariffs. They also found that dynamic tariffs can lead to significant consumer cost savings. Another study also looked at the impact of dynamic pricing [14]. It used a real Dutch low-voltage grid with photovoltaic systems and electric vehicles and real data from 2023 to study the effects of different adoption rates of dynamic electricity pricing on voltage dips and power peaks. In the study, it was put forward that dynamic electricity pricing can lead to concentrated power peaks due to EVs charging at the same, cheapest time of day. For lower percentages of households with a dynamic price contract (10-30%), this reduced the moments of undervoltage and overloading of the transformer, as part of the charging was shifted to a time when most electric vehicles were not charging. However, as the percentage of households with dynamic contracts increased, the undervoltage and overloading problems became more severe than without dynamic contracts. The concurrency of charging is significantly increased

in this case, as everyone charges at the cheapest time. This study was also carried out at the Delft University of Technology in collaboration with Stedin and the same supervisors. The research described in the rest of the thesis is considered a follow-up study of [14], where its models are used as a basis for this thesis.

## 1.2. Focus point

Taking into account the summarised research, a knowledge gap is found in a direct comparison of different types of heat pumps on the low-voltage grid, considering transformer overload and undervoltage. Although [33] compares GSHPs and ASHPs, they are always assisted by an auxiliary heater. Due to advances in heat pump technology, this is no longer always the case today. Therefore, this thesis will focus on comparing ASHPs and GSHPs with different control methods, namely on/off, modulating, and dynamic electricity price-based. Furthermore, hybrid heat pumps with natural gas and resistive-electric auxiliary heaters will also be included in the comparison. Moreover, the influence of dynamic electricity prices will be included in the analysis. Lastly, three scenarios for 2035 and three for 2050 will be simulated. Electric vehicle charging, photovoltaic production, and other non-flexible demands will also be considered during these simulations.

## 1.3. Project Objective

Due to the shift in the energy source for domestic heating from natural gas to electricity, increasing concerns are raised about its impact on the electricity grid. Since every household in a neighbourhood is subjected to the same cold temperatures during winter as its neighbours, electric loads due to heating might cause overloading in the grid. This thesis, therefore, aims to analyse the effect of heating with heat pumps on a low-voltage grid, where distinctions will be made between different types of heat pumps. Its impact will be measured with the overloading of the central transformer connecting the grid to a higher voltage level and the undervoltage that might occur in the lines of the grid. These simulations will be performed with the DIGSILENT PowerFactory simulation tool [15].

The main research question for this thesis is as follows:

*What is the impact of heat pump penetration on the low-voltage grid for future winter scenarios, looking at local grid constraints (transformer overloading and undervoltage)?*

This question leads to a number of sub-questions, which are presented here.

1. *What is the impact of different types of heat pumps on local grid constraints?*
2. *How do dynamic energy prices influence the impact on the local grid constraints caused by heat pumps and home electric vehicle chargers?*
3. *How does the presence of domestic hot water production influence the impact on the local grid constraints?*

## 1.4. Research approach

To answer these questions, this thesis conducts a case study on an existing low-voltage grid in the Stedin operating area for a period of two weeks in the winter of 2021. The period of 4 to 17 February 2021 is chosen because this period was the coldest in the last 10 years and had outside temperatures of  $-10^{\circ}\text{C}$ , for which most heat pump systems in the Netherlands are dimensioned. Different technologies will be placed in this grid that produce or demand electricity and will be simulated to examine the influence of different electrical loads on this grid. This case study will use a combination of models, an overview of which can be seen in figure 1.1.

The grid used contains 155 households, and its topology is taken from a project called GO-e, which has collected data on the low-voltage grid in the Netherlands, including anonymised low-voltage grids in Gaia [39] format, which will be converted into a PowerFactory model. The technologies are placed

in these households. Information about the low-voltage grids in the Netherlands, the selection of this grid and its modelling are explained in chapter 2.

Secondly, households' non-flexible electricity consumption is added, including general electricity consumption such as lighting and the use of household appliances. In addition, photovoltaic systems can be placed on the houses, depending on the desired penetration rate of this technology. Next, electric vehicle charging is implemented in two ways. Public charging points are included by using charging profiles from the research centre for EV charging called ElaadNL. For home EV charging, charging sessions from home chargers are collected from the GO-e project and fed into an optimisation model that either optimises with dynamic electricity prices or without dynamic electricity prices, resulting in full power charging from the start. A more detailed description of non-flexible demand, PV production and EV charging can be found in chapter 4.

A thermal model is used to determine the demand for space heating profiles of the different types of heat pumps. This model uses the ambient temperature in the neighbourhood together with the thermal parameters of the house and then controls the heat pump to maintain a specific temperature in the house. In addition to space heating, domestic hot water (DHW) demand profiles are included in the heat pump demand model to include DHW production in the electricity demand profile. If the heat pump is assumed to be controlled and optimised based on dynamic energy prices, these prices are included in the optimisation. Dynamic gas prices are used if the heat pump has a natural gas auxiliary heater. These models are described in more detail in chapter 5.

Once all the power demand profiles of the loads have been determined, a quasi-dynamic simulation is carried out in Powerfactory and transformer overload and voltage limit problems are analysed. In addition to comparing the different types of heat pumps for current penetration rates of EV charging, PV systems and dynamic energy prices, possible scenarios for 2030 and 2050 are also simulated. The results of all these simulations can be found in chapter 6. Some discussion points and limitations are then presented in chapter 7, and conclusions and recommendations are given in 8.

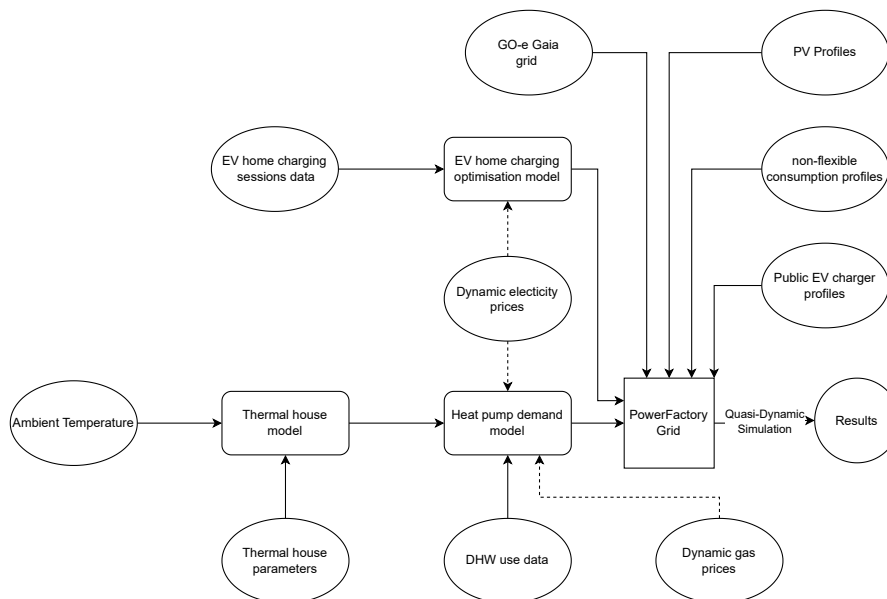


Figure 1.1: Overview of the models used in this thesis.

# 2

## Low-voltage Grid

The Netherlands has an unbundled electricity market, which means that the supply and generation of electricity cannot be carried out by the same company that operates the transmission and distribution system. The high voltage (>150 kV) transmission system is operated by a company called Tennet, which is the only Transmission System Operator (TSO) in the country. The distribution systems with a lower voltage than 150kV are operated by 6 Distribution System Operators (DSO), of which the company involved in this thesis, Stedin, is one. The DSOs in the Netherlands are responsible for the medium-voltage grid, which is mainly used for regional transport of electricity and connections to large consumers and industrial loads, and the low-voltage grid. The low-voltage grid is primarily used to connect households and small businesses. Stedin's operating area covers the province of Zeeland and most of the provinces of Zuid-Holland and Utrecht. A map of the operating areas of the individual DSOs can be seen in figure 2.1.



Figure 2.1: Operating areas of the DSOs in The Netherlands

### 2.1. Grid constraints

As mentioned earlier, the increase in electricity consumption in the Netherlands is putting a strain on the current electricity grid. As demand grows, more and more regions in the Netherlands are experiencing grid congestion. This means that the capacity of the grid in that area is fully utilised and new customers cannot be connected or additional capacity cannot be given to existing customers. For grid congestion, the distinction is made between congestion for the supply and demand sides. The regions currently experiencing this, as of March 2025, can be seen in figures 2.2 and 2.3 for demand and supply, respectively. White regions have enough unused transport capacity, yellow regions have limited capacity, orange regions are under investigation and have a waiting list for new connections, and red

regions have a shortage of transport capacity and a waiting list.

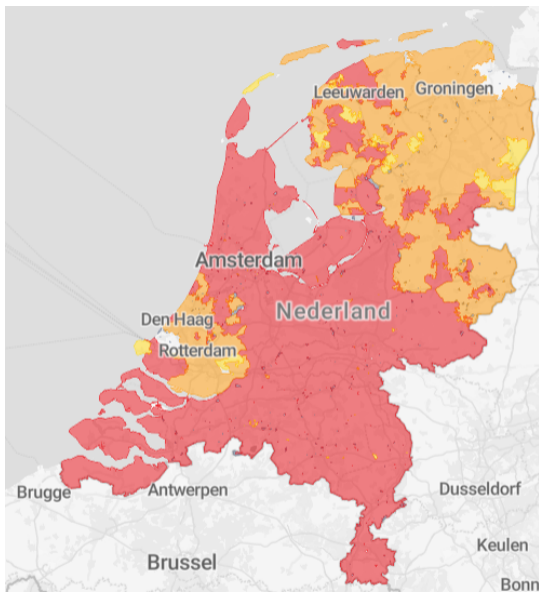


Figure 2.2: Regions in the Netherlands with grid congestion for demand.

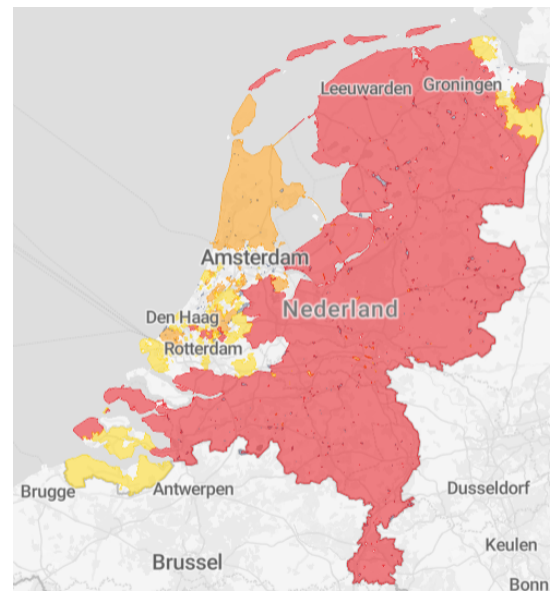


Figure 2.3: Regions in the Netherlands with grid congestion for supply.

One factor limiting the grid's transport capacity is component overload. For example, when the current through a transformer or cable becomes too high for a prolonged period, the component overheats, increasing the likelihood of failure.

In addition, to maintain a sufficient quality of electricity in the Dutch grid, grid operators must comply with the Electricity Grid Code (Netcode Electriciteit [30]), which contains rules for connecting customers to the grid, transporting electricity and operating the grids. Among other things, the voltage characteristics are specified in this code. For connection to the grid with a voltage level of 1 kV or less, which is the case in low-voltage grids, the grid code imposes restrictions on the following phenomena.

- Slow voltage variations at the connection point
- Fast voltage variations at the connection point
- Asymmetry of the phase voltages (phase imbalance) at the connection point
- Harmonic distortion at the connection point

Since the resolution of the simulations done in this thesis is 1 hour, fast voltage variations are not picked up and, therefore, will not be covered in this thesis. Furthermore, asymmetry and harmonic distortions are also not considered in this thesis. For the slow voltage variation, two constraints are given:

- The voltage level should not exceed  $\pm 10\%$  of the nominal voltage (230V) for 95% of the average values of 10 minutes during one week.
- The voltage level should not exceed  $+10\%$  or  $-15\%$  of the nominal voltage for all average values of 10 minutes during one week.

For this thesis, these two limits will be taken into account, but for hourly average values since the simulation resolution is 1 hour. Furthermore, it is assumed that 5% of the voltage deviation is reserved for the medium voltage grid, so 5% is subtracted from the restrictions. This means that if the following limits are exceeded for an individual connection, this will be marked as a voltage problem.

- The voltage level should not exceed  $\pm 5\%$  of the nominal voltage (230V) for 95% of the average values of 10 minutes during one week.
- The voltage level should not exceed  $+ 5\%$  or  $-10\%$  of the nominal voltage for all average values of 10 minutes during one week.

Overloading problems will also be considered. This will be done by observing the apparent power flowing through the central transformer, which is rated at 250 kVA. Therefore, a power problem will be marked when this rated capacity is exceeded because prolonged periods of overloading can lead to its failure. The cables are assumed to be dimensioned on the transformer. Therefore, their loading will not be considered in this thesis.

## 2.2. Chosen grid

In this thesis, a real Dutch low-voltage grid published by the 'Gebouwde Omgeving Electrificatie' (GO-e) project [20] is used. This project was a collaboration between Dutch DSOs, universities, and companies in the energy sector that looked at a broad range of aspects of bringing flexible consumption into the Dutch grid. Among other things, they published a study in 2023 in which they anonymised existing Dutch low-voltage grids so that they can be used in grid impact studies [21]. These grids are subdivided into eight archetype neighbourhoods. Each of the three participating DSOs provided five grid sections for each of the eight archetypes, totalling 120 grids.

These archetypes are chosen to represent all types of neighbourhoods in The Netherlands and are plotted in figure 2.4 and defined as follows [23]:

- **Archetype 1 Pre-housing bill (<1920):** This archetype mainly consists of buildings built before the Housing Act was introduced in 1920. 2% of the neighbourhoods in the Netherlands fall into this category. It is a densely populated area with predominantly apartments and mixed energy labels [29], but more C and D labels than A or B.
- **Archetype 2 Pre-war residences:** 1% of neighbourhoods fall into this archetype, which is dominated by residences built between 1920 and 1946. This archetype also mainly consists of apartments and has a mixed energy label present, but the A and B labels are more present than the C and D labels.
- **Archetype 3 Post-war terraced houses:** The houses in this archetype were mainly built between 1970 and 2010 and constitute around 8% of the neighbourhoods in the Netherlands. It consists of a mixture of primarily chained houses and apartments. It has a low-to-medium population density and a mix of energy labels.
- **Archetype 4 Post-war tenements:** These neighbourhoods also consist mainly of buildings built from 1970 to 2010, and 8 % of the neighbourhoods can be classified as this archetype. Most of the houses are rented apartments with a mix of energy labels.
- **Archetype 5 Corporation residences:** With building periods being a mix between 1920-2010 and newer, this archetype has a medium population density consisting mainly of multiple-family homes. 6% of the neighbourhoods can be classified as this archetype. Residence corporations own a large share of these houses, with a high percentage of C, D and E energy labels.
- **Archetype 6 Detached houses:** Detached homes between 1874 and 1920 and 1946 and 1960 dominated this archetype. 20% of the neighbourhoods can be classified as this. It has a low population density, with energy labels mainly in the F and G categories.
- **Archetype 7 Rural areas:** 26 % of the neighbourhoods fall into the Rural areas archetype. It is dominated by terraced houses and apartments in rural areas built in 1874-1920 and 1946-1960. Energy labels are mainly C, D and E.
- **Archetype 8: Industry and limited population** This archetype has many industrial buildings built between 1970 and 2010. This type of neighbourhood has a presence of 11% in the Netherlands and does not have a specific energy label mentioned.

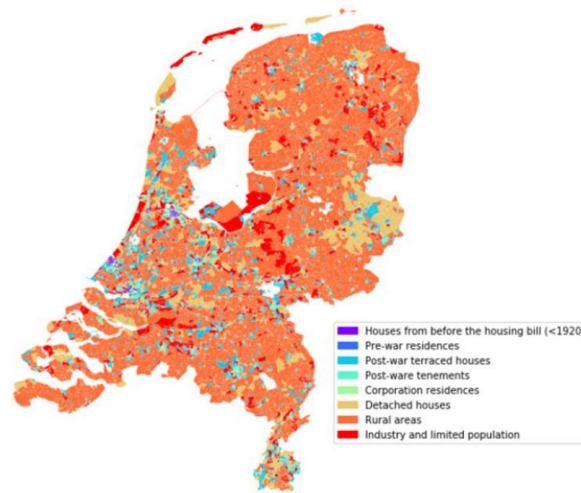


Figure 2.4: Maps of Dutch neighbourhoods and their archetypes [23]

This research is done in collaboration with Stedin, whose service area is mainly in the Randstad area. In this area, the majority of people live in the cities, where post-war terraced houses are most common. Therefore, archetype 3 is chosen as the grid type for this thesis.

## 2.3. Powerfactory model

In the previous work of the authors of [14], a certain grid was chosen for archetype 3, post-war terraced houses. The selected grid was called *BU3.5 2030* and is also selected for this thesis. It consists of a large, meshed grid with multiple external grid connections. A radial section was chosen for the simulation from this large grid. This part consists of one external grid connection connected with a transformer that lowers the voltage from 10 kV of the external grid to 400 V phase-to-phase (230 V phase-to-ground), five branches, and 155 busbars representing the households. The grid is depicted in figure 2.5. This thesis uses a converted version of the low-voltage grid in PowerFactory used in [14]. The original grid file was published as a Gaia LV Network Design [39] file by GO-E. In this conversion, the geographical coordinates are not considered; therefore, the grid view in figure 2.5 does not represent the physical layout of the neighbourhood, improving anonymisation.

Furthermore, figure 2.6 shows a zoom-in on one of the households. It can be seen that three loads and a PV system are connected to the busbar. The load starting with 'ev' represents the EV charger load, the 'hp' load represents the heat pump load, and the load with only the busbar number represents the non-flexible load. The 'pc' load represents a public EV charger. In reality, these will not be located in a household, but this simplification is made because of the short distances between a public charger and a house. The 'zon' symbol represents the PV system. Each load can be switched on (black lines) or off (grey lines). For example, if a certain percentage of households have a heat pump, a random set of heat pumps corresponding to that fraction will be switched on, and the rest will be kept out of service so they do not influence the simulation.

In addition, each load has a profile taken from a separate CSV file, which is the output of the Python demand profile models for home and public EV chargers, HP demand, PV production and non-flexible profiles. This CSV contains multiple profiles, one of which is randomly selected for each load. Finally, each load is assumed to have a power factor of 1. In reality, this will not be the case, but due to the small distances in this network, this simplification can be justified.

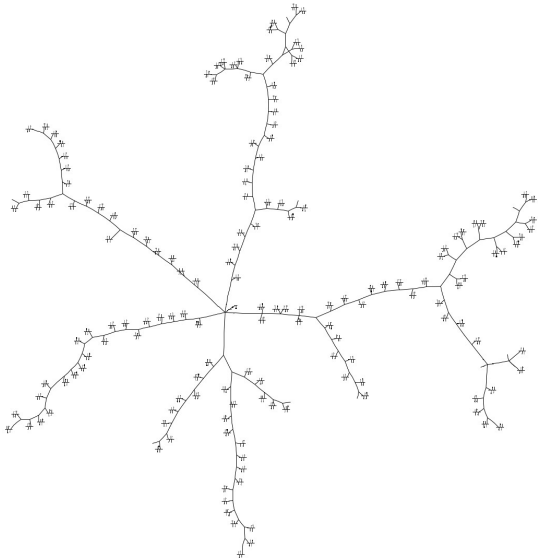


Figure 2.5: Screenshot of grid used for simulation

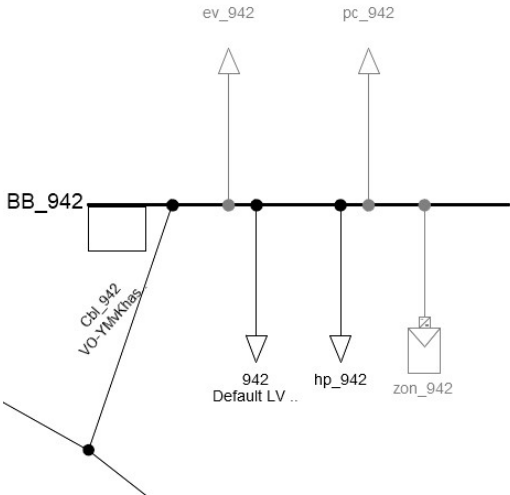


Figure 2.6: Zoomed-in screenshot of a household connected to the grid.

# 3

## Dynamic Energy Pricing

In general, there are three types of energy contracts in the Netherlands: fixed, variable, and dynamic. Fixed energy contracts have a fixed price for electricity and natural gas during their one- to three-year term. Variable contracts have a price of energy that changes each quarter, half a year, or a year, depending on your contract, with terms of one to three years. Dynamic contracts are based on the day-ahead market and have different electricity prices every hour [54]. Each day at 13:00, these hourly prices are announced for the next calendar day[6]. The natural gas price followed its daily market with a fixed price for the whole day. This kind of contract is increasingly popular in the Netherlands, and their use has increased to more than 5 % of all energy contracts by November 2024 [markt\_energiemonitor\_2024].

In figure 3.1, the average electricity price during the day of each month is shown for 2024. It can be seen that generally, there are two peak moments in price during the day. One in the morning and a higher one in the early evening. Furthermore, the influence of the high amount of solar capacity can be seen in this figure. During times when solar production is high, which happens during the middle of the day and more in summer, electricity prices drop. With an increasing share of wind energy [25], cheap electricity moments will also increasingly occur during periods with strong winds instead of only during high solar irradiance.

Uur/Maand	Januari	Februari	Maart	April	Mei	Juni	Juli	Augustus	September	Oktober	November	December
00:00	€ 0.06265	€ 0.05279	€ 0.06207	€ 0.06110	€ 0.08623	€ 0.08434	€ 0.08664	€ 0.09255	€ 0.07875	€ 0.07075	€ 0.09510	€ 0.07827
01:00	€ 0.06034	€ 0.04964	€ 0.05887	€ 0.05539	€ 0.07887	€ 0.07661	€ 0.07445	€ 0.08657	€ 0.07498	€ 0.06642	€ 0.09056	€ 0.07071
02:00	€ 0.05916	€ 0.04699	€ 0.05713	€ 0.05210	€ 0.07462	€ 0.07346	€ 0.07075	€ 0.08267	€ 0.07117	€ 0.06555	€ 0.08670	€ 0.06631
03:00	€ 0.05579	€ 0.04488	€ 0.05601	€ 0.05051	€ 0.07240	€ 0.06888	€ 0.06698	€ 0.07922	€ 0.07106	€ 0.06328	€ 0.08331	€ 0.06124
04:00	€ 0.05517	€ 0.04493	€ 0.05615	€ 0.05186	€ 0.07138	€ 0.06870	€ 0.06689	€ 0.07983	€ 0.07045	€ 0.06234	€ 0.08231	€ 0.06091
05:00	€ 0.05887	€ 0.04882	€ 0.05797	€ 0.05764	€ 0.07523	€ 0.07099	€ 0.07031	€ 0.08527	€ 0.07421	€ 0.06748	€ 0.08645	€ 0.06651
06:00	€ 0.06669	€ 0.05974	€ 0.06744	€ 0.07139	€ 0.08534	€ 0.08623	€ 0.08430	€ 0.10229	€ 0.09141	€ 0.08477	€ 0.09598	€ 0.07880
07:00	€ 0.08090	€ 0.07268	€ 0.07714	€ 0.08754	€ 0.09014	€ 0.09189	€ 0.08767	€ 0.10503	€ 0.11444	€ 0.11098	€ 0.11754	€ 0.09944
08:00	€ 0.09593	€ 0.08032	€ 0.07549	€ 0.08092	€ 0.07945	€ 0.08014	€ 0.07952	€ 0.09025	€ 0.10984	€ 0.12009	€ 0.13018	€ 0.13152
09:00	€ 0.09297	€ 0.07479	€ 0.06365	€ 0.06501	€ 0.05760	€ 0.05964	€ 0.05966	€ 0.07022	€ 0.08518	€ 0.09884	€ 0.12414	€ 0.14057
10:00	€ 0.08588	€ 0.06787	€ 0.05334	€ 0.05089	€ 0.03928	€ 0.04125	€ 0.04145	€ 0.04935	€ 0.06163	€ 0.08143	€ 0.11418	€ 0.13132
11:00	€ 0.07948	€ 0.06325	€ 0.04373	€ 0.03907	€ 0.02477	€ 0.02941	€ 0.02722	€ 0.03431	€ 0.04298	€ 0.07067	€ 0.10345	€ 0.12187
12:00	€ 0.07450	€ 0.05821	€ 0.03769	€ 0.02752	€ 0.01061	€ 0.01932	€ 0.01817	€ 0.02277	€ 0.03065	€ 0.06255	€ 0.09977	€ 0.11570
13:00	€ 0.07327	€ 0.05579	€ 0.03548	€ 0.01673	€ 0.00033	€ 0.01045	€ 0.00901	€ 0.02144	€ 0.02544	€ 0.05955	€ 0.10161	€ 0.11731
14:00	€ 0.07730	€ 0.05919	€ 0.03920	€ 0.01393	€ 0.00373	€ 0.00732	€ 0.00481	€ 0.01012	€ 0.02339	€ 0.06175	€ 0.10991	€ 0.12337
15:00	€ 0.08447	€ 0.06448	€ 0.04949	€ 0.01878	€ 0.00636	€ 0.01329	€ 0.01096	€ 0.02049	€ 0.03223	€ 0.07316	€ 0.12484	€ 0.13847
16:00	€ 0.09311	€ 0.07009	€ 0.06138	€ 0.03016	€ 0.03441	€ 0.02834	€ 0.02478	€ 0.03513	€ 0.05338	€ 0.09165	€ 0.14849	€ 0.15431
17:00	€ 0.10686	€ 0.08142	€ 0.08119	€ 0.05109	€ 0.06394	€ 0.05225	€ 0.05046	€ 0.06068	€ 0.08666	€ 0.12078	€ 0.19199	€ 0.20073
18:00	€ 0.10671	€ 0.09349	€ 0.09980	€ 0.07507	€ 0.08654	€ 0.07667	€ 0.07595	€ 0.09634	€ 0.11696	€ 0.13105	€ 0.17055	€ 0.15204
19:00	€ 0.09756	€ 0.08354	€ 0.10074	€ 0.10258	€ 0.10846	€ 0.10499	€ 0.10299	€ 0.13833	€ 0.12478	€ 0.14441	€ 0.24481	€ 0.13577
20:00	€ 0.08611	€ 0.07257	€ 0.08278	€ 0.10979	€ 0.12484	€ 0.12647	€ 0.13773	€ 0.11020	€ 0.13127	€ 0.10974	€ 0.12137	€ 0.11394
21:00	€ 0.07958	€ 0.06642	€ 0.07202	€ 0.08842	€ 0.11098	€ 0.12353	€ 0.12172	€ 0.12879	€ 0.10163	€ 0.09433	€ 0.10862	€ 0.09607
22:00	€ 0.07627	€ 0.06371	€ 0.06893	€ 0.07565	€ 0.09514	€ 0.10849	€ 0.10234	€ 0.10959	€ 0.08884	€ 0.09014	€ 0.10627	€ 0.09060
23:00	€ 0.07114	€ 0.05776	€ 0.06396	€ 0.06714	€ 0.08581	€ 0.09020	€ 0.08692	€ 0.09796	€ 0.08063	€ 0.07899	€ 0.09685	€ 0.07861

Figure 3.1: The average hourly electricity prices in €/kWh per month for 2024 (excluding taxes) [5]

### 3.1. Influence on the consumer electricity consumption

Due to varying prices during the day, consumers might shift parts of the electricity demand to cheaper hours of the day. Some of the devices that are suitable for this are listed below.

- **Heat pumps and other electrical heating:** The exact time of heating buildings can be shifted due to the thermal mass of the building. If a building is heated to a higher temperature than needed before a time when the electricity price is high, the temperature will lower in the time that electricity is more expensive, but it can still be above the desired temperature if the building is preheated sufficiently. With the increasing use of heat pumps and other electrical heating, the effect of load shift due to dynamic electricity prices will increase with it.
- **Electric vehicles:** During charging, electric cars are often plugged into a charger longer than necessary to fully charge, especially when they are charged at home. This gives rise to an opportunity for either the car or the charger to optimise the charging session so that it uses the most power during times when the electricity price is low. This leads to the synchronisation of the charging profiles of different electric vehicles and causes a high peak load if many cars follow this way of charging [14].
- **Home batteries:** In addition to storing solar panel electricity, home batteries can make the owner a profit based on the prices on the day-ahead market. In this case, batteries can store electricity during hours when the price of electricity is low and discharge when prices are high, making a profit.
- **Solar Panels:** If a household has a dynamic energy contract, it is beneficial to turn off its solar panels when electricity prices are negative. When the household produces electricity during these hours, it will have to pay to send this to the grid. Even if the power produced is lower than the electricity consumption, it is beneficial to turn off the solar panels, as using electricity earns money during that period.
- **Other devices:** In addition to the devices mentioned above, appliances such as dishwashers, washing machines, and dryers increasingly have features to delay their program. This gives rise to the opportunity to plan its run during times of cheap electricity.

Next to the direct effect of dynamic prices, Dutch consumers can benefit from a net metering scheme (Salderingsregeling) until 2027, which allows them to offset their own production, for example, from solar panels, with their consumption on an annual basis, if they do not have a dynamic electricity contract [28]. Therefore, for consumers with a fixed or variable contract, there is no incentive to use their own solar energy directly when they produce it. However, some electricity suppliers currently charge an extra fee for feeding solar electricity into the grid [16]. This fee and the forthcoming abolition of net metering will reduce the value of the solar energy fed into the grid and, therefore, incentivise consumers to use their own solar energy directly.

In this thesis, devices that can react to dynamic prices are heat pumps, electric vehicle home chargers, and photovoltaic systems. The rest of the electrical loads are considered inflexible. The strategy to increase the self-consumption of solar energy will not be included.

### 3.2. Determination of price

As mentioned previously, the price of electricity is based on the hourly prices of the day-ahead market. On top of that, a fixed amount of energy tax is levied on the kWh prices and a purchase fee that the energy supplier adds to the price to factor in their acting as a middleman. In all of this, VAT has to be added to obtain the final price that consumers pay, resulting in a price calculation shown in equation 3.1.

$$Total\ price = market\ price \cdot (1 + VAT) + Energy\ Tax_{incl.\ VAT} + purchase\ fee_{incl.\ VAT} \quad (3.1)$$

The energy tax for electricity in the Netherlands, including VAT, is  $0,1317 \frac{\text{€}}{\text{kWh}}$  [3], and the purchase fees vary with each energy supplier and are usually around  $0,02 \frac{\text{€}}{\text{kWh}}$ . Here, a purchase fee, including tax, is taken as  $0,02534 \frac{\text{€}}{\text{kWh}}$  based on that fee at one of the largest suppliers, Eneco [19]. This price calculation is only for the purchase of electricity. Prices for feeding PV electricity into the grid are not considered in this thesis.

For this thesis, a simulation period is chosen between 4 and 17 February 2021, but to avoid unrealistic start-and-stop effects, the dynamic price control demand simulations for heat pumps are run for an additional 2 days before and after the grid analysis period. These days are then removed before this data is fed into the network simulation. The electricity prices for a dynamic contract can be seen in figure 3.2.

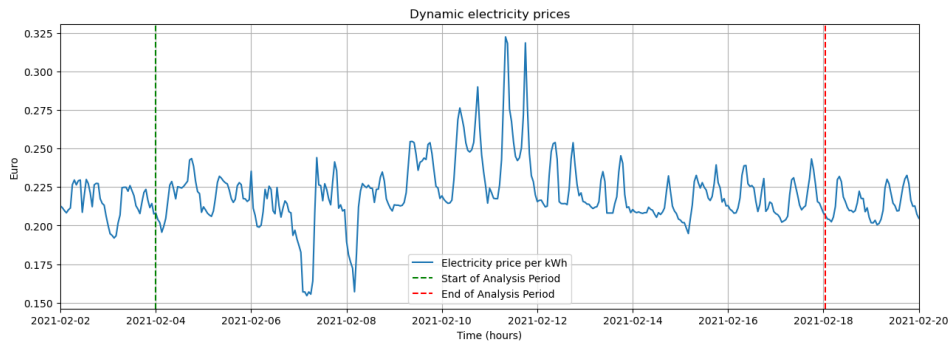


Figure 3.2: Dynamic electricity prices during simulation period

The daily price of natural gas is also determined in the same way as in Equation 3.1. However, the energy tax, including VAT, for natural gas is  $0.4216 \frac{\text{€}}{\text{m}^3}$  and the purchase fee used is  $0.093 \frac{\text{€}}{\text{m}^3}$ , including VAT from Eneco [19]. Due to the significant increase in natural gas prices at the time of writing compared to 2021, it was decided to use the daily gas prices of the same period from 2 to 19 February, but in 2025. This is done to make a more realistic assumption about the choice to use the natural gas auxiliary heater for economic reasons. Furthermore, the energy density of  $31.65 \frac{\text{MJ}}{\text{m}^3}$  for natural gas is used to calculate the price per kWh, based on the average value in the Dutch natural gas grid [41]. The resulting natural gas prices used in this thesis are shown in figure 3.3.

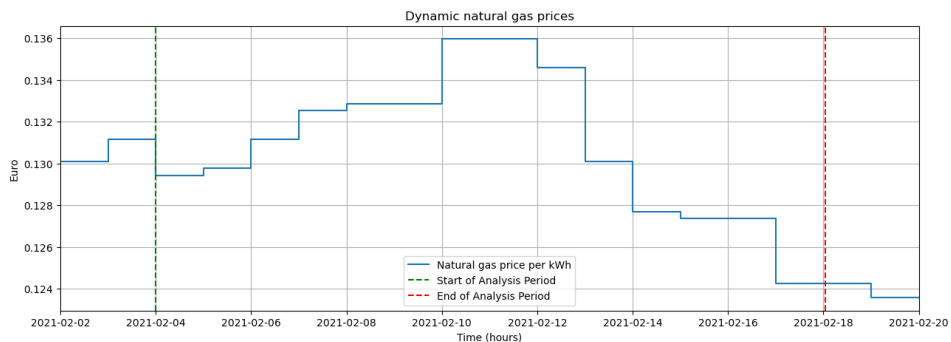


Figure 3.3: Dynamic natural gas price during simulation period

# 4

## Household Electricity Consumption

The electricity consumption of each household on the grid is divided into five different parts, as discussed in Section 2.3. Non-flexible consumption is discussed in Section 4.1, the EV charging profiles for home charging are explained in Section 4.2, public EV charging in Section 4.3, and the photovoltaic production profiles are discussed in section 4.4. Due to the focus on heat pumps in this thesis, their electricity demand is discussed in a separate chapter 5

### 4.1. Non-flexible Consumption

In addition to household loads that are quite flexible in their use, like EV chargers and heat pumps, households also have some loads that are not flexible. These loads include lighting, electronic appliances such as televisions, refrigerators, dishwashers and washing machines.

To obtain the profiles for non-flexible consumption, the same approach as is in [14] is used. The GO-e project [21], already mentioned earlier, also published profiles for non-flexible consumption. This data set consists of base load profiles for 1 year divided into categories based on their total annual consumption, ranging from 500 kWh per year to 15000 kWh. These profiles are then combined into a data set that takes into account the distribution of the number of people per household, resulting in a set of 595 households representing this distribution. This distribution is given in table 4.1. Furthermore, the data is converted to an hourly resolution to match the simulation resolution.

Number of people	Percentage of households	Yearly electricity usage
1 person	39%	1500 kWh
2 people	32%	2500 kWh
3 people	12%	3500 kWh
4 people	12%	4000 kWh
5 people	5%	4500 kWh

Table 4.1: Distribution of households and their yearly electricity consumption in The Netherlands [14]

Lastly, the year is changed in the data set so that it matches the period simulated in this thesis. Example profiles for each total annual consumption are plotted in figure 4.1.

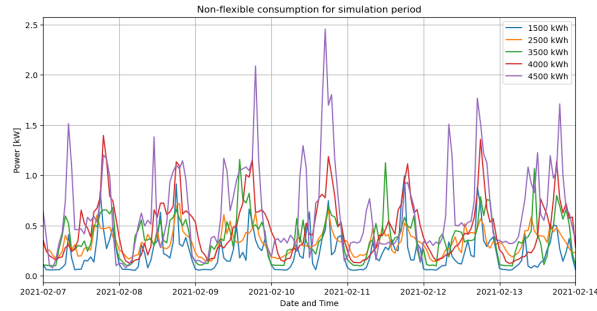


Figure 4.1: Example of non-flexible profiles for each household class

## 4.2. Electric Vehicle Home Charging model

In 2023, 4% of households had an electric car in the Netherlands [10], of which 69% have a charger at home [42]. This means that 2.7 % of the households have an electric vehicle charger at home. Because of the large amount of energy required to charge an EV and its dependence on household electricity price, it can be beneficial to consider the price of electricity when charging, besides the need to have enough capacity for your next journey.

To obtain the charging profiles of these chargers, the same method as [14] is used. In the GO-e project already mentioned in section 2.2, they generated a large set of charging sessions based on national charging records. The charging sessions of 950 households were chosen to be used, which contain data from 1 week and include the following information:

- Household ID
- Arrival time
- Departure time
- Energy to be charged
- Maximal charging power (3-11 kW)

If charging is not optimised for dynamic electricity prices, it is assumed that the charger will charge its battery at maximum power when connected until the battery is fully charged. To get the charging profiles for the 2 weeks simulated in this thesis, the same charging session data was used but with the corresponding electricity prices of the corresponding week and then put back-to-back. A single charging profile without price optimisation is shown in figure 4.2, and the combined power profile of the 950 households can be seen in figure 4.3.

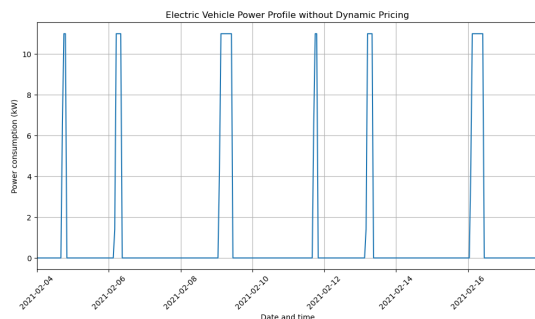


Figure 4.2: Single EV non-optimised charging profile for one household.

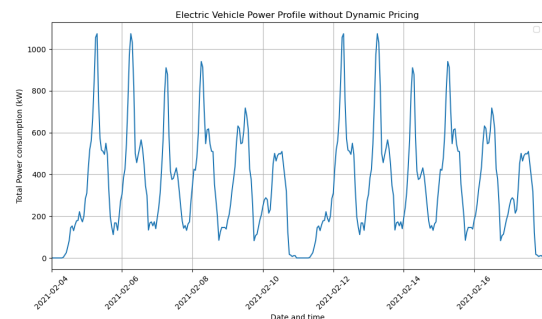


Figure 4.3: Sum of all 950 non-optimised EV charging profiles

### 4.2.1. Charging optimisation for dynamic electricity pricing

We assume that if a household is assigned a dynamic electricity price contract, it will base its charging behaviour on this contract if it has an EV charger. For optimal charging based on dynamic energy prices, a model described in [38] is used, which is shown in equation 4.1.

$$\min_p \sum_{t \in T} c_t p_t \Delta t \quad \text{s.t.}$$

$$\begin{aligned} e_t &= 0, \quad t \leq t^a; \\ e_t &= e_{t-1} + p_{t-1} \Delta t, \quad t^a < t \leq t^d; \\ e_t &= \bar{e}, \quad t \geq t^d; \\ p_t &= 0, \quad t < t^a; \\ 0 &\leq p_t \leq \bar{p}, \quad t^a \leq t < t^d; \\ p_t &= 0, \quad t \geq t^d \end{aligned} \quad (4.1)$$

Here,  $c_t$  are the prices described in Section 3.2,  $p_t$  and  $\bar{p}$  are the power at time  $t$  and the maximum capacity of the charger,  $e_t$  and  $\bar{e}$  the energy at time  $t$  and the maximum capacity of the battery,  $t^a$  and  $t^d$  the arrival and departure times and  $\Delta t$  is the time step of the optimisation, which is 1 hour. In the model, it is assumed that the battery should always be fully charged if that is possible. In reality, this might not be the case if, for example, prices during the whole session are very high or users want to have their car charged sooner to allow for unexpected early departures. A resulting charging profile can be seen in figure 4.4, and the sum of all optimised charging profiles is depicted in figure 4.5, including the electricity price. Here, it can be seen that the charging peaks concentrate around the minima of the electricity price.

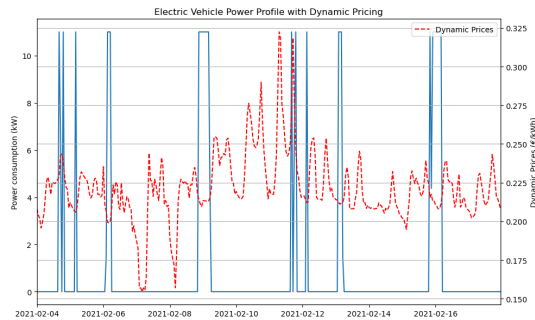


Figure 4.4: Single EV optimised charging profile for one household.

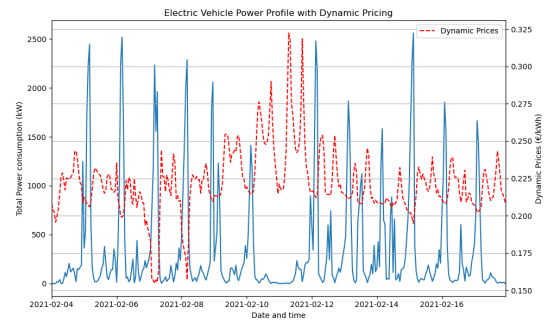


Figure 4.5: Sum of all 950 optimised EV charging profiles

## 4.3. Electric Vehicle Public Charging model

Because not every home is suitable for a home charger, for example, because it does not have a driveway, public charging points are increasingly often installed on the street. ElaadNL, a research institute that focuses on electric vehicle charging, has published an online profile generator for low-voltage public charging points [17]. This generator uses real charging session data to simulate the profiles, taking into account seasonality and distribution over time. The charging points can have one or two sockets, but for this thesis, the one with two sockets is considered.

The generator can provide regular profiles and smart charging profiles. For regular charging, the available power per socket is 11 kW and 17.25 kW per charging point. For smart charging, a dynamic profile, for which the power limit can be specified every 15 minutes, or a static profile can be selected for the power limits. For this thesis, the standard static profile is chosen if smart charging is assumed. In the standard static profile, the power available per socket is reduced from 11 to 4 kW between 17:00 and 23:00. The power limit is then increased by 1 kW per hour until full capacity is reached at 6:00. This type of smart charging is a rough estimate of a smart charging profile that will be implemented in the

real world, but since this thesis does not focus on smart charging, this profile is assumed to be sufficient. More information about the generator can be found in the introduction section on the generator's website [17].

1550 charging profiles are generated for the year 2023, as 2021 is not available, for 2 to 16 February to take into account the correct weekdays and weekend days. Then, the year is changed to 2021, and 2 days are added to the date stamp to match the simulation period. The average of the 1550 profiles of both regular charging and static smart charging can be seen in figure 4.6.

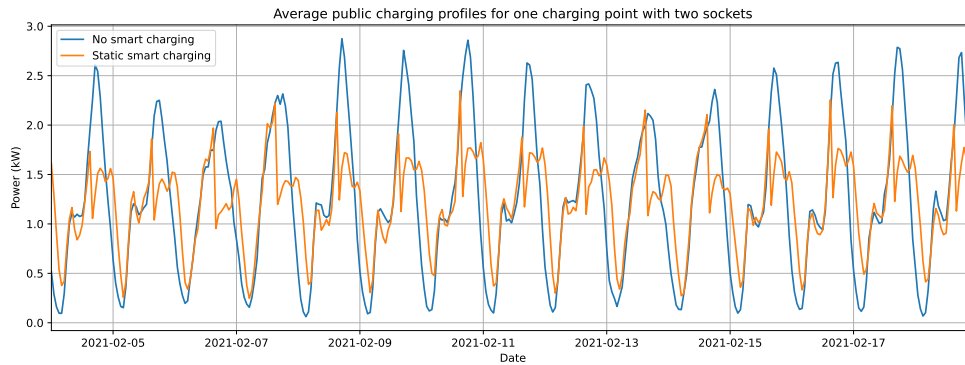


Figure 4.6: Average public charger profiles for regular and static smart charging

This figure clearly shows the power reduction in the peak period for the static smart charging profile. Furthermore, the difference can be seen between weekdays and weekend days, where the average power during the weekend is lower.

ElaadNL also provides outlooks on the number of public EV chargers in a given area [18]. As the location of the specific grid is known internally in Stedin, the current and forecast number of charging points could be retrieved from this. In 2025, there are 7 public EV chargers in the area that is modeled in this thesis.

## 4.4. Solar Panels

As the chosen neighbourhood consists mainly of terraced houses, households have a roof on which to install a photovoltaic system, which is popular in the Netherlands. In 2022, the average PV system on a house in the Netherlands had a peak capacity of 3.76 kW [11]. In 2023, 32 % of the houses in the Netherlands had a PV system [35]. For the model in this thesis, a rounded percentage of 30% of households with a PV system was used.

The PV production profile is taken from a Stedin-collected data set for the same two weeks. This data set was created by retrieving feed-in data from large solar parks in Stedin's operating area. After that, the feed-in power was normalised to a 1 kW peak. From this profile, the period corresponding to the simulation period of this thesis was selected, and the power was multiplied by the average capacity of 3.76 kW. This profile is then assigned to each PV system in the grid, taking into account whether or not it is out of service. In addition, PV production is shut down if the price is negative during any hour, but negative prices do not occur during the period considered. The resulting PV system production profile can be seen in figure 4.7.

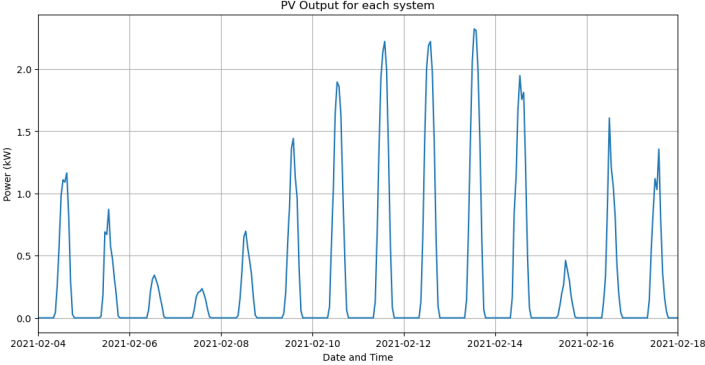


Figure 4.7: Photovoltaic power output for each system

# 5

## Heat Pump Electricity Consumption

Domestic heat pumps are becoming increasingly popular as an alternative to natural gas boilers in the Netherlands, with 16% of households having one in 2022 [9][7]. In this chapter we will first discuss the operating principles, then the heating requirements, then the different types of heat pumps, the control methods including simulation results of the heat pump demand and finally their cooling ability.

### 5.1. Working principles

A heat pump extracts heat from a source and then transforms this heat to a higher temperature using a thermodynamic cycle. The heat pump's source of heat can be either air or water and, in residential applications, moves the heat in or out of the building [48]. The thesis focusses only on the heating of buildings. The heat pump works on the basis of the refrigerant phase that changes during the thermodynamic cycle. This is illustrated in figure 5.1.

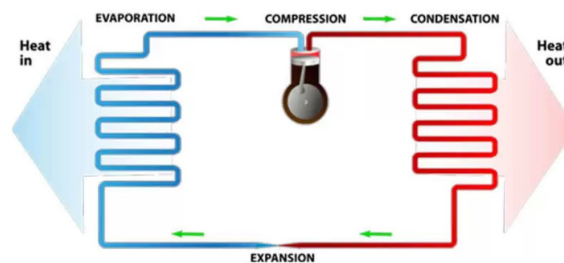


Figure 5.1: Schematic of a heat pump [44]

First, the refrigerant with a low pressure is run through an evaporator connected to the heat source. In there the refrigerant is evaporated by the low-temperature heat because of the low pressure. Secondly, the refrigerant is compressed by the compressor, which is the part that uses electricity, resulting in high pressure and increased temperature. Third, the high-pressure gas is run through a condenser connected to the heat sink, usually the water of the heating system or the domestic hot water tank. Here, the refrigerant condenses and thus gives off its heat. Lastly, the refrigerant is passed through an expansion valve to lower the pressure and temperature needed for the evaporator, and then the cycle starts again.

The efficiency of a heat pump is generally expressed by the Coefficient Of Performance (COP). The COP is given by the following formula.

$$COP = \frac{|Q|}{W} \quad (5.1)$$

Here,  $Q$  is the useful heat provided by the heat pump and  $W$  is work done by the compressor. The electrical work provided by the compressor is decided by the manufacturer, but, as can be seen in formula 5.1, the actual heat output depends on the COP during that time. Therefore, the maximum heat output of a heat pump can be lower if the source temperature is lower. For this thesis, the COP is determined using equation 5.2, which comes from a study that used quadratic regression of heat pump manufacturer's data [43] and a correction factor ( $CF$ ) that fits this formula to the measured performance of heat pumps.

$$\text{COP} = \begin{cases} CF \cdot (6.08 - 0.09 \cdot \Delta T + 0.0005 \cdot \Delta T^2), & \text{ASHP} \\ CF \cdot (10.29 - 0.21 \cdot \Delta T + 0.0012 \cdot \Delta T^2), & \text{GSHP} \end{cases} \text{ with } \Delta T = T^{\text{sink}} - T^{\text{source}} \text{ and } CF = 0.85 \quad (5.2)$$

Here,  $T^{\text{sink}}$  is the temperature of the heat sink, which for domestic heat pumps is the delivery temperature of the heat distribution system. The delivery temperature to floor heating or radiators for heat pumps is usually between 30 and 55°C. For the purposes of this work, all heat pumps are assumed to have a delivery temperature of 55°C to ensure that power consumption is not underestimated.  $T^{\text{source}}$  is the temperature of the source where the heat pump takes its heat from. This is the outside air for air-source heat pumps and the ground for ground-source heat pumps.

These COP fits are based on heat pump data that were introduced until 2018. A study by [51] in 2022 used a similar approach to create a fit for ASHPs based on newer heat pumps. This fit might improve the accuracy of the model, however, I found this study when the simulations were already finished. Therefore, this was not taken into account.

Heat pumps can have fixed or variable speed compressors. Heat pumps with fixed-speed compressors can only be turned off or run on full electric power and are called on-off heat pumps. With heat pumps with variable-speed compressors, the electric power of the compressor and, thus, the output heat flow of the heat pump can be modulated. These kinds of heat pumps are, therefore, also called modulating heat pumps. In this thesis, both types of heat pump are simulated, in which modulating heat pumps can vary their power between 30% and 100% of their rated power.

Heat pumps in residential buildings are used mainly for heating spaces and domestic water. The usage, types, and control methods of heat pumps that are covered in this report are discussed in the remainder of this chapter.

## 5.2. Space Heating demand

Most of the energy that a residential heat pump produces is used for space heating. For a 2-person household in a poorly insulated corner terraced house built in 1970, this is about 75% of the gas used when heated by a gas boiler [26]. To simulate the heat demand for space heating, a model described in [2] is used. This model consists of a house with four rooms for which both convective and conductive heat losses through the wall, roof, and double-glazed windows are considered. A schematic overview of the model can be seen in figure 5.2.

In the model, heat losses to the ground, heat transfer between rooms, and the heat gained by radiation through the windows are not taken into account. Radiative heat gains can decrease the need for heating with a heat pump, but since solar radiation is relatively low in winter, they are considered to be out of scope. This leads to a more conservative estimate of the heat demand.

Equations 5.3 to 5.5 are used to calculate the convective losses through the walls, windows and roof and the parameters of it are provided in [49], which are based on a C-label house in the Netherlands [29] and are described in appendix part A.1.

$$\dot{Q}_{\text{roof}} = \frac{T_{\text{in}} - T_{\text{out}}}{\frac{1}{h_{\text{air-roof}}A_{\text{roof}}} + \frac{L_{\text{roof}}}{k_{\text{roof}}A_{\text{roof}}} + \frac{1}{h_{\text{roof-air}}A_{\text{roof}}}} \quad (5.3)$$

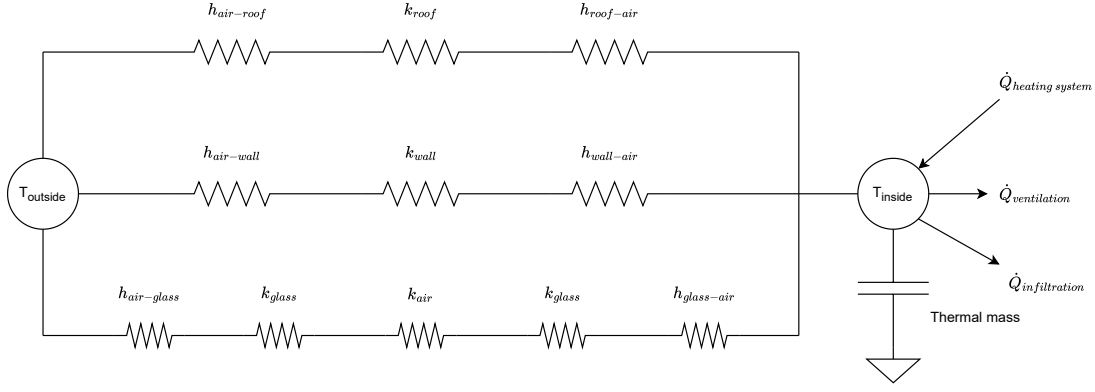


Figure 5.2: Thermal model for space heating demand

$$\dot{Q}_{\text{wall}} = \frac{T_{\text{in}} - T_{\text{out}}}{\frac{1}{h_{\text{air-wall}}A_{\text{wall}}} + \frac{L_{\text{wall}}}{k_{\text{wall}}A_{\text{wall}}} + \frac{1}{h_{\text{wall-air}}A_{\text{wall}}}} \quad (5.4)$$

$$\dot{Q}_{\text{glass}} = \frac{T_{\text{in}} - T_{\text{out}}}{\frac{1}{h_{\text{air-glass}}A_{\text{glass}}} + \frac{L_{\text{glass}}}{k_{\text{glass}}A_{\text{glass}}} + \frac{L_{\text{air}}}{k_{\text{air}}A_{\text{glass}}} + \frac{L_{\text{glass}}}{k_{\text{glass}}A_{\text{glass}}} + \frac{1}{h_{\text{glass-air}}A_{\text{glass}}}} \quad (5.5)$$

$T_{\text{in}}$  and  $T_{\text{out}}$  are the temperatures inside the house and outside. The  $h$  represents the heat transfer coefficients,  $k$  the thermal conductivity,  $A$  the surface and  $L$  the thickness of the materials. The ventilation loss is calculated with equation 5.6.

$$\dot{Q}_{\text{ventilation}} = c_a \rho_a q_v (T_{\text{in}} - T_{\text{out}}) \quad (5.6)$$

In this equation,  $c_a$  is the specific heat capacity of air,  $\rho$  the density of air, and  $q_v$  is the ventilation air flow. This air flow is calculated by the empirical equation 5.7 proposed in [24], which was originally published in imperial units but converted to metric units in this thesis, resulting in equation 5.6.

$$q_v = C_{\text{surf}} \cdot A_{\text{cf}} + C_{\text{room}} \cdot (N_r + 1) \quad (5.7)$$

Where the surface constant  $C_{\text{surf}}$  is  $0.0001524 \frac{\text{m}}{\text{s}}$ , the building conditioned area  $A_{\text{cf}}$  is taken to be  $156.65 \text{m}^2$ , which is the roof area of the house, the room constant  $C_{\text{room}}$  is  $0.00354 \frac{\text{m}^3}{\text{s}}$  and  $N_r$  is the number of rooms, which is 4. The ventilation losses are calculated using equation 5.8.

$$\dot{Q}_{\text{infiltration}} = c_a \rho_a q_i (T_{\text{in}} - T_{\text{out}}) \quad (5.8)$$

The variables  $c_a$  and  $\rho$  are the same as in equation 5.6, and the infiltration air flow  $q_i$  is given by equation 5.9.

$$q_i = A_{\text{es}} A_u \sqrt{C_s |\Delta T| + C_w u^2} \quad (5.9)$$

Here,  $A_{\text{es}}$  is the exposed area of the building, taken to be  $119.6 \text{m}^2$ ,  $A_u$  is the unit leakage area, taken to be  $0.007$ .  $C_s$  is the stacking coefficient, which is  $0.027 \frac{\text{m}^2}{\text{s}^2 \text{K}}$  here.  $\Delta T$  is the difference between the inside and outside temperature,  $C_w$  the wind coefficient of  $5.018$  and  $u$  the wind speed of  $1 \frac{\text{m}}{\text{s}}$ .

Internal heat gains like occupants, ovens, stoves, and lighting are neglected in this model. Therefore, the total heat flow can be calculated with the equation 5.10.

$$\dot{Q}_{\text{total}} = \dot{Q}_{\text{heating system}} - \dot{Q}_{\text{roof}} - \dot{Q}_{\text{wall}} - \dot{Q}_{\text{glass}} - \dot{Q}_{\text{ventilation}} - \dot{Q}_{\text{infiltration}} \quad (5.10)$$

$\dot{Q}_{heating\ system}$  is the heat provided by the heat pump system. After this, the new house temperature at the next time step can be calculated with equation 5.11.

$$T_{in,t+1} = T_{in,t} + \frac{\dot{Q}_{total}}{mc_{total}} \Delta t \quad (5.11)$$

With  $T_{in,t}$  and  $T_{in,t+1}$  being the inside temperature at the current and next time stamp,  $\Delta t$  the size of the timestamp and  $mc_{total}$  the total thermal mass defined in equation 5.12.

$$mc_{total} = m_{air}c_a + m_{roof}c_{roof} + m_{windows}c_{windows} + m_{walls}c_{walls} \quad (5.12)$$

$m_{air}$ ,  $m_{roof}$ ,  $m_{windows}$  and  $m_{walls}$  are the respective masses of the air, roof, windows and walls.  $c_a$ ,  $c_{roof}$ ,  $c_{windows}$  and  $c_{walls}$  are the specific heat of the air, roof, windows and walls. These values can be found in Appendix A.1.

The thermal demand is then calculated by providing a set point for the inside temperature of the house that the heat pump has to maintain, as well as the outside temperature during the period, depicted in figure 5.3. The resolution of the model that determines the heat pump's power demand is 15 minutes. Once the demand has been determined, the 15-minute values are averaged to hourly values before being used in the PowerFactory model, which has an hourly resolution.

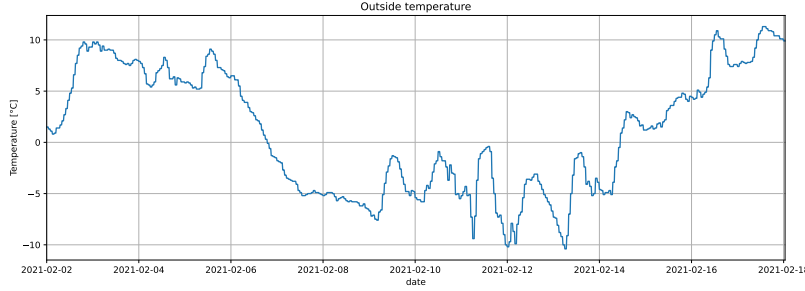


Figure 5.3: Outside temperature during the thermal simulation

### Modifications to the original model

In this thesis, some changes are made to the thermal model of [2]. Firstly, when the thermal model is used for the optimisation for dynamic energy prices, equation 5.9 is set to a constant value with equation 5.13 to improve the speed of optimisation.

$$q_i = A_{es}A_u \sqrt{C_s |T_{set,mean} - T_{out,mean}| + C_w u^2} \quad (5.13)$$

Here,  $T_{set,mean}$  is the mean set point temperature of the houses, which is  $20^\circ C$ ,  $T_{out,mean}$  is the mean of the outside temperature during the simulation period, which is  $1.7^\circ C$ .

In addition, a scaling factor for the heat loss  $S_Q$  is added to the total heat flow in the equation 5.10, chosen randomly between 0.7 and 1.3 uniformly for each house to give variability to the thermal behaviour of the houses, resulting in the equation 5.14.

$$\dot{Q}_{total} = \dot{Q}_{heating\ system} - S_Q(\dot{Q}_{roof} - \dot{Q}_{wall} - \dot{Q}_{glass} - \dot{Q}_{ventilation} - \dot{Q}_{infiltration}) \quad (5.14)$$

Lastly, equation 5.12 is modified to include a scaling factor  $S_{mc}$ , which is randomly chosen between 0.7 and 1.3 uniformly to, like the heat loss scaling factor, provide variability to the thermal behaviour of the houses. These scaling factors are chosen independently of each other. Since the walls are made of 1

slab of concrete in the model and houses built after 1920 usually have a cavity wall in the Netherlands [27], the thermal mass of the walls in the original model is divided in half to account for this in this thesis.

$$m c_{total} = S_{mc} (m_{air} c_a + m_{roof} c_{roof} + m_{windows} c_{windows} + 0.5 \cdot m_{walls} c_{walls}) \quad (5.15)$$

$S_{mc}$  is the scaling factor of the thermal mass, which is randomly chosen between 0.7 and 1.3 uniformly to, like the heat loss scaling factor, provide variability to the thermal behaviour of the houses. The inside temperature of each house is initialised randomly between  $T_{set} - 1^\circ C$  and  $T_{set}$  uniformly.

### 5.3. Domestic Hot Water production

In addition to space heating, the heat pump also provides domestic hot water, except in a gas-hybrid set-up, where the natural gas boiler does this. When the heat pump provides the DHW, the power is insufficient to supply enough hot water for a shower instantly. Therefore, a storage tank buffers the hot water.

To determine the DHW usage of the simulated households and the size of the DHW tank, a Python package called PYSIMDEUM [45] is used. This package is developed to model and simulate stochastic residential water demand at the end-use level. In this package, a house is built based on the kind of household provided as input. Here, the choices are a one-person household, a two-person household, or a family household. Based on this information, the software fills the house with different types of people, including age group and gender, and if they are working, using Dutch statistics on inhabitants. In addition, it places end-use devices such as a water-saving shower head or a washing machine in the house. Then, the water use of the household is simulated and can be split into total use and hot water use. For this research, a mix of households is taken based on the current mix of households in the Netherlands provided by Statistics Netherlands (CBS) [8]. In 2024, 40% of the households were one-person, 32% were two-person, and 28% were family households, which are assumed to hold three or more persons. Therefore, each household in the grid simulation will be assigned a unique DHW use profile based on the spread of household types. One of these profiles is depicted in figure 5.4.

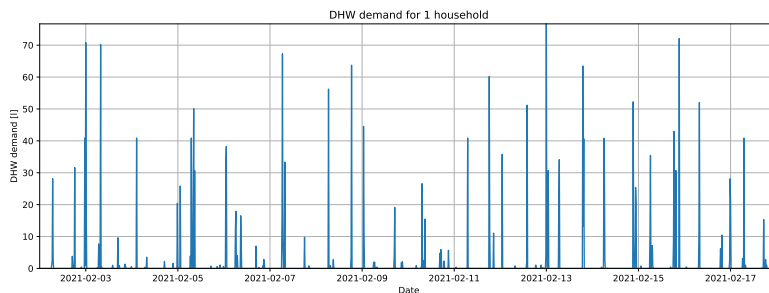


Figure 5.4: Domestic hot water demand for one of the households

Based on the maximum demand in an hour from these profiles, a tank volume of 300 L is chosen for each household. The tank is assumed to be a cylinder with a length of 1.66m and a radius of 0.24m. This is bigger than that placed on average in the Netherlands, but a bigger DWH tank does not influence the electricity demand significantly, and therefore, it justifies the simplification.

To determine the temperature of the water within the DHW tank, it is assumed that the temperature of the water is uniformly distributed within the tank. This results in the heat balance inspired by [37] and given in equations 5.16.

$$Q_{t+1} = Q_t - Q_{used,t} - \dot{Q}_{loss} \cdot \Delta t + \dot{Q}_{HP} \cdot \Delta t \quad (5.16)$$

Where  $Q_{t+1}$  is the heat inside the tank in the next time step,  $Q_t$  the heat at the current time step,  $Q_{used,t}$  the heat used by DHW use,  $\dot{Q}_{loss}$  the heat that leaks into the environment,  $\dot{Q}_{HP}$  the heating power

supplied by the heat pump and  $\Delta t$  the time duration of the time step in seconds. This equation can now be written in terms of volume and temperature, which is done in equation 5.17

$$V_{tank}C_w(T_{t+1} - T_{tap}) = V_{tank}C_w(T_t - T_{tap}) - V_{used}C_w\left(\frac{T_{t+1} + T_t}{2} - T_{tap}\right) - U_{tank}A_{tank}(T_t - T_{in}) \cdot \Delta t + \dot{Q}_{HP} \cdot \Delta t \quad (5.17)$$

Where  $V_{tank}$  is the volume of the DHW tank,  $C_w$  the specific heat of water,  $T_{Tank,t}$ , the temperature of the tank at time step  $t$ ,  $T_{tap}$ ,  $V_{used}$  the volume of water used for the DHW appliances,  $U_{tank}$  the heat transfer coefficient of the tank, which in this report is  $0.5 \frac{W}{m^2K}$  based on an example DWH tank [22],  $A_{tank}$  the surface area of the tank, and  $T_{in}$  the inside temperature of the house. Solving for  $T_{Tank,t+1}$  results in equation 5.18

$$T_{Tank,t+1} = \frac{1}{V_{tank}C_w + 0.5V_{used}C_w} \cdot (V_{tank}C_w(T_{Tank,t} - T_{tap}) + (V_{tank}C_w + V_{used}C_w)T_{tap} - 0.5V_{used}C_wT_{Tank,t} + U_{tank}A_{tank}(T_{Tank,t} - T_{in})\Delta t + \dot{Q}_{HP} \Delta t) \quad (5.18)$$

The initial temperature of each DHW tank is randomly chosen between 45°C and 50°C uniformly.

## 5.4. All-Electric Heat Pumps

In this thesis, all-electric heat pumps are defined as heat pumps that do not use an auxiliary heating system. This heat pump configuration accounts for 75 % of heat pump sales in the Netherlands in the period 2021 to 2023 [52]. These heat pumps usually use either the ground or the outside air as a heat source. The All-Electric heat pumps in this thesis have a rated heating capacity of  $8kW_{thermal}$  at a source temperature of 7°C and a supply temperature of 35°C. The rated capacity at these conditions can usually be found in the technical specifications of a heat pump. The rated electric power of the heat pump is then calculated by dividing the thermal capacity by the COP under these conditions.

### 5.4.1. Air-Source Heat Pump

Air-source heat pumps that heat water for space heating and DHW were, by 2023, the most popular type of heat pump in the Netherlands with a 76% market share, excluding air-to-air heat pumps, also known as air conditioners [9]. ASHPs use the outside air as a heat source, where the evaporator of the heat pump is placed outside, and air is forced onto it, most of the time with a fan. Therefore, the temperature of the heat source is dependent on the outside temperature. Due to the variability of outside temperature, the COP varies during the day and seasons.

### 5.4.2. Ground-source Heat Pump

Ground-source heat Pumps had a 24 % market share, excluding air-to-air heat pumps in the Netherlands [7] in 2023. Here, the source of heat comes from the ground. Instead of letting air flow against the evaporator, water is used to provide heat to the evaporator. This water is pumped through a loop that is placed under the ground either horizontally at a depth between 1 and 2 meters or vertically at a depth between 60 and 100 meters or sometimes even more [12], also called a well. Because the heat source is the ground, the temperature stays relatively constant throughout the year and is usually around 10-12 ° C [50], which is higher than the air temperature during cold days. Therefore, the COP of these types of heat pumps is higher and more stable during the cold winter days in the Netherlands. This COP is determined using equation 5.2 from [43].

In addition to individual wells, a kind of district heating network called a source network, or in Dutch 'zeer lage temperatuur (ZLT) netwerk' can be used. In this case, the water that provides heat to the evaporator comes from a network of water pipes that runs through the streets. The supply temperature

of the water in this network is usually around 10°C [36]. The heat provided to the water in the network can either come from collective wells in the network, low-temperature residual heat, such as cooling of data centres, or a heat exchanger with a body of water, such as a river or lake. For this thesis, a constant source temperature for GSHPs of 10 ° C is taken.

### 5.4.3. Control methods

The control of the heat pump is usually based on a specific temperature that the occupant of the house likes. The heat pump then turns on and off or modulates its power to keep the temperature close to the set point that the occupant provides. In this thesis, the set point temperature of each house is randomly chosen with a uniform distribution between 18 and 22 ° C and is set for the whole simulation period.

If DHW production is also done by the heat pump, it is prioritised over space heating. This means that if the temperature of the DHW tank drops below 45°C, the heat pump provides its heat to the DHW in the next time step, giving full power for the whole time step or a fraction of its power until the tank is 50 ° C. In reality, an on-off heat pump can not give a fraction of its power, but it is assumed that it runs at full power for a fraction of the time step, averaging to this fraction of power. To avoid any unrealistic initialisation phenomenon, the first 2 days of the heat pump demand simulation are discarded before being fed to the PowerFactory grid simulation. Now, the two different control methods will be described.

#### On-off control

The model for an on-off heat pump turns on the heat pump till the set temperature is met and then turns it off again. If the temperature has decreased to 1 ° C below the set point, the heat pump is turned on again until the setpoint is reached. This control method is described in equation 5.19.

$$P_{HP,t} = \begin{cases} P_{HP,rated}, & T_{in,t} \leq T_{set} - 1^{\circ}C \\ P_{HP,t-1}, & T_{set} - 1^{\circ}C < T_{in,t} < T_{set} \\ 0, & T_{set} \leq T_{in,t} \end{cases} \quad \text{with } T_{set} \sim \mathcal{U}(18, 22) \quad (5.19)$$

If the temperature of the house in the first time step is between  $T_{set} - 1^{\circ}C$  and  $T_{set}$ ,  $P_{HP,t-1}$  is randomly chosen between  $P_{HP,rated}$  and 0 with a 50/50 chance on both. The results of the heat pump demand simulation of one of the houses can be seen in figure 5.5.

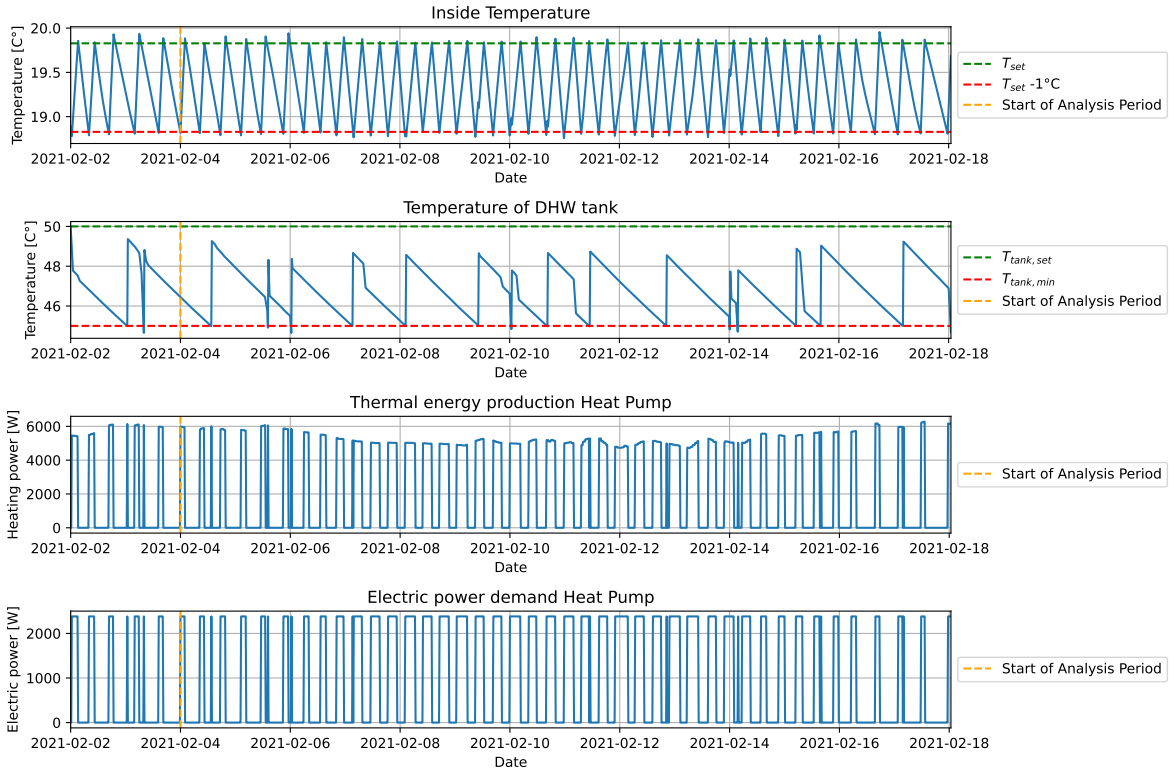


Figure 5.5: Results of the heat pump demand for one house with an all-electric **ASHP** with **on-off** control

The effect of the lower COP due to the lower outdoor temperature can be clearly seen in the thermal energy production graph. The thermal power is reduced in the middle of the simulation period when the outdoor temperature is at its lowest. In addition, the electric power graph shows that the heat pump has to be switched on more often during the cold period because the heat demand is higher due to the lower temperatures, and the heat pump's thermal yield is lower due to the lower COP. The on-off control method can also be clearly seen in the bouncing of the indoor temperature between the setpoint and the minimum temperature.

### Modulating control

For a modulating heat pump, the heat pump provides 100 % electric power if the temperature is  $1^\circ\text{C}$  or more below the set point. Between  $1^\circ\text{C}$  and  $0^\circ\text{C}$  below the set point, it modulated linearly between 100% and 30% of its electrical power, and if the temperature is above the set point, the heat pump is turned off. This control method is described in equation 5.20 and visually depicted in figure 5.6. The results of the simulation for one house can be seen in figure 5.7.

$$P_{\text{HP},t} = \begin{cases} P_{\text{HP},\text{rated}}, & T_{\text{in},t} < T_{\text{set}} - 1^\circ\text{C} \\ (0.3 + 0.7(1 - T_{\text{in},t} - (T_{\text{set}} - 1))) \cdot P_{\text{rated}}, & T_{\text{set}} - 1^\circ\text{C} < T_{\text{in},t} < T_{\text{set}} \\ 0, & T_{\text{set}} \leq T_{\text{in},t} \end{cases} \quad \text{with } T_{\text{set}} \sim \mathcal{U}(18, 22) \quad (5.20)$$

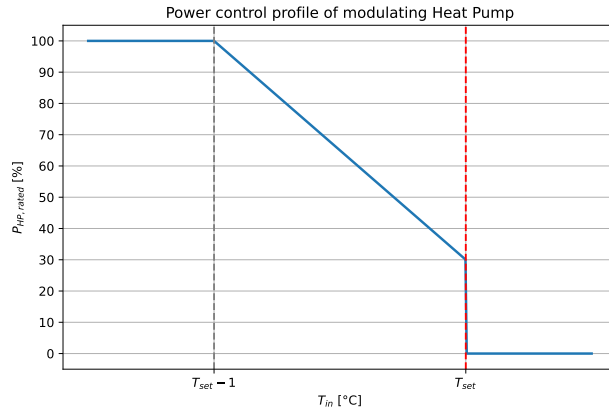


Figure 5.6: Power control profile of modulating Heat Pump

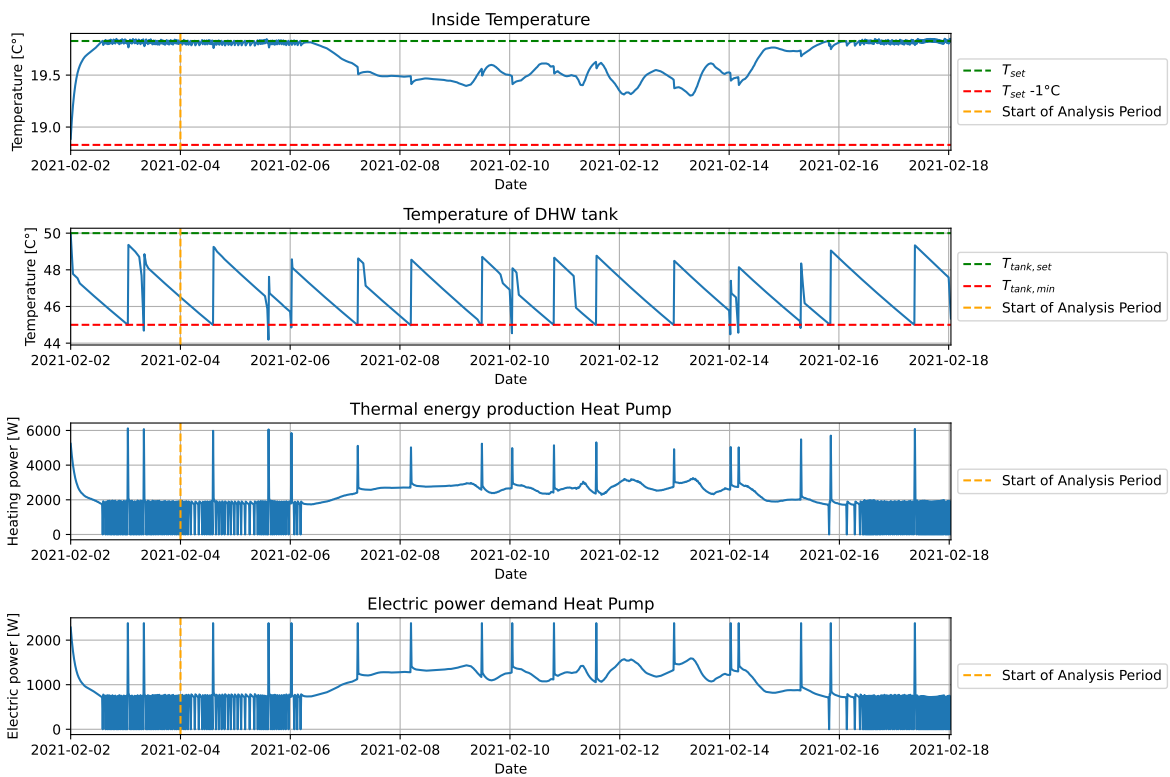


Figure 5.7: Results of the heat pump demand for one house with an all-electric ASHP with modulating control

From this graph, it can be seen that the modulating control provides a more constant indoor temperature. During the warmer phase of the simulation period, in the beginning and end, the heat pump operates in an on-off controlled manner due to the lower limit of 30% of the heat pump output. When it gets colder outside, the heat pump starts to modulate and maintains a relatively constant power demand, except for the peaks for domestic hot water production. The relative constant power is considerably lower than the maximum power it can deliver.

## 5.5. Hybrid Heat Pumps

GSHPs usually provide all the heat throughout the year because their output and COP are relatively independent of the outside temperature. However, ASHPs can be designed to provide heating for most

of the year but have a backup heater for a small percentage of the year when outside temperatures are too low to provide sufficient output. This can be done to save investment costs, as the backup heating is cheaper than a heat pump with more capacity. This is usually the case with electric resistance backup heaters. Another option is to use a natural gas boiler as a backup heater. With the latter option, the boiler can also provide cheaper heating if the COP falls below a certain threshold where the electricity required is more expensive than natural gas. If the heating system is equipped with a natural gas auxiliary heater, the DHW is usually also produced by the boiler.

For the electric resistive hybrid system, the heat pump has a rated capacity of  $6kW_{thermal}$  and a  $2kW_{thermal}$  resistive heater, assumed to have 100% efficiency. With the gas-hybrid system, the heat pump has a rated capacity of  $4kW_{thermal}$  and a natural gas boiler with a capacity of  $4kW_{thermal}$ . It is assumed that the natural gas boiler can produce  $31.65MJ$  of heat from  $1m^3$ , assuming 100% efficiency compared to the average lower heating value of natural gas in the Netherlands [41].

The auxiliary heaters are switched on in addition to the heat pump if the heat loss during this time period is greater than the heat pump alone can provide at the outdoor temperature during that time step. A resulting simulation of the electric resistive hybrid heat pump can be seen in figure 5.8.

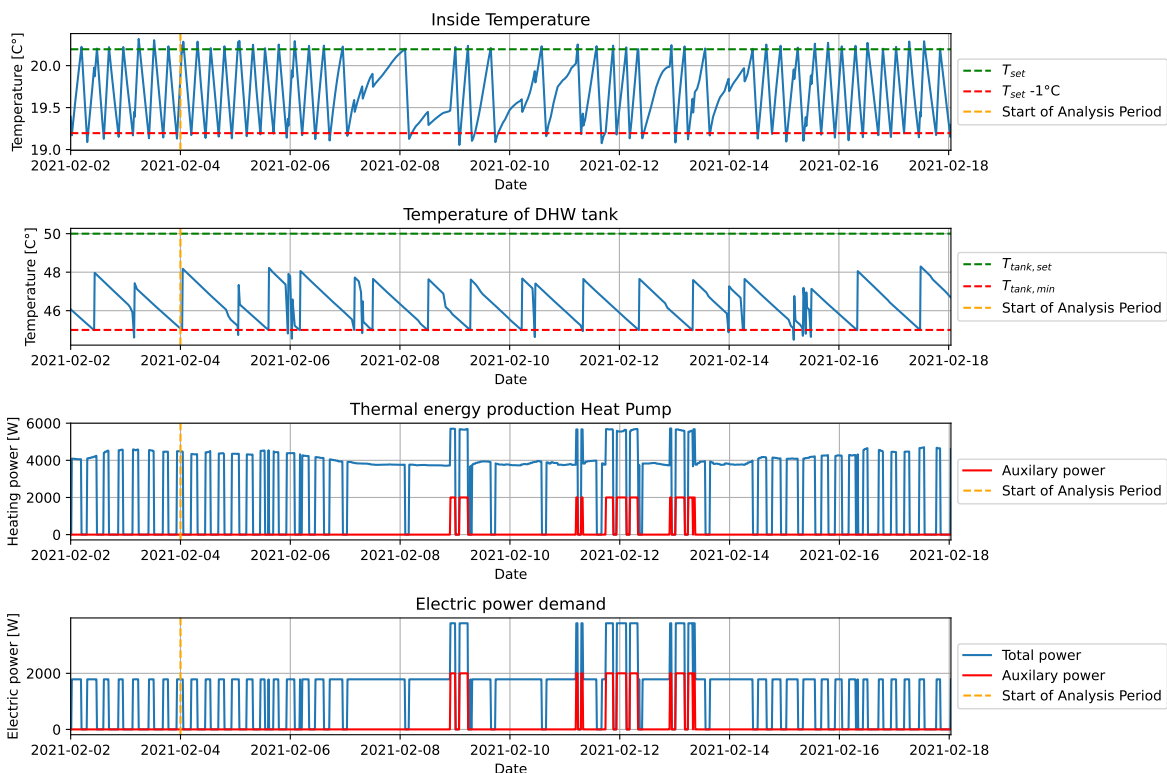


Figure 5.8: Results of the heat pump demand for one house with an electric resistive hybrid ASHP with on-off control

During the coldest period in the middle of the simulation period, it can be seen that the heat pump starts to struggle to reach the setpoint indoor temperature, as the slope of the indoor temperature rise decreases. Often, at moments when this slope is close to zero, the electric resistive auxiliary heater kicks in, causing the internal temperature to rise significantly again. At times when the auxiliary heater is activated, the electrical power consumed by the system more than doubles. The simulation results of the gas hybrid heat pump can be seen in figure 5.9.

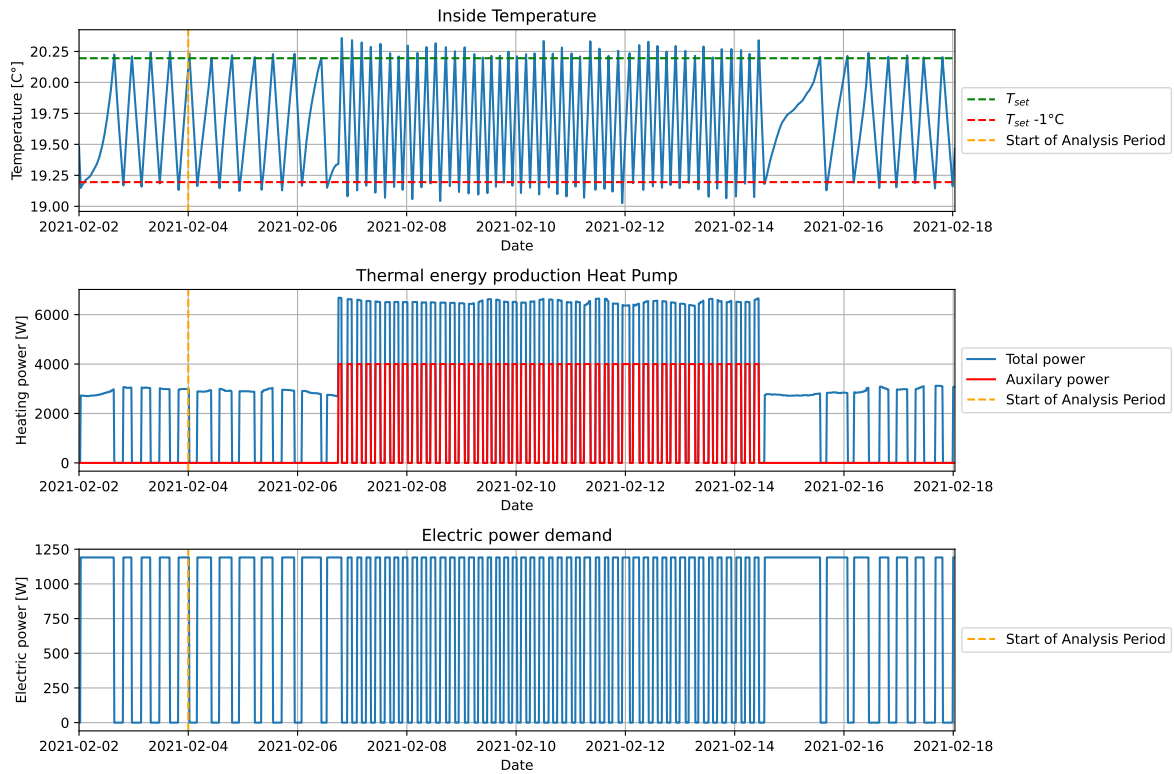


Figure 5.9: Results of the heat pump demand for one house with a gas hybrid **ASHP** with **on-off** control

In this simulation, the auxiliary heater kicks in much more often. This is to be expected as the heat pump has a lower capacity than the electric resistive hybrid system. Here, the natural gas boiler always operates alongside the heat pump during the coldest period of the simulated 2 weeks. However, this does not increase the electricity demand of the systems as the boiler uses natural gas instead of electricity.

## 5.6. Dynamic energy price-based control

Heat pumps can also be controlled while optimising for dynamic energy prices. This is simulated in this thesis using an optimisation model that minimises the cost of electricity needed for the heat pump. This model uses weather data, DHW use and hourly electricity prices as known inputs and uses the same thermal model, assuming perfect foresight. The set temperature is given as a minimal temperature constraint and is again randomly chosen with a uniform distribution between 18 ° C and 22 ° C, and for the DHW tank, the minimum temperature is always 45 ° C. For the dynamic prices optimisation model, the first and last 2 days are thrown away before being fed to the grid simulation to prevent any unrealistic initialisation or finishing phenomena. The optimisation model for the all-electric heat pumps is given in equation 5.21.

$$\begin{aligned}
& \min_p \sum_{t \in T} c_{electricity,t} P_{hp,t} \Delta t \\
& \text{s.t.} \\
& 0 \leq P_{hp,t} \leq P_{hp, \text{rated}}; \\
& T_{in, \text{set}} \leq T_{in,t}, \quad t \geq t^i; \\
& T_{in,t} \leq T_{in, \text{set}} + 2^\circ\text{C}; \\
& \frac{T_{in,t+1} + T_{in,t}}{\Delta t} = \frac{COP_t \cdot P_{sh,t} - S_Q(\dot{Q}_{\text{roof}} - \dot{Q}_{\text{wall}} - \dot{Q}_{\text{glass}} - \dot{Q}_{\text{ventilation}} - \dot{Q}_{\text{infiltration}})}{mC_{\text{total}}}; \quad (5.21) \\
& T_{\text{tank}, \text{min}} \leq T_{\text{tank},t}, \quad t \geq t^i; \\
& T_{\text{tank},t+1} = \frac{1}{V_{\text{tank}}C_w + 0.5V_{\text{used},t}C_w} \cdot (V_{\text{tank}}C_w(T_{\text{Tank},t} - T_{\text{tap}}) + (V_{\text{tank}}C_w + V_{\text{used},t}C_w)T_{\text{tap}} \\
& \quad - 0.5V_{\text{used},t}C_wT_{\text{Tank},t} + U_{\text{tank}}A_{\text{tank}}(T_{\text{Tank},t} - T_{in})\Delta t + COP_t \cdot P_{DHW,t} \Delta t); \\
& P_{HP,t} = P_{sh,t} + P_{DHW,t}
\end{aligned}$$

In this model,  $c_{electricity,t}$  is the price of electricity at time  $t$ ,  $P_{HP,t}$  is the total power demanded by the heat pump at time  $t$ , and  $P_{sh,t}$  and  $P_{DHW,t}$  are the respective proportions that the heat pump provides for space and water heating.  $t^i$  is the time step from which the minimum temperature constraints are active. This time step is set to 4 hours to provide the optimization some time to reach this minimum temperatures is the DHW use is significant in the first hours. The initial inside temperature is set to  $T_{in, \text{set}}$ , and the initial tank temperature is randomly chosen between 45°C and 50°C uniformly. The resulting simulation of the heat pump demand is depicted in figure 5.10.

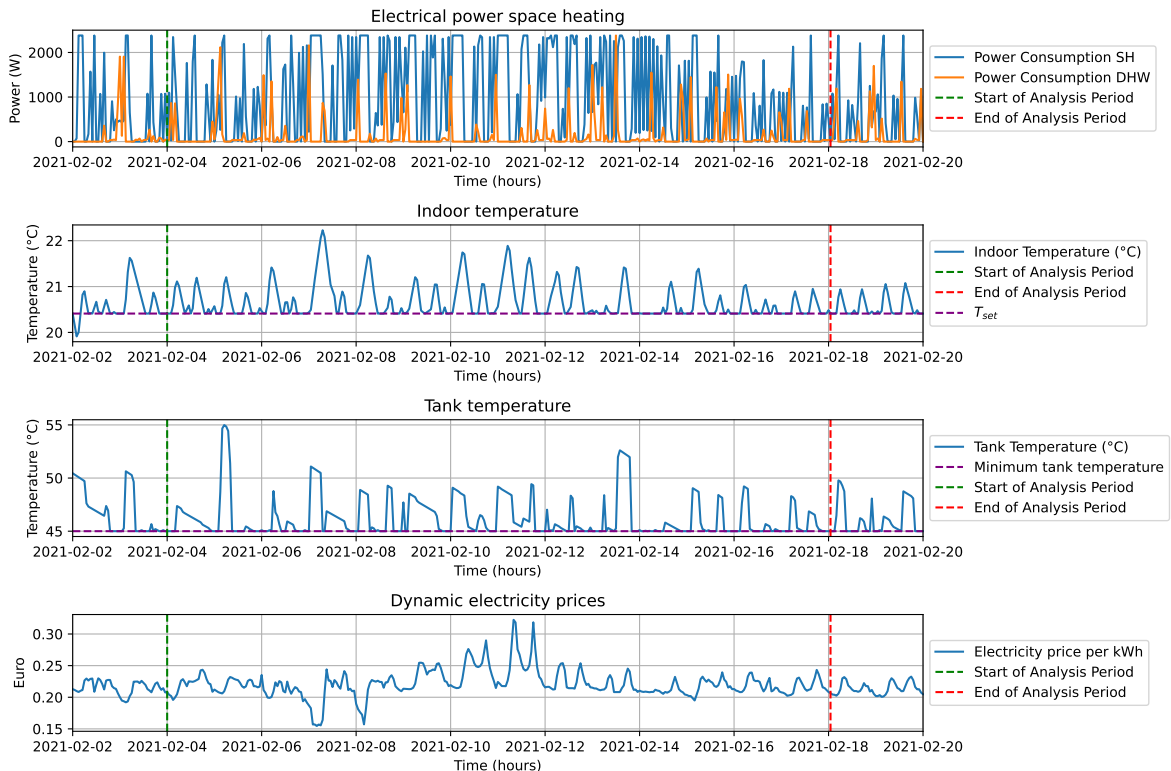


Figure 5.10: Results of the heat pump demand for one house with an all-electric ASHP with dynamic price control

These graphs show that the optimisation uses the buffering capacity of the DHW tank and the thermal

mass of the house to minimise the cost, which can be seen with the increase of the inside and DHW tank temperature during times of cheap electricity.

For the electric restive hybrid heat pumps, the optimisation is a bit different, where  $P_{aux,t}$  is added for the power the auxiliary heater is providing, which is limited with a  $P_{aux,rated}$  of  $2kW$ . The resulting model is given by equation 5.22 and the resulting simulation for one house is depicted in figure 5.22.

$$\begin{aligned}
 & \min_P \sum_{t \in T} c_{electricity,t} (P_{hp,t} + P_{aux,t}) \Delta t \\
 & \text{s.t.} \\
 & 0 \leq P_{hp,t} \leq P_{hp,rated}; \\
 & 0 \leq P_{aux,t} \leq P_{aux,rated}; \\
 & T_{in,set} \leq T_{in,t}, \quad t \geq t^i; \\
 & T_{in,t} \leq T_{in,set} + 2^\circ C; \\
 \square H \quad & \frac{T_{in,t+1} + T_{in,t}}{\Delta t} = \frac{COP_t \cdot P_{sh,t} + P_{aux,t} - S_Q(\dot{Q}_{roof} - \dot{Q}_{wall} - \dot{Q}_{glass} - \dot{Q}_{ventilation} - \dot{Q}_{infiltration})}{mC_{total}}; \\
 & T_{tank,min} \leq T_{tank,t}, \quad t \geq t^i; \\
 & T_{tank,t+1} = \frac{1}{V_{tank}C_w + 0.5V_{used,t}C_w} \cdot (V_{tank}C_w(T_{Tank,t} - T_{tap}) + (V_{tank}C_w + V_{used,t}C_w)T_{tap} \\
 & \quad - 0.5V_{used,t}C_wT_{Tank,t} + U_{tank}A_{tank}(T_{Tank,t} - T_{in})\Delta t + COP_t \cdot P_{DHW,t} \Delta t); \\
 & P_{HP,t} = P_{sh,t} + P_{DHW,t}
 \end{aligned} \tag{5.22}$$

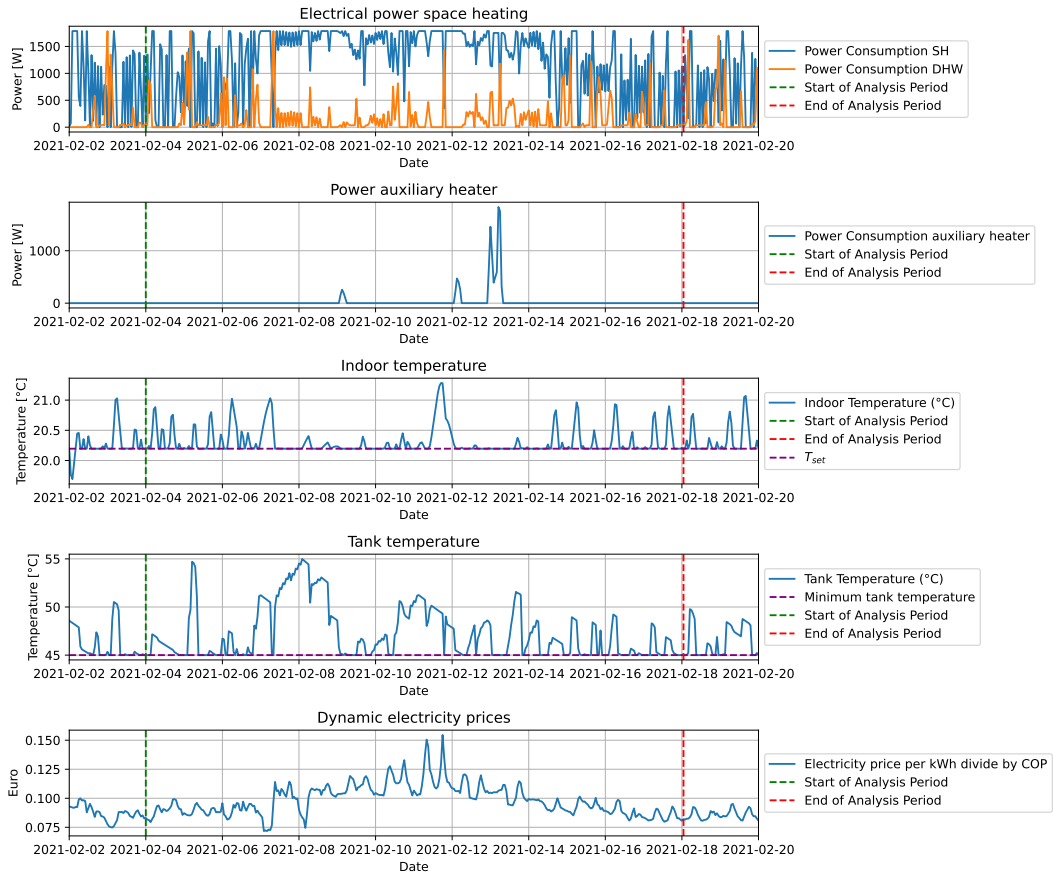


Figure 5.11: Results of the heat pump demand for one house with an **electric resistive hybrid ASHP** with **dynamic price control**

During the coldest week, the heat pump is first utilised for 100% before the auxiliary heater is used due to the high cost of using the electric resistance heater. The use of the auxiliary heater is minimised in the optimisation, which can be seen, for example, in the increase in internal temperature just before the second use of the auxiliary heater. This buffering minimises the peak of the auxiliary heater required afterwards.

For the gas-hybrid heat pump. The optimisation does not include DHW production, and the price of natural gas per  $kWh$  of heat produced,  $c_{gas,t}$  is added, resulting in the model described by equation 5.23 and the simulation results of one house are depicted in figure 5.23.

$$\min_p \sum_{t \in T} c_{electricity,t} P_{hp,t} \Delta t + c_{gas,t} P_{aux,t} \Delta t$$

s.t.

$$0 \leq P_{hp,t} \leq P_{hp,rated};$$

$$0 \leq P_{aux,t} \leq P_{aux,rated};$$

$$T_{in,set} \leq T_{in,t}, \quad t \geq t^i;$$

$$T_{in,t} \leq T_{in,set} + 2^\circ C;$$

$$\frac{T_{in,t+1} + T_{in,t}}{\Delta t} = \frac{COP_t \cdot P_{sh,t} + P_{aux,t} - S_Q(\dot{Q}_{roof} - \dot{Q}_{wall} - \dot{Q}_{glass} - \dot{Q}_{ventilation} - \dot{Q}_{infiltration})}{mC_{total}}$$

(5.23)

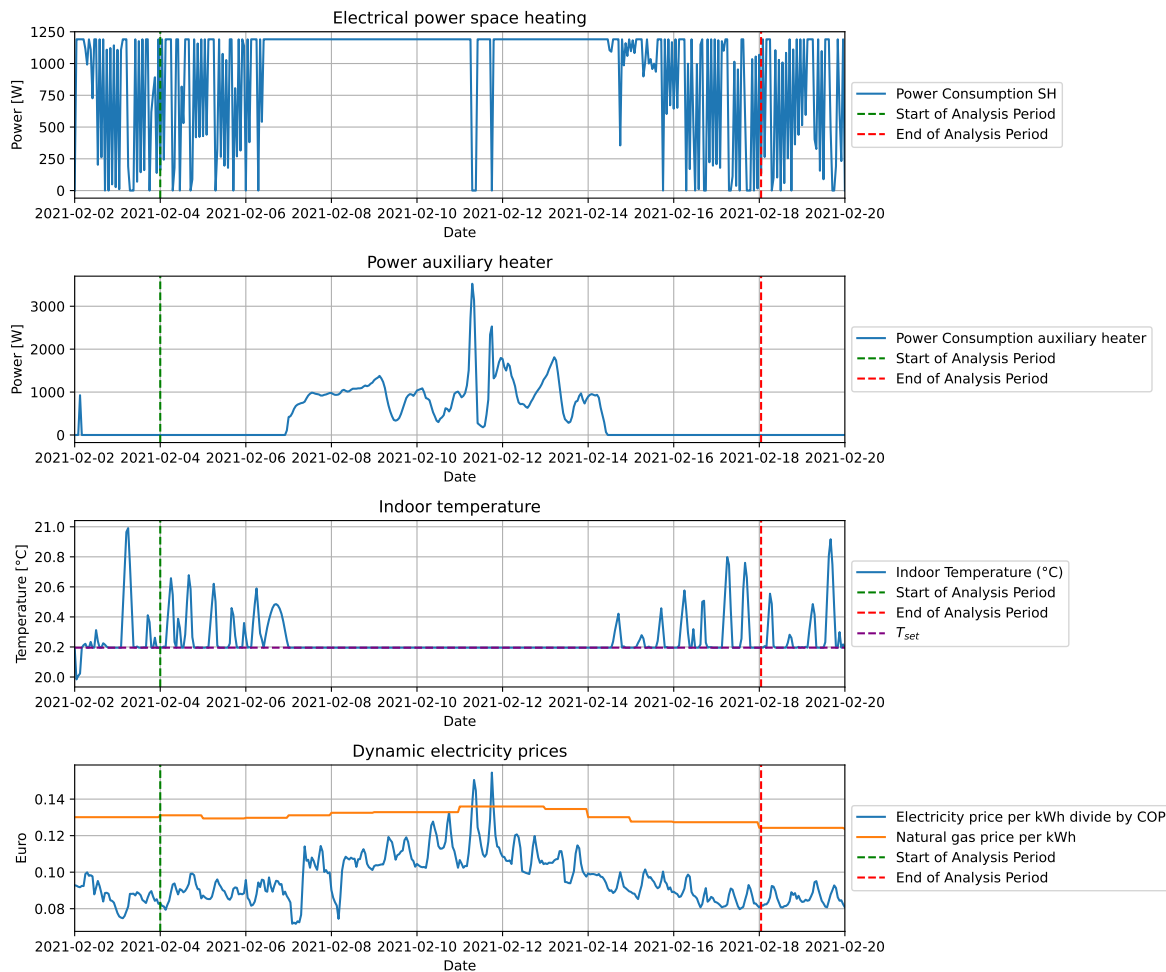


Figure 5.12: Results of the heat pump demand for one house with a **natural gas hybrid ASHP** with **dynamic price control**

To ensure that the energy prices are comparable magnitude in figure 5.12, the electricity price is divided by the COP at this time step. This ensures that the energy prices plotted represent the price of the heat it provides and that the most cost-effective choice can be seen in the graph. It can be seen that in the middle of the simulation period, the COP of the heat pump drops to such a low level that heating with natural gas becomes cheaper. The effect of this can be seen in the electric power of the heat pump, which drops to zero during the period when natural gas heating is cheaper, and the natural gas boiler takes care of all the heating. During the times when heating with the heat pump is cheaper, the heating power of the boiler is only used when the heat pump alone cannot provide enough heat.

## 5.7. Cooling

Both ASHPs and GSHPs can often be used to provide cooling to the house if the radiators or floor heating is suitable for it. ASHPs use active cooling where the outside air is used, which in summer is hotter than the temperature the system cools with. Therefore, it uses the thermodynamic cycle with the compressor that uses comparable amounts of electricity as heating. GSHPs use passive cooling, which uses the cool ground temperature that is lower than the temperature the systems cool with. Therefore, this way of cooling only needs a small pump to pump the cool water out of the ground or the source network without using a thermodynamic cycle, which uses much less electricity. Furthermore, with an individual well, the ground is heated during the passive cooling of the house. The ground then increases in temperature, increasing the COP during winter. The simulation of cooling is not considered in this thesis.

# 6

## Results

In this chapter, the results of the simulations are given for each type of heat pump by presenting their respective effects on the overloading of the central transformer and voltage problems. The difference in the two control types, on-off and modulating, can be seen as well. Then, the influence of dynamic energy prices and domestic hot water production is portrayed. The effects of different types of heat pumps, dynamic pricing, and DHW production are simulated for the current adoption rate of PV systems, EV chargers, and dynamic tariffs and are depicted for multiple adoption rates of heat pumps. The final part of this chapter discusses the results of some simulated scenarios for 2030 and 2050. The current adoption rates of the technologies considered, together with the forecasts for these rates for 2030 and 2050, are presented in table 6.1

Table 6.1: Adoption rates considered in the simulations

Penetration rate	Current	2030	2050
PV	30%	45% <sup>1</sup>	85% <sup>1</sup>
EV home chargers	2.7%	5.7% <sup>1</sup>	15.6% <sup>1</sup>
EV public chargers	7	14	31
HP	16%	24% <sup>1</sup>	100%
Dynamic tariff	3%	10% <sup>1</sup>	30% <sup>1</sup>

<sup>1</sup> These values are based on internal discussion and forecasts from SETIAM, Stedin's Energy Transition Impact Assessment Model.

For each set-up of the simulation, i.e. a given number of public and home chargers, PV systems, households with a dynamic energy contract and number and type of heat pumps, 30 different runs are performed, with the placement of these loads and tariffs being shuffled for each run. This is done to average out particular favourable and unfavourable placements of the loads for the total impact. The shuffling of the runs is done in the same way for each set up to ensure that the simulations of the setups can be well compared.

### 6.1. All-Electric Heat Pumps

First, the All-Electric heat pumps will be discussed. This means that the heat pump is providing all the heat demand in both space heating and domestic hot water without backup heating by natural gas or resistive electric heating.

In figure 6.1 the apparent power through the central transformer can be seen for the on-off air source heat pumps for different adoption rates, where the mean is represented by the line and the shading represents the 10th and 90th percentile of the 30 runs performed per adoption rate.

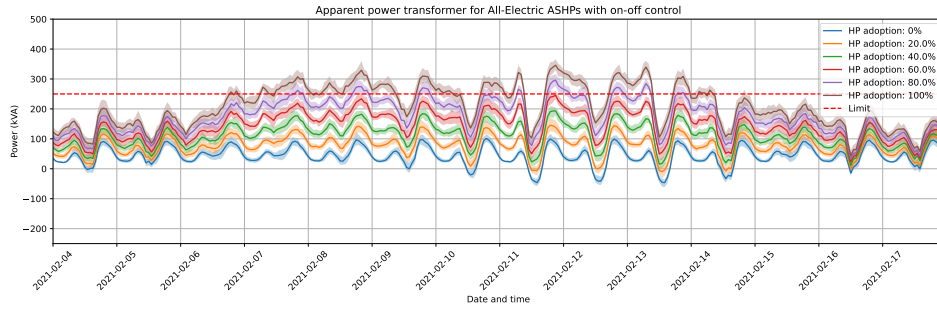


Figure 6.1: Apparent power through the transformer during the simulation period for **ASHPs** with **on-off** control for a variety of heat pump penetration levels

The effect of the outside temperature (figure 6.2) can be seen in the power profile, where in the middle of the simulation period, when the temperature is lowest, the power, on average, is the highest. It can be seen that for adoption rates of 80 % or more, the limit of the transformer is exceeded. This can be seen more clearly in figures 6.3 to 6.6, where the maximum exceedance of the limit per run is shown with a box plot, where the box represents the 25th to 75th percentile, the whiskers the minimum and maximum, and the stripe the median. The 10th and 90th percentiles are also represented by the shading.

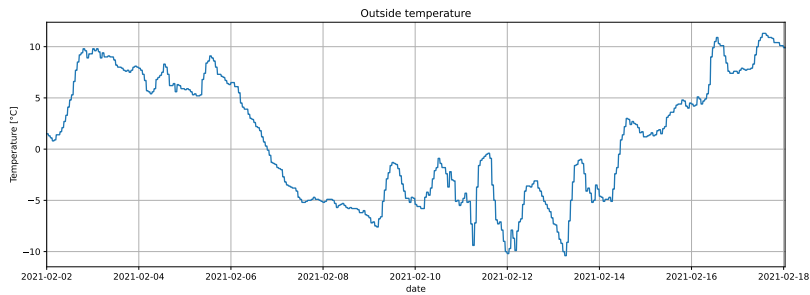


Figure 6.2: Outside temperature during the thermal simulation

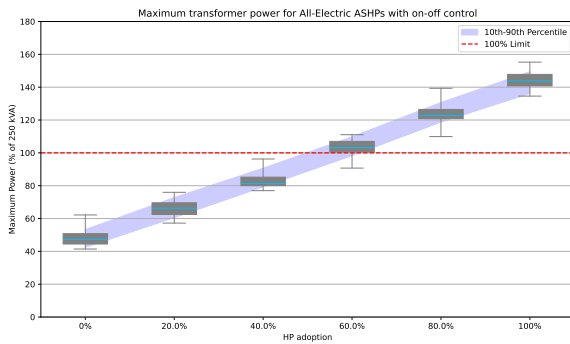


Figure 6.3: Maximum power through the transformer in percentage of the rated capacity for 30 runs per adoption rate for **on-off ASHPs**.

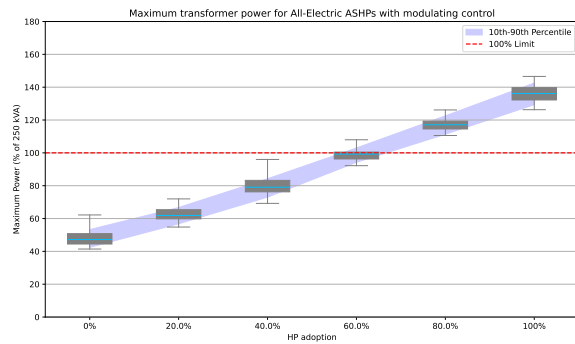


Figure 6.4: Maximum power through the transformer in percentage of the rated capacity for 30 runs per adoption rate for **modulating ASHPs**.

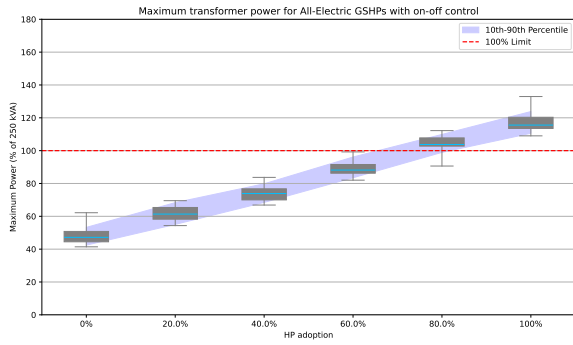


Figure 6.5: Maximum power through the transformer in percentage of the rated capacity for 30 runs per adoption rate for **on-off GSHPs**.

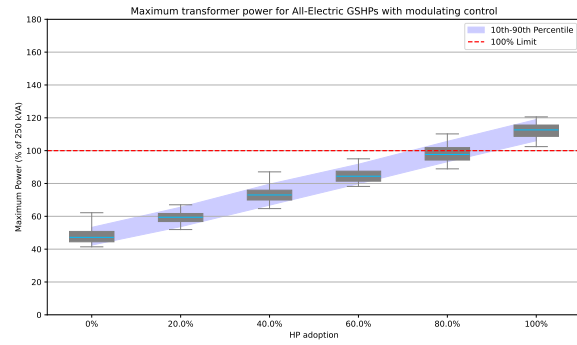


Figure 6.6: Maximum power through the transformer in percentage of the rated capacity for 30 runs per adoption rate for **modulating GSHPs**.

When comparing these plots, it can be seen clearly that the maximum power through the transformer is higher for the ASHPs than for GSHPs. The median of the maximum power for the 100 % adoption rate is 24% higher for ASHPs than GSHPs with on-off heat pumps and 20% for modulating heat pumps. Next to that, on-off heat pumps have a higher maximum power than modulating heat pumps, with 6% for ASHPs and 3% for GSHPs. Therefore, the all-electric heat pump with the lowest power limit exceedance is the GSHP with modulating control. Its power profile is depicted in figure 6.7, and the power profiles of the remaining heat pumps can be found in Appendix section B.1.

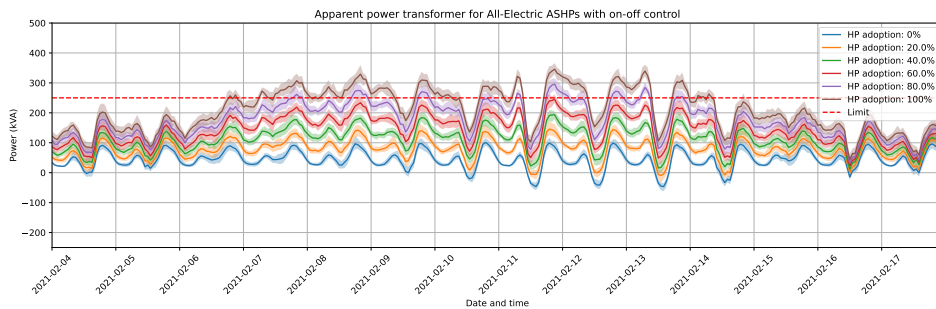


Figure 6.7: Apparent power through the transformer during the simulation period for **GSHPs with modulating control**.

Looking at the voltage deviation, the points at the far end of the grid will generally show the most deviation. The point farthest from the transformer in this grid is *Cbl\_718*, and its voltage profile will be used to show the variation. The profile for ASHPs with on-off control is depicted in figure 6.8, where the lines represent the mean and the shading the 10th to 90th percentile of 30 runs. When looking at the total voltage limit violations of the grid code for each household, explained in Section 2.1, the attention can be drawn to figures 6.9 to 6.12 where the total amount of grid code violations at a household is counted for both weeks and summed.

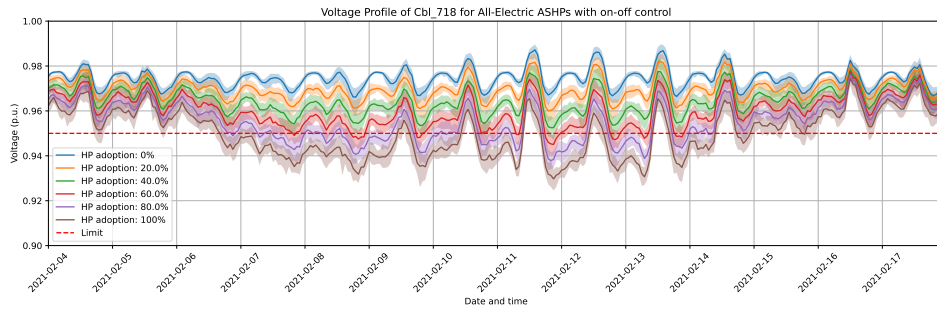


Figure 6.8: Voltage profile at CBL\_718 for **ASHPs** with **on-off** control

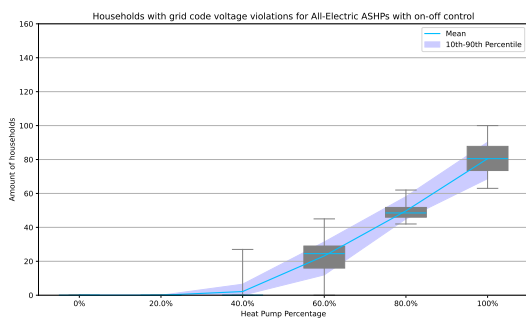


Figure 6.9: Amount of households with voltage grid code violations for 30 runs per adoption rate for **on-off ASHPs**.

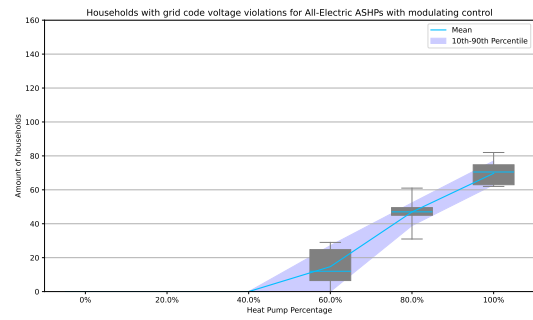


Figure 6.10: Amount of households with voltage grid code violations for 30 runs per adoption rate for **modulating ASHPs**.

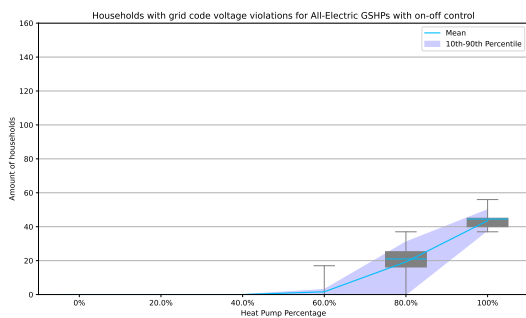


Figure 6.11: Amount of households with voltage grid code violations for 30 runs per adoption rate for **on-off GSHPs**.

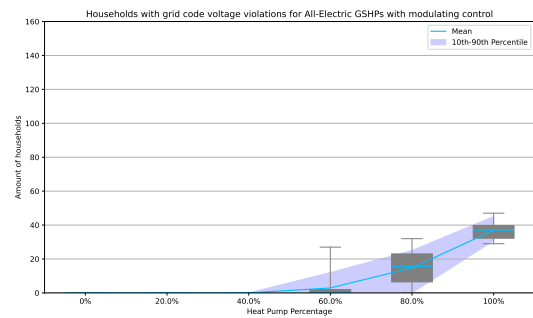


Figure 6.12: Amount of households with voltage grid code violations for 30 runs per adoption rate for **modulating GSHPs**.

With the grid code violations, the same difference in grid problems can be seen as for the power. When again looking at the median of the 100 % adoption rate, the ASHPs have more voltage grid code violations than GSHP, 80% more for on-off heat pumps and 92% more for modulating heat pumps. Furthermore, on-off heat pumps perform worse for voltage grid code violations with an increase of 14% in violations compared to modulating heat pumps for ASHPs and 22% for GSHPs. Therefore, GSHPs with modulating control have the lowest number of voltage limit violations. The voltage profile for *Cbl\_718* with modulating GSHPs can be seen in figure 6.13. The voltage profiles for all other heat pump types can be found in Appendix section B.2. No overvoltages were observed during the simulations.

In figure 6.14 an overview of the low-voltage grid is given, where households with voltage limit problems are circled in red.

It can be seen that voltage limit problems tend to occur at the ends of the network, where many loads

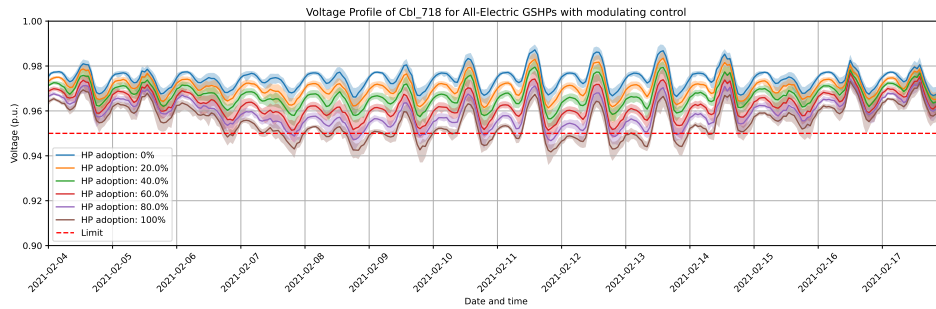


Figure 6.13: Voltage profile at CBL\_718 for **ASHPs** with **on-off** control

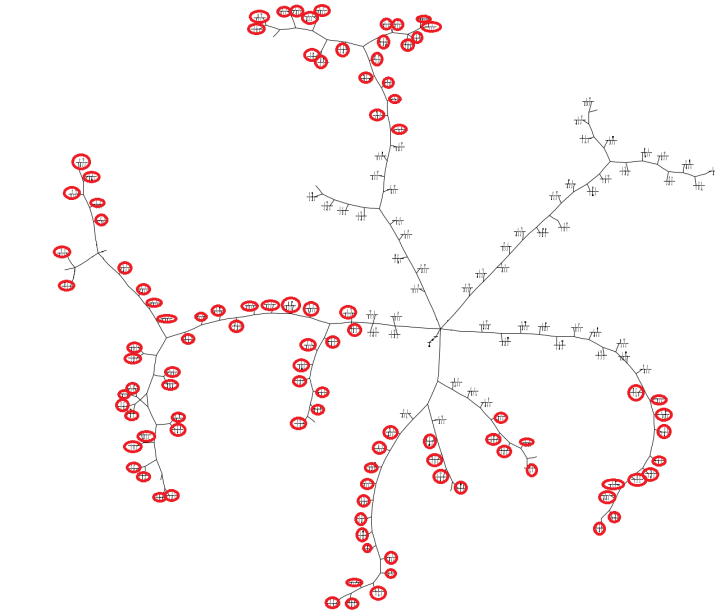


Figure 6.14: Overview of the low-voltage grid where the households circled in red are experiencing grid limit violations beyond the grid code for the worst performing heat pump (**on-off controlled ASHPs**)

before they have already caused the voltage to drop significantly. Because the total power drawn here is high, some branches are almost completely encircled from the ends to almost the transformer in the middle. One branch stands out. The top right branch has no voltage limit violations beyond the grid code. This can be explained by the relatively small number of houses combined with a relatively short cable connecting the branch to the transformer. The physical length is not visible in the figure 6.14, but the length of the cable that connects the transformer to the branch without voltage problems is 20 m, while the other branches either have a cable of 38 m or longer, or have a larger number of houses.

### Discussion

Looking at the results for All-Electric heat pumps, GSHPs can significantly reduce the impact on the grid compared to ASHPs for overloading and undervoltage. Therefore, a large amount of additional investment in grid upgrades can be reduced by opting for more GSHPs in households. However, this comes at the cost of additional investment at the household level. Whereas an ASHP can be easily installed outdoors without any additional infrastructure (except a grid connection), GSHPs need a water source to connect to. This water source can be achieved by drilling a personal well or by setting up a collective system in the neighbourhood, where several wells are drilled under the street, or one or more thermal storages can be built. In the second case, there is also the possibility of feeding low-temperature residual heat into the collective system, for example, by cooling supermarkets. In all cases, upfront investment costs will be higher than for ASHPs, and future research is required to decide whether these costs outweigh the additional grid upgrades needed for ASHPs.

In these simulations, modulating heat pumps produce a lower maximum power peak compared to on-off heat pumps, and they also caused fewer voltage problems. Therefore, modulating heat pumps are superior to their on-off counterparts in terms of grid impact. As they are also more efficient in terms of electricity use [4], it can be assumed that this technology will naturally become dominant if residents have a choice. However, it is possible that homeowners who do not pay the electricity bill will opt for the cheaper option, which in most cases will be the on-off controlled heat pump. Because of the smaller impact of the control method, it is up to the government to decide whether it is worthwhile to steer towards modulating heat pumps, for example, through subsidies.

## 6.2. Hybrid Heat Pumps

Next, the heat pumps with backup heating are simulated. These simulations are only carried out for ASHPs, as GSHPs do not normally require auxiliary heating due to their relatively constant source temperature. The two types of auxiliary heating are a natural gas boiler and an electric resistance heater, and both options can have an on-off and modulating type of control. For heat pumps with a natural gas boiler, it is assumed that the DHW production is also carried out by the boiler, and no electricity is used for this.

First, the power profiles with resistive electric auxiliary heating are depicted in figure 6.15 and the gas hybrid in figure 6.16. The rest of the power profiles can be found in Appendix Section B.1. In the first figure, a greater power capacity exceedance can be seen than for all-electric ASHPs (figure 6.1) for resistive electric backup heating. This is to be expected since part of the heating power of the resistive electric heater is done with a COP of 1. For the natural gas auxiliary heater, a lower power consumption is observed. This can be explained by the extra heat provided by the natural gas boiler that does not require electricity and the lack of DHW production. In figures 6.17 to 6.20, the maximum power of the 30 runs is plotted against the adoption rate of heat pumps.

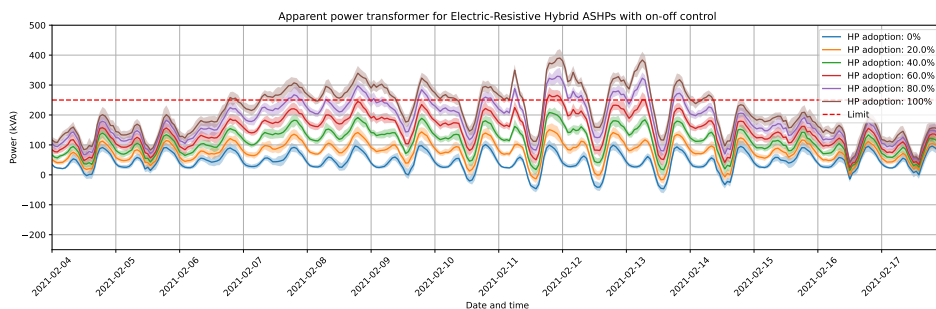


Figure 6.15: Apparent power through the transformer during the simulation period for **ASHPs with on-off control and resistive electric auxiliary heaters**.

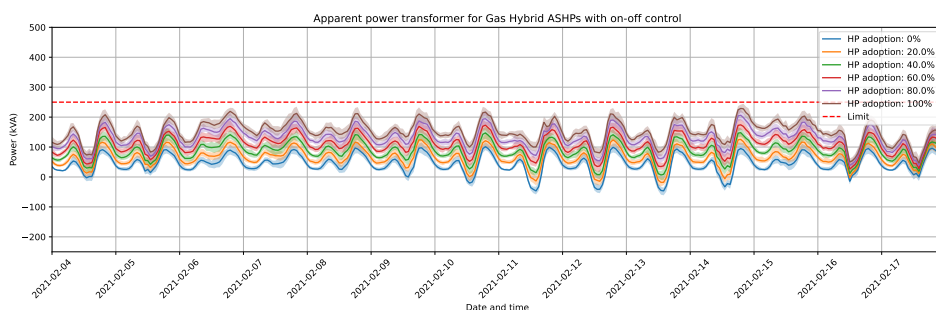


Figure 6.16: Apparent power through the transformer during the simulation period for **ASHPs with on-off control and natural gas auxiliary heaters**.

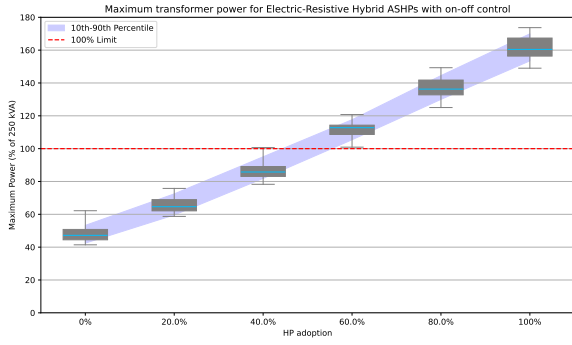


Figure 6.17: Maximum power through the transformer in percentage of the rated capacity for 30 runs per adoption rate for on-off ASHPs with resistive electric auxiliary heaters.

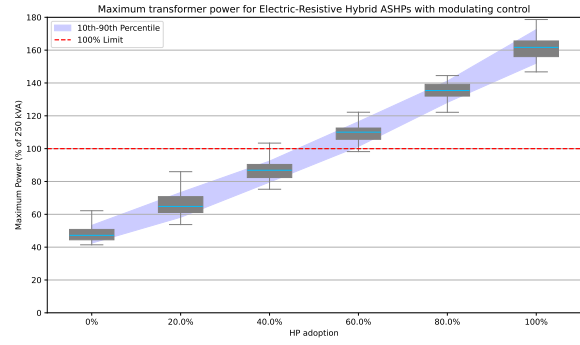


Figure 6.18: Maximum power through the transformer in percentage of the rated capacity for 30 runs per adoption rate for modulating ASHPs with resistive electric auxiliary heaters.

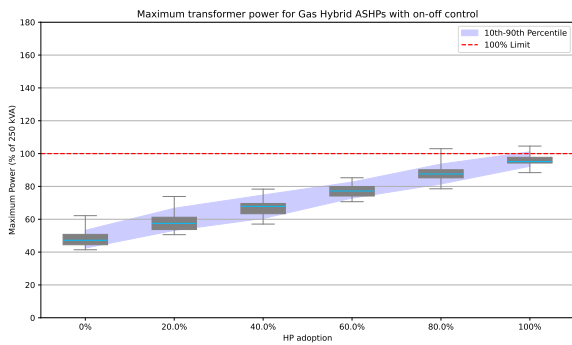


Figure 6.19: Maximum power through the transformer in percentage of the rated capacity for 30 runs per adoption rate for on-off ASHPs with natural gas auxiliary heaters.

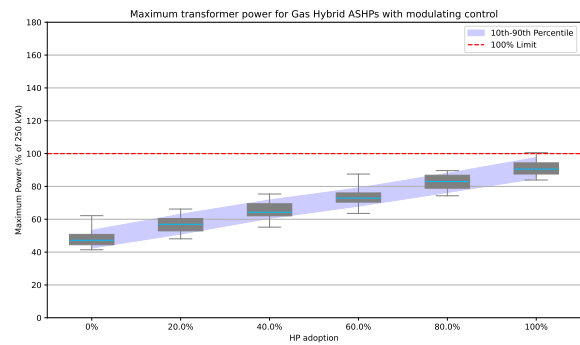


Figure 6.20: Maximum power through the transformer in percentage of the rated capacity for 30 runs per adoption rate for modulating ASHPs with natural gas auxiliary heater.

Heat pumps with resistive electric backup heating have a greater maximum power through the transformer than All-Electric ASHPs with 12% with on-off control and 19% with modulating control, looking at the median of the 100 % adoption rate. For gas hybrid systems, the maximum power through the transformer was decreased compared to the All-Electric ASHP with 52% for on-off controlled and 49% for modulating control.

The voltage profiles for *CBL\_718* for the electric hybrid and gas hybrid system are provided in figures 6.21 and 6.22, respectively. As can be seen, the voltage limit of 0.95 is exceeded by the electric hybrid system but hardly by the gas hybrid one. The voltage profiles for all hybrid heat pumps can be found in Appendix Section B.2. Looking at the number of voltage grid code violations in figures 6.23 to 6.26, there is no grid code violation for gas hybrid systems for any HP adoption rate.

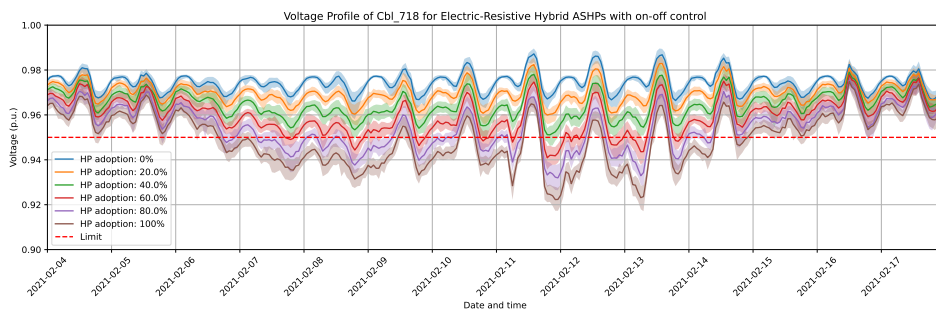


Figure 6.21: Voltage profile at CBL\_718 for ASHPs with on-off control and resistive electric auxiliary heaters

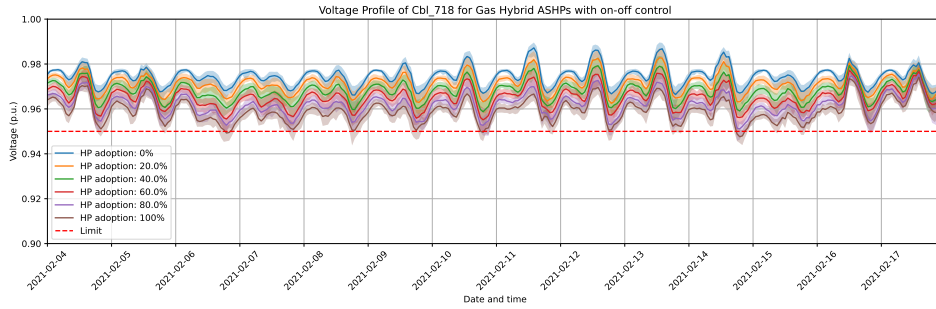


Figure 6.22: Voltage profile at CBL\_718 for **ASHPs with on-off control and natural gas auxiliary heaters.**

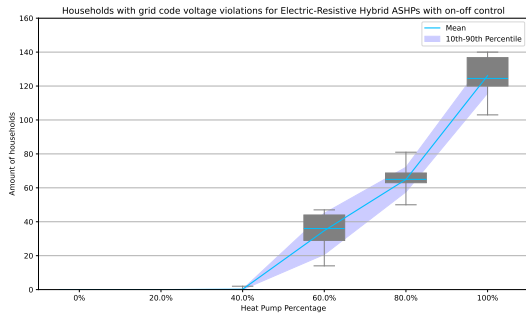


Figure 6.23: Amount of households with voltage grid code violations for 30 runs per adoption rate for **on-off ASHPs with resistive electric auxiliary heaters.**

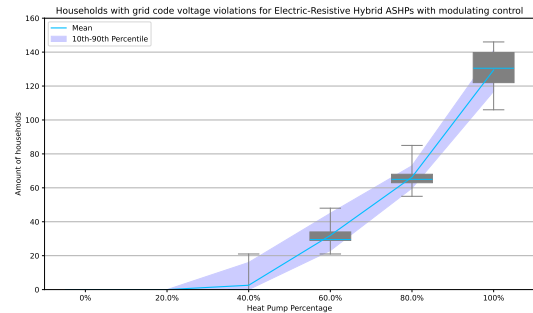


Figure 6.24: Amount of households with voltage grid code violations for 30 runs per adoption rate for **modulating ASHPs with resistive electric auxiliary heaters.**

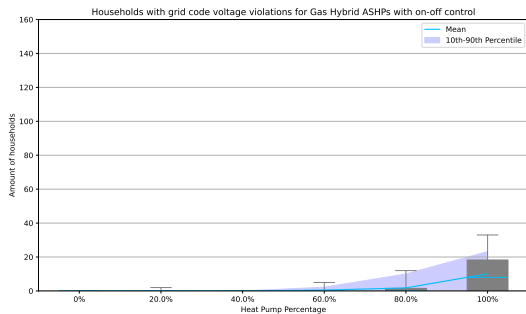


Figure 6.25: Amount of households with voltage grid code violations for 30 runs per adoption rate for **on-off ASHPs with natural gas auxiliary heaters.**

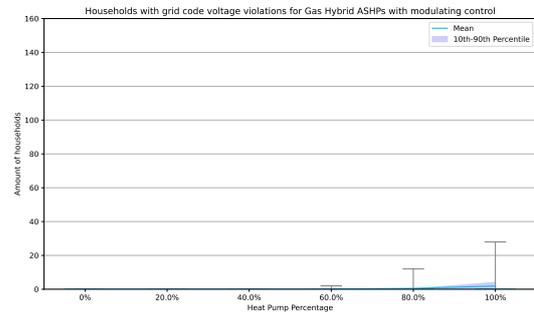


Figure 6.26: Amount of households with voltage grid code violations for 30 runs per adoption rate for **modulating ASHPs with natural gas auxiliary heaters.**

The number of grid violations regarding voltage levels is significant for electric hybrid systems. The median for the adoption rate of 100% of the electric hybrid system is 54% higher than for the All-Electric ASHP with on-off control and 85% for modulating control. Gas-hybrid heat pumps have a significantly lower number of grid violations, with a 90% reduction compared to all-electric ASHPs with on-off control. With modulating control, gas hybrid ASHPs even have a median number of grid violations of 0 for 100% heat pump adoption.

Discussion

The results show that resistive electric backup heating can significantly impact both overloading and undervoltage. Heat pumps can currently provide sufficient capacity without backup heating, and while resistive heating is slightly cheaper than increasing the capacity of the heat pump, this reduction in the investment cost of the heat pump comes at the cost of a significant impact on the electricity grid and,

therefore, potential upgrade costs. Therefore, electric hybrid heat pumps have an additional impact on the low-voltage grid, which is way bigger than the investment costs it saves for the heat pump. An important side note is the use of resistive electric elements for anti-legionella protection in the hot water tank. Although not simulated in this thesis, it is suspected that the impact of this on the grid is insignificant, as the duration is quite short and will not be the same for each house.

The impact of hybrid heat pumps is less than that of their all-electric counterparts. The simulations show that with a 100% penetration rate, there will be no problems with overloading or undervoltage for this grid. Although this type of system does not completely eliminate the use of natural gas, it can be a good solution as a transition to the gas-free goal in 2050 while keeping the impact on the grid manageable.

### 6.3. Influence of Dynamic Pricing

After looking at the effect of different types of heat pumps, the effect of dynamic energy tariffs is presented. One type of heat pump is chosen as an example, namely the all-electric heat pump with on-off control, and it is placed in all households. Then, the percentage of households with a dynamic electricity contract is changed from 0 to 100%. For the rest of the adoption information, the 'current' values are used, given in table 6.1. The corresponding profiles can be seen in figure 6.27 and figure 6.28.

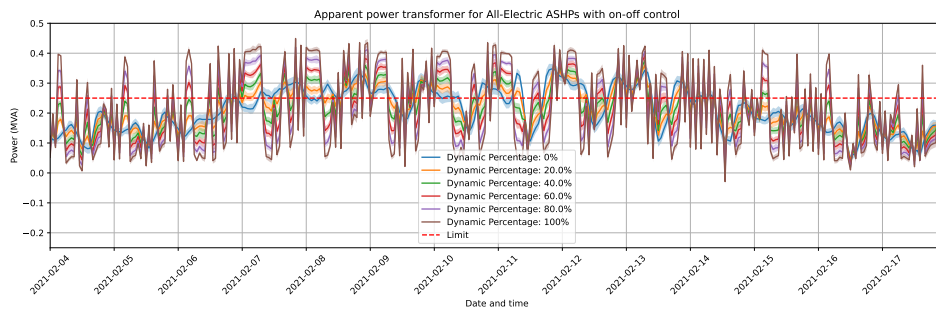


Figure 6.27: Apparent power through the transformer for 100% adoption of **All-Electric ASHPs** with **on-off** control with different percentages of dynamic contracts

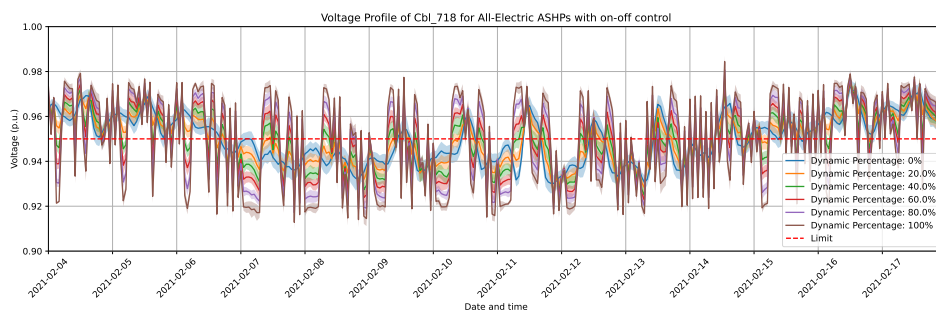


Figure 6.28: Voltage profile at CBL\_718 for 100% adoption **All-Electric ASHPs** with **on-off** control with different percentages of dynamic contracts

In these plots, you can see that an increasing part of the load is shifted to different times due to the price difference. This causes higher peak loads with an increasing amount of dynamic contract because of synchronisation of the electricity demand. This effect can be further seen in figure 6.29 for the maximum power through the transformer and in figure 6.30 for voltage violations.

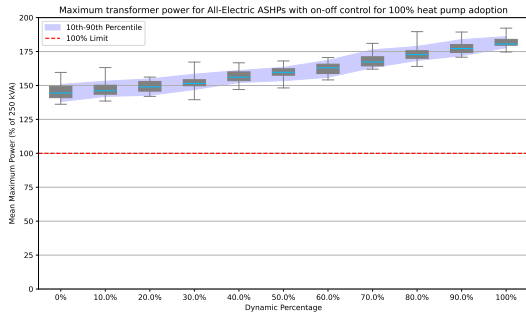


Figure 6.29: Maximum power through the transformer in percentage of the rated capacity for 30 runs per dynamic electricity tariff adoption rate for **All-Electric on-off ASHP**.

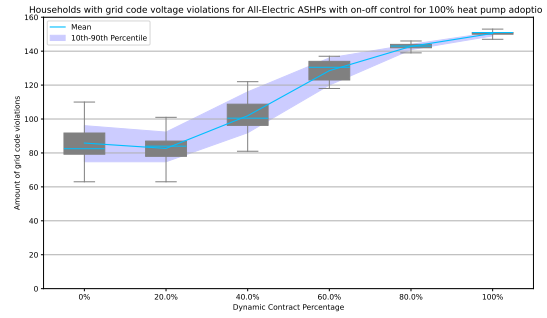


Figure 6.30: Amount of households with voltage grid code violations for 30 runs per dynamic electricity tariff adoption rate for **All-Electric on-off ASHP**.

The effect of dynamic contracts on the maximum power is quite small for the first 10% to 20%, but it increases with 25% for 100% dynamic contracts compared to 0%. The same trend can be seen in the number of voltage limit violations, where the effect is minimal up to 20%, but rises to 151 households for 100% dynamic contracts. Therefore, almost all of the 155 households will experience voltage limit violations by then. This is an increase of 83% compared to the absence of dynamic contracts.

After this, the influence of dynamic prices is also simulated for the current adoption rate of heat pumps of 16%. This is also done for the on-off control ASHP. The resulting power and voltage profiles at the farthest point are presented in figures 6.31 and 6.32. The maximum power and voltage problems plots are given in figures 6.33 and 6.34.

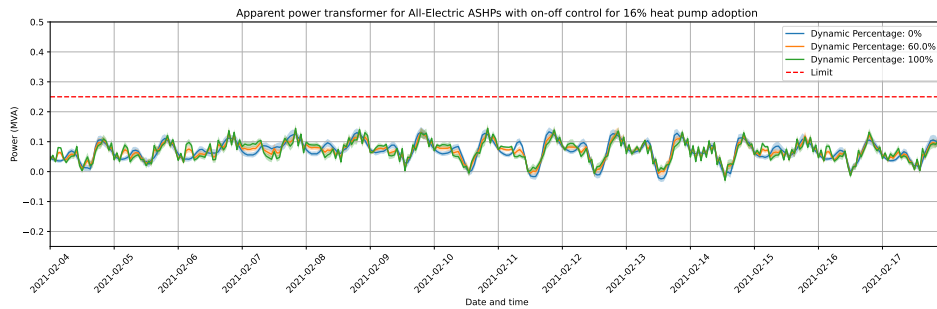


Figure 6.31: Apparent power through the transformer for 16 % adoption of **All-Electric ASHPs** with **on-off** control with different percentages of dynamic contracts

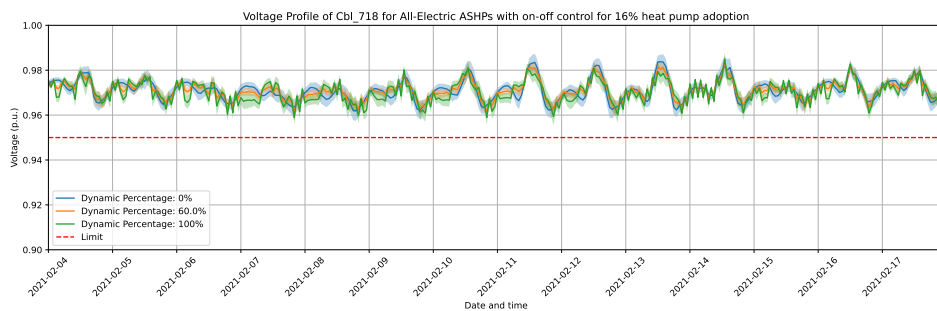


Figure 6.32: Voltage profile at CBL\_718 for 16 % adoption of **All-Electric ASHPs** with **on-off** control with different percentages of dynamic contracts

The graphs show that the influence of dynamic tariffs will not have a significant impact on both power and voltage at the current penetration rate of heat pumps and EV home chargers. This is also confirmed by the maximum power and number of voltage violations plots shown in figures 6.33 and 6.34.

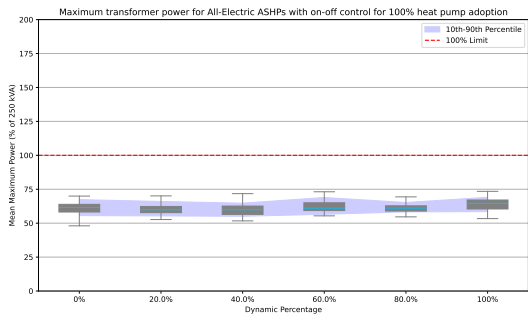


Figure 6.33: Maximum power through the transformer in percentage of the rated capacity per dynamic electricity tariff adoption rate for 16 % adoption of **All-Electric on-off ASHP**.

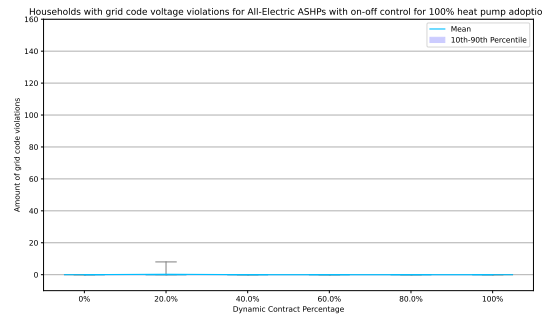


Figure 6.34: Amount of households with voltage grid code violations per dynamic electricity tariff adoption rate for 16 % adoption of **All-Electric on-off ASHP**.

Discussion

For the current adoption rate of EV home chargers and heat pumps, dynamic contracts have a minimal impact on the low-voltage grid for these simulations. When the neighbourhood has full adoption of ASHPs, dynamic contracts become a problem when more than 20% of households have one. However, the homes in the simulation have a fixed indoor temperature setpoint. This results in the heating demand being spread over the day. Households may change their set temperature during the day. For example, it is likely that many households will increase the temperature when they get home from work, which is usually around the same time for many people. Therefore, a peak in heat pump demand can be caused by this phenomenon. This can be partly counteracted by dynamic prices, as electricity prices are generally higher at times when many people come home from work, which shifts part of this peak to another time. Therefore, there may be some benefits of dynamic tariffs that are not taken into account in these simulations.

However, since dynamic tariffs can save consumers money, as noted in [46], the growth of this type of contract should be carefully monitored to ensure that its popularity does not become so large that it causes problems in the grid.

6.4. Influence of Domestic Hot Water Production

For the same type of heat pump (All-Electric ASHP with on-off control), an analysis is done on the effect of DHW production on power and voltage. The resulting graphs where the profiles with and without DHW are depicted can be found in figures 6.35 and 6.36.

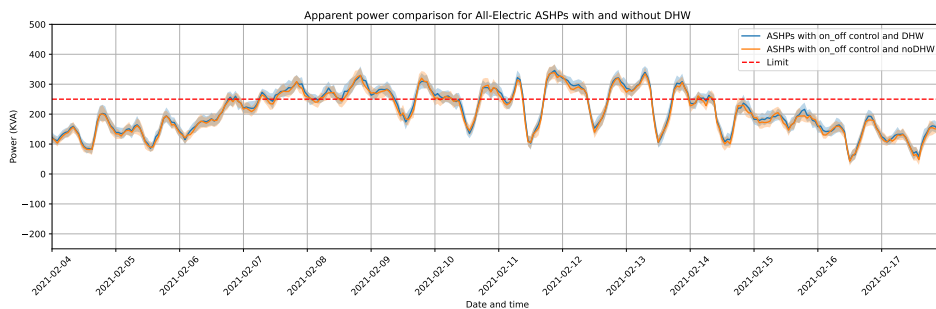


Figure 6.35: Apparent power through the transformer for All-Electric ASHPs with and without domestic hot water production.

Here, it can be seen that the effect is minimal and that DHW production causes a very slight increase in power and a dip in voltage because of the energy needed for it. Furthermore, there does not appear to be an effect on concurrency, which is further confirmed by a simulation in which only the demand for heat pumps is used, as depicted in figure 6.37, where the total power of 155 heat pumps during the simulation period was divided by the total rated power. Furthermore, the maximum power and voltage

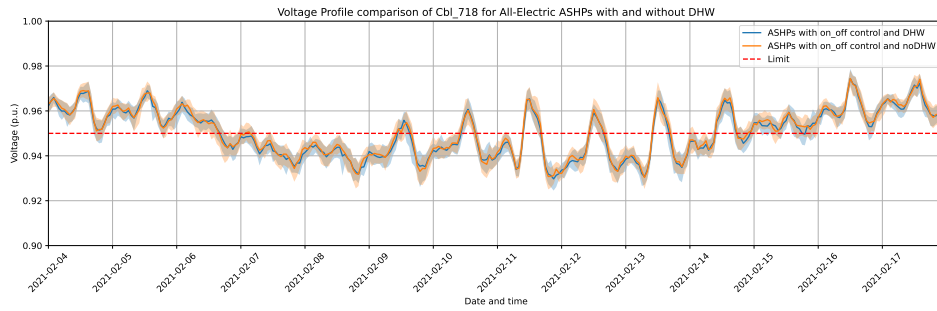


Figure 6.36: Voltage profile at CBL\_718 for All-Electric ASHPs with and without domestic hot water production.

violations for the case without DHW production are shown in figures 6.38 and 6.39.

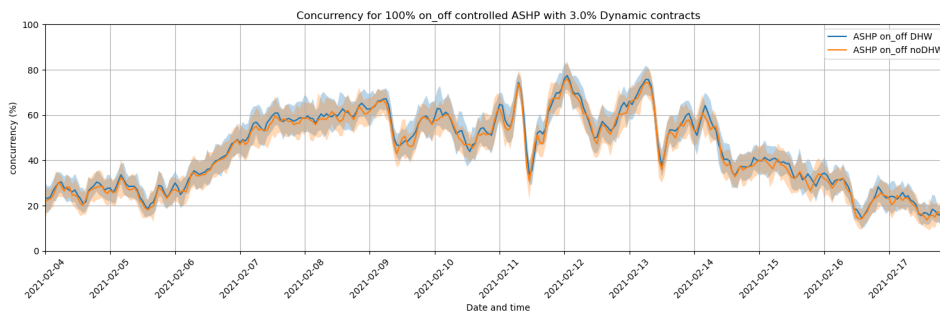


Figure 6.37: Concurrency for only heat pumps loads with and without domestic hot water production.

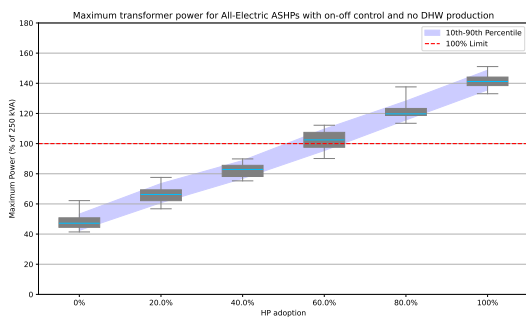


Figure 6.38: Maximum power through the transformer in percentage of the rated capacity for 30 runs per HP adoption rate for All-Electric on-off ASHP without DHW production.

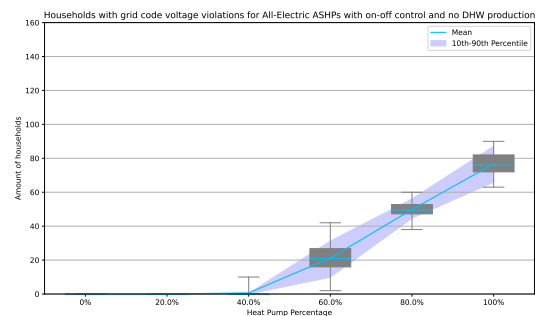


Figure 6.39: Amount of households with voltage grid code violations for 30 runs per HP adoption rate for All-Electric on-off ASHP without DHW production.

The median of the maximum power for the adoption rate 100% is slightly higher, at 2%, with domestic hot water production than without it. Voltage violations increase by 7% if DHW production is included for the same adoption rate.

### Discussion

At the beginning of this research, it was hypothesised that the production of domestic hot water could cause a drop in concurrency. The heat pumps could be synchronised due to the same temperature variations experienced by all, and individual pumps demand for domestic hot water could disrupt this synchronisation. However, as these results show, domestic hot water production does not reduce concurrency and increases the maximum power only slightly. This increase can be considered insignificant.

## 6.5. Scenarios

Three different scenarios are now simulated for two years in the future. The first 'natural growth' scenario is the authors' expectation of the mix of heat pump types in 2030 and 2050 if no electric backup heating is installed in the heat pump, the second 'natural growth with electric backup heating' scenario takes into account that a portion of these heat pumps have electric backup heating, and the third 'GSHP ready' scenario is chosen where either a source network is built in the neighbourhood where everyone can connect, or many people decide to drill their own source for a GSHP. These scenarios are shown in the table 6.2, where the percentages represent the mix of heat pumps in this scenario. This means that with a heat pump penetration rate of 50%, 35% of these heat pumps in 2030 for the natural growth scenario will be gas hybrid, totalling 27 gas hybrid heat pumps for 155 households. An adoption rate of 100% is assumed for all 2050 scenarios, as the aim of this work is to look at the effect of a whole neighbourhood switching to a heat pump. The rest of the adoption information is already given in table 6.1 on page 33. Public EV charging is also assumed to have a smart charging profile in 2030 and 2050, where all public EV chargers are assigned one of the static smart charging profiles of the Elaad profile generator [17]. Due to time limitations, the scenarios are only simulated for modulating control. Since this type of control is more energy efficient [4], it is assumed that this will be the dominant technology in the future. Finally, the same data is used for non-flexible load, EV home charging, PV production, outdoor temperature, and domestic hot water demand as for the "current" simulations.

Table 6.2: The mix of heat pumps in the future scenarios

Scenarios	2030	2050
Natural Growth	35% gas-hybrid ASHP 65% all-electric ASHP	100% all-electric ASHP
Natural Growth with Electric Auxiliary Heating	35% Gas-Hybrid ASHP 65% Electric Resistive Hybrid ASHP	65% Electric Resistive Hybrid ASHP 35% All-Electric ASHP
GSHP Ready	15% gas-hybrid ASHP 15% All-Electric ASHP 70% GSHP	100% GSHP

### 6.5.1. Scenarios for 2030

In 2030, it is assumed that the percentage of households with a PV system has increased to 45%, 5.7% of households have an EV home charger, 10% have a dynamic energy contract, 14 public EV charging points are available and 24% of households have a heat pump.

#### Natural growth

In this scenario, a mix of All-Electric and Gas-Hybrid ASHPs is present in the neighbourhood, which results in the power and voltage profiles shown in figures 6.40 and 6.41.

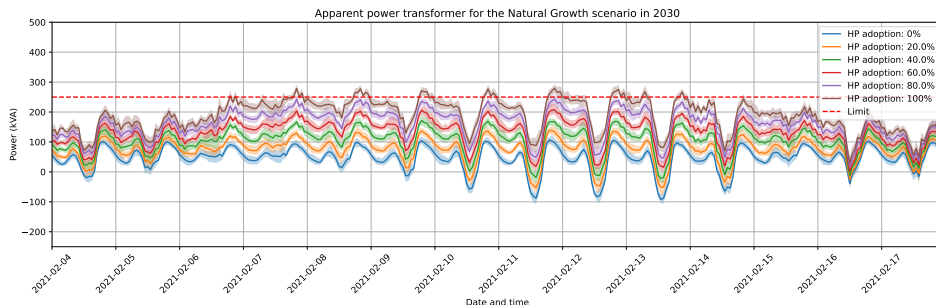


Figure 6.40: Apparent power through the transformer for a mix of 65% **All-Electric ASHPs** and 35% **Gas-Hybrid ASHPs** in 2030

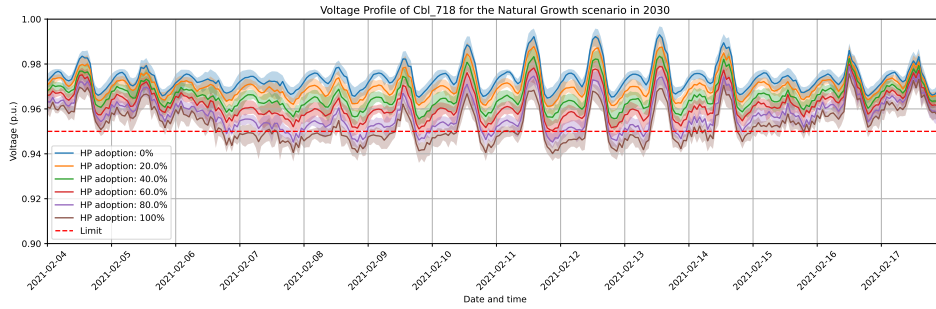


Figure 6.41: Voltage profile at CBL\_718 for a mix of 65% **All-Electric ASHPs** and 35% **Gas-Hybrid ASHPs** in 2030

These profiles show that the power and voltage limits are only exceeded at higher heat pump penetration rates. This is further confirmed by the graphs of maximum power and voltage limit violations in figures 6.42 and 6.43.

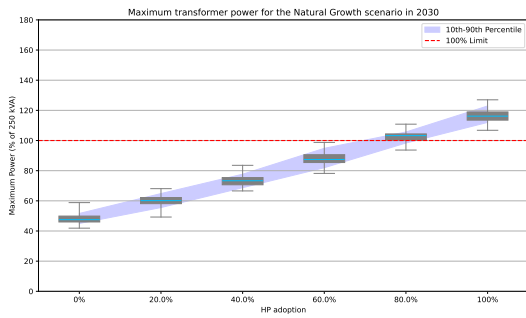


Figure 6.42: Maximum power through the transformer in percentage of the rated capacity for a mix of 65% **All-Electric ASHPs** and 35% **Gas-Hybrid ASHPs** in 2030

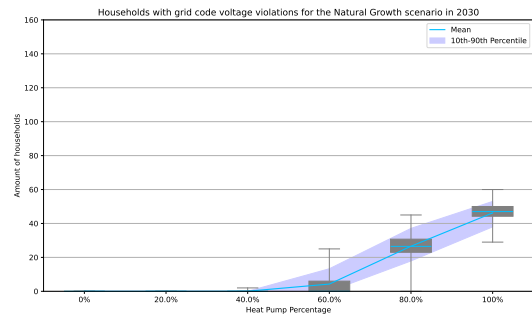


Figure 6.43: Amount of households with voltage grid code violations for a mix of 65% **All-Electric ASHPs** and 35% **Gas-Hybrid ASHPs** in 2030

It can be seen that voltage limit problems only occur from a 40% adoption rate, and overloading problems only occur from more than 60%. As the expected penetration rate of heat pumps in 2030 is 24%, this scenario is not expected to cause any problems for the low-voltage grid.

### Natural growth with Electric Auxiliary Heating

In this scenario, a similar mix of ASHPs is present as in the natural growth scenario. However, all of the All-Electric ASHPs have been changed to Electric-Resistive Hybrid ASHPs. This results in the power and voltage profiles shown in figures 6.44 and 6.45.

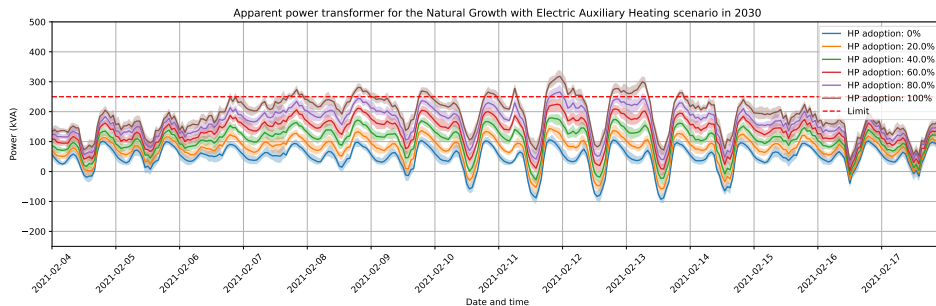


Figure 6.44: Apparent power through the transformer for a mix of 65% **Electric-Resistive Hybrid ASHPs** and 35% **Gas-Hybrid ASHPs** in 2030

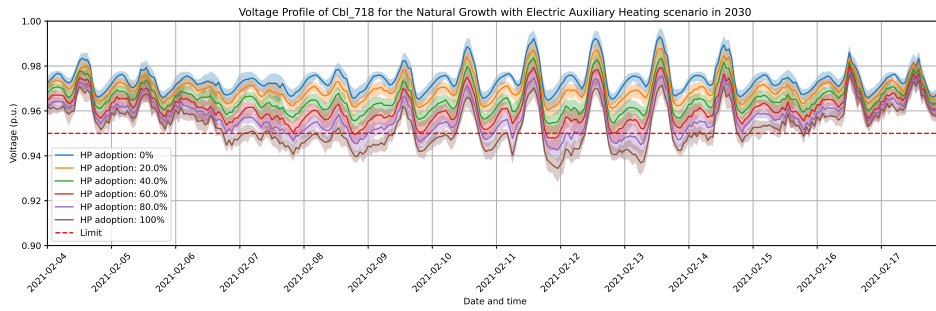


Figure 6.45: Voltage profile at CBL\_718 for a mix of 65% **Electric-Resistive Hybrid ASHPs** and 35% **Gas-Hybrid ASHPs** in 2030

Compared to the profiles for the natural growth scenario without electric backup heating, these profiles exceed the limits slightly earlier. The figures 6.46 and 6.47 give a better idea of this.

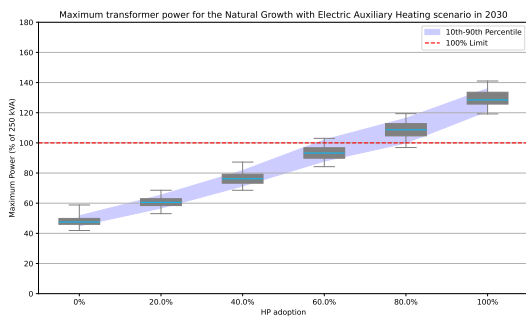


Figure 6.46: Maximum power through the transformer in percentage of the rated capacity for a mix of 65% **Electric-Resistive Hybrid ASHPs** and 35% **Gas-Hybrid ASHPs** in 2030

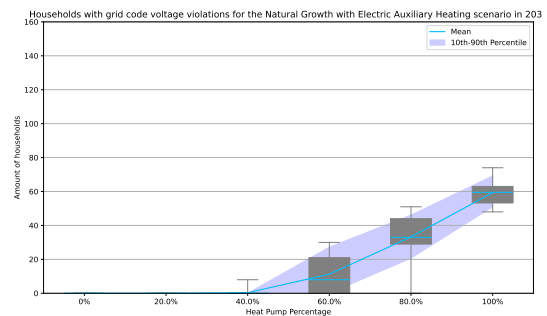


Figure 6.47: Amount of households with voltage grid code violations for a mix of 65% **Electric-Resistive Hybrid ASHPs** and 35% **Gas-Hybrid ASHPs** in 2030

Although overload and voltage problems occur at a lower penetration rate of heat pumps than in the natural growth scenario without electric backup heating, they still do not occur at the expected penetration rate of 24%. This means that this scenario for 2030 is not expected to cause any problems for the low-voltage grid.

**GSHP Ready**

In this scenario, many households choose to install an GSHP. This results in a mix of 70% all-electric GSHPs with 15% all-electric ASHPs and 15% gas-hybrid ASHPs. This results in the following power and voltage profiles in figures 6.48 and 6.49.

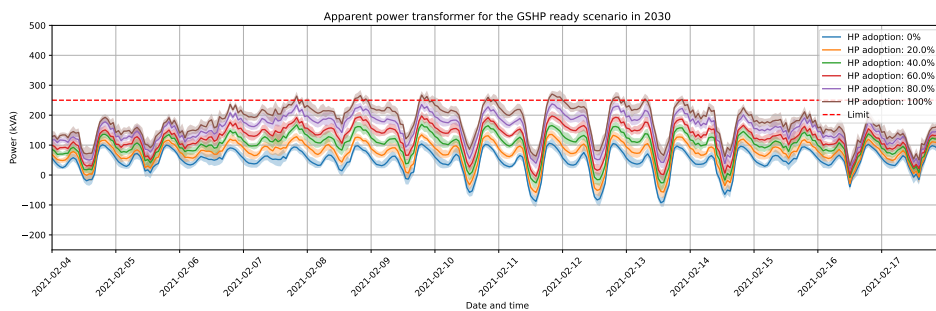


Figure 6.48: Apparent power through the transformer for a mix of 70% **All-Electric GSHPs**, 15% **All-Electric ASHPs** and 15% **Gas-Hybrid ASHPs** in 2030

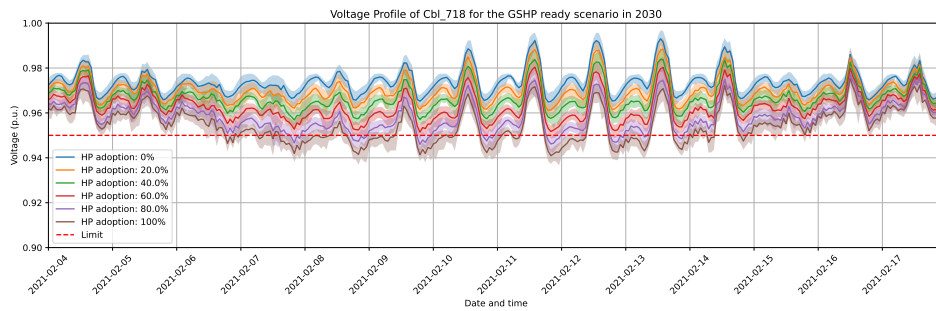


Figure 6.49: Voltage profile at CBL\_718 for a mix of 70% **All-Electric GSHPs**, 15% **All-Electric ASHPs** and 15% **Gas-Hybrid ASHPs** in 2030

The power limit is barely exceeded in this profile, and the voltage limit is only exceeded at 80% and 100% heat pump adoption. These limits are further examined in figure 6.50 and 6.51, where the maximum power and voltage limit violations are plotted.

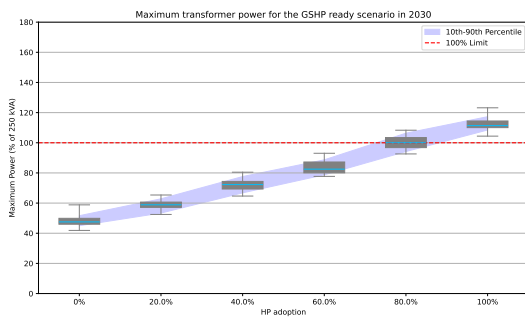


Figure 6.50: Maximum power through the transformer in percentage of the rated capacity for a mix of 70% **All-Electric GSHPs**, 15% **All-Electric ASHPs** and 15% **Gas-Hybrid ASHPs** in 2030

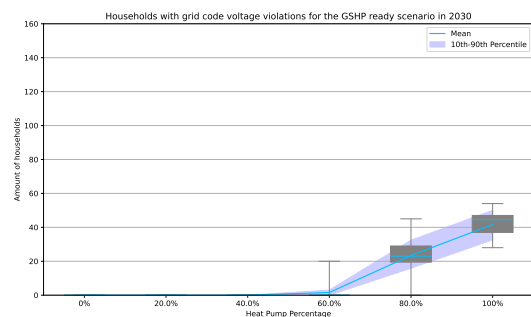


Figure 6.51: Amount of households with voltage grid code violations for a mix of 70% **All-Electric GSHPs**, 15% **All-Electric ASHPs** and 15% **Gas-Hybrid ASHPs** in 2030

It can be seen that the overload and voltage limits are exceeded later than in the first two scenarios. This means that also in this scenario there will be no grid limit problems in 2030.

### Discussion of 2030 scenarios

These simulations for the 2030 scenarios show that with the predicted number of heat pumps, grid limit problems are not expected to occur by 2030. As most low-voltage grids will not be upgraded by 2030, each scenario presented here is feasible for that year.

## 6.5.2. Scenarios for 2050

By 2050, 85% of households are expected to have a PV system. In addition, 15.6% have an EV home charger, 30% have a dynamic energy contract, and everyone has a heat pump. There are also 31 public EV charging points in the neighbourhood.

### Natural growth

For 2050, the other loads are present in larger amounts, as well as the amount of dynamic energy contract compared to 2030. The results can be seen in figures 6.52 and 6.53.

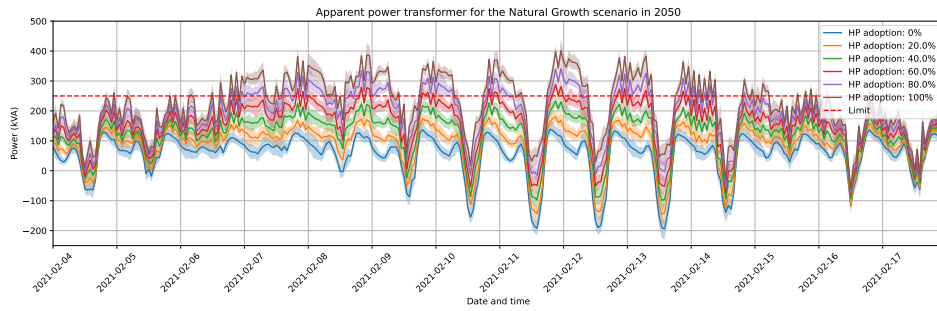


Figure 6.52: Apparent power through the transformer for 100% All-Electric ASHPs in 2050

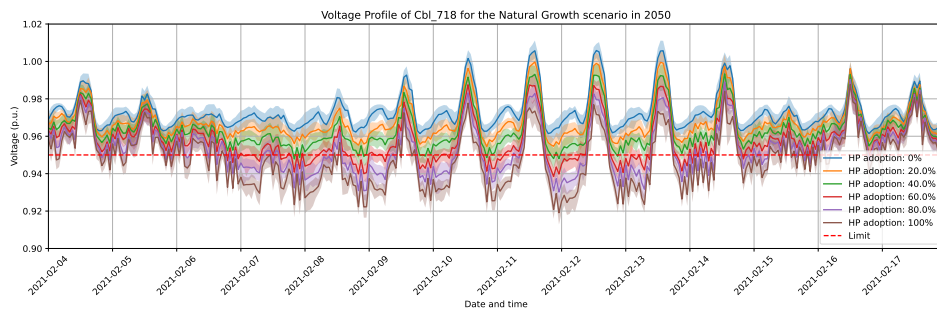


Figure 6.53: Voltage profile at CBL\_718 for 100% All-Electric ASHPs in 2050

The voltage limits are exceeded earlier than for the 2030 case, which is to be expected with these increased loads. In addition, the voltage peaks are also higher than for 2030. This can be explained by the high number of solar systems in the neighbourhood. In the power profile, the sharper drops and peaks can be seen, which are also present in the higher dynamic tariff profiles in section 6.3. Looking at figures 6.54 and 6.55, the maximum power and voltage limit violation plots can be seen.

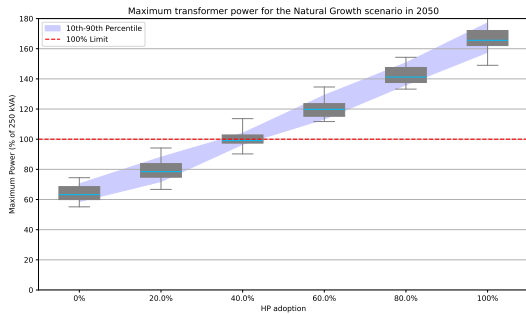


Figure 6.54: Maximum power through the transformer in percentage of the rated capacity for 100% All-Electric ASHPs in 2050

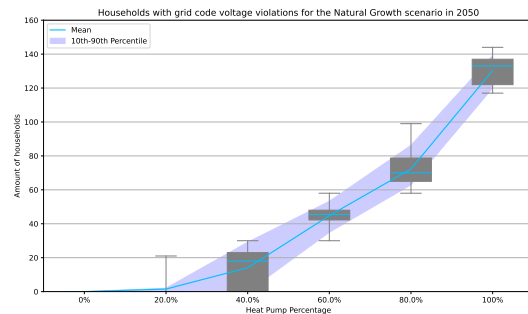


Figure 6.55: Amount of households with voltage grid code violations for 100% All-Electric ASHPs in 2050

First, the increased non-heat pump loads are clearly visible here for 0% heat pump adoption. The median of the maximum power here increases with 34% from 47% to 63% of the rated capacity. Furthermore, these graphs show that the limits are exceeded by about 40% for both overload and voltage limit problems. For 100% heat pump adoption, the median of the maximum power through the transformer is 166%. Assuming that everyone has a heat pump this year, the current grid will not be able to cope with this number of heat pumps without upgrades.

Natural growth with Electric Auxiliary Heating

For 2050, the natural growth scenario is also simulated with electric backup heating. The resulting power and voltage profiles are shown in figures 6.56 and 6.57.

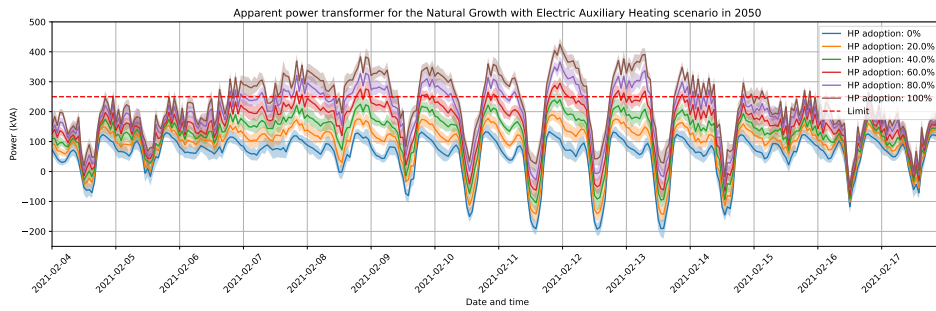


Figure 6.56: Apparent power through the transformer for a mix of 65% **Electric-Resistive Hybrid ASHPs** and 35% **All-Electric ASHPs** in 2050

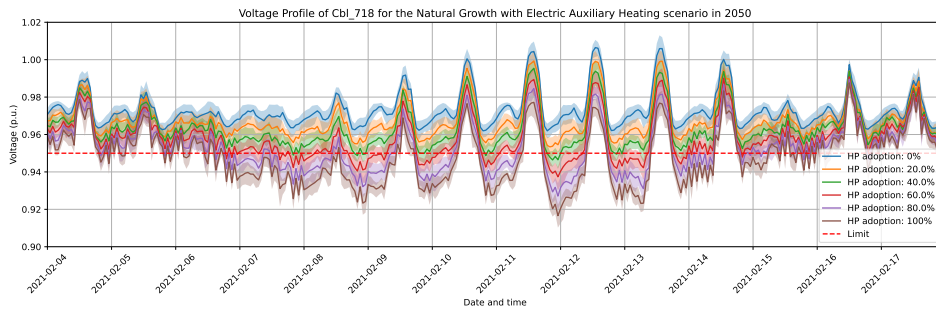


Figure 6.57: Voltage profile at CBL\_718 for a mix of 65% **Electric-Resistive Hybrid ASHPs** and 35% **All-Electric ASHPs** in 2050

The differences between natural growth and this scenario are harder to see in these profiles. However, the effect of electric backup heating can be seen during the power peaks around 12 and 13 February, where the peak is higher with electric backup heating. This effect can also be seen for the voltage profile, with lower voltage drops on these days. The maximum power and voltage limit violation plots in figures 6.58 and 6.59 can be further examined to better classify the differences.

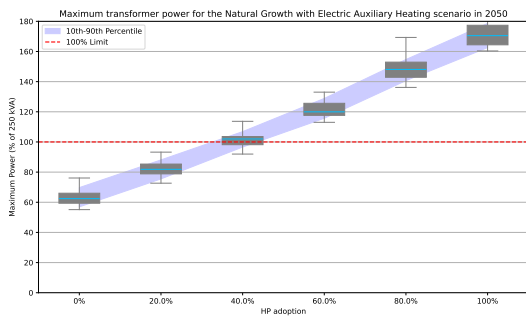


Figure 6.58: Maximum power through the transformer in percentage of the rated capacity for a mix of 65% **Electric-Resistive Hybrid ASHPs** and 35% **All-Electric ASHPs** in 2050

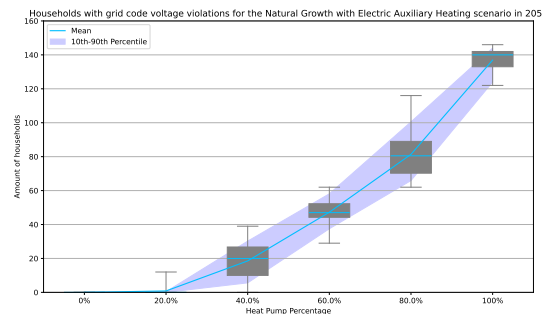


Figure 6.59: Amount of households with voltage grid code violations for a mix of 65% **Electric-Resistive Hybrid ASHPs** and 35% **All-Electric ASHPs** in 2050

As in the natural growth scenario without electric backup heating, the limits for both voltage and overload are long exceeded for a 100% heat pump penetration rate. The median of the maximum power for 100%

is slightly higher here at 170%, an increase of 2%. This means that this scenario will also cause serious problems in the low-voltage grid if it is not upgraded.

### GSHP Ready

In this scenario all households have a GSHP installed. The power profile of the transformer and the voltage profile of the farthest household from the transformer are shown in figures 6.60 and 6.61.

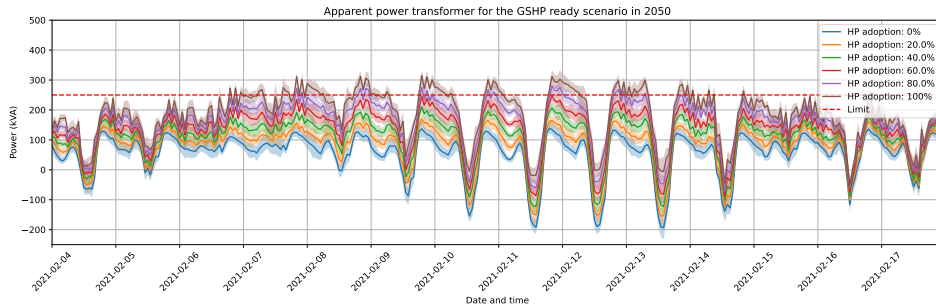


Figure 6.60: Apparent power through the transformer for 100% All-Electric GSHPs in 2050

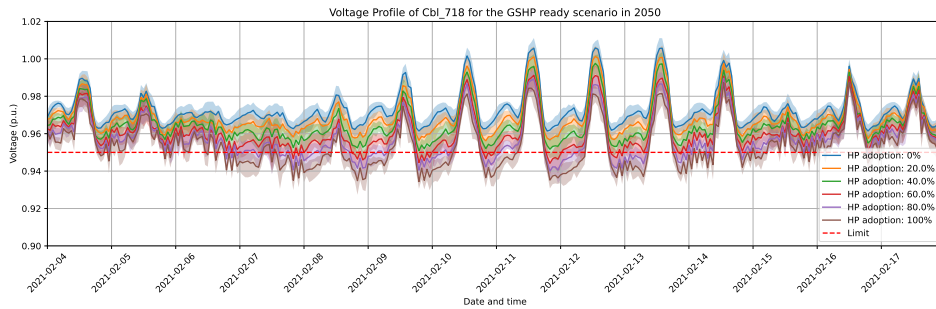


Figure 6.61: Voltage profile at CBL\_718 for 100% All-Electric GSHPs in 2050

The better COP of GSHPs at colder temperatures is clearly visible in these two profiles. In the ASHP scenarios, the limits were exceeded with higher peaks and longer overloading duration compared to those of the GSHP-ready scenario. The duration of voltage drop below the limit is comparable but less severe for the GSHP ready scenario. In addition to these profiles, the maximum power and voltage limit violation plots are shown in figures 6.62 and 6.63.

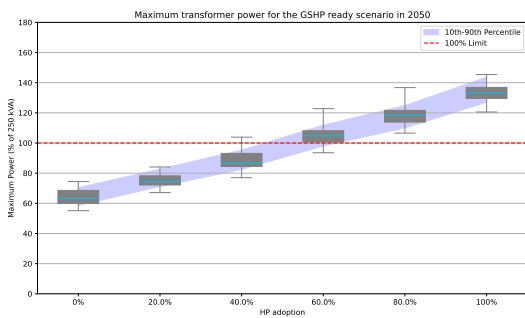


Figure 6.62: Maximum power through the transformer in percentage of the rated capacity for 100% All-Electric GSHPs in 2050

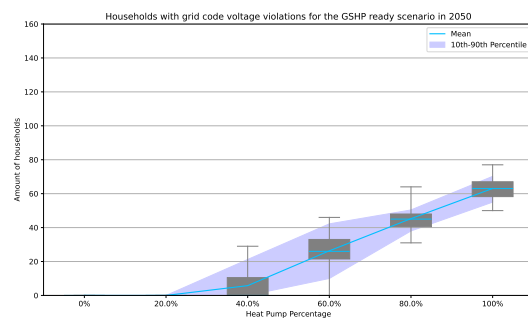


Figure 6.63: Amount of households with voltage grid code violations for 100% All-Electric GSHPs in 2050

Like the natural growth scenarios, voltage limit problems already occur at 40% heat pump adoption.

In the GSHP ready scenario, power limits are generally exceeded at a heat pump adoption rate of 50%, compared to 40% for the ASHP scenarios. This means that at 100% heat pump adoption, the maximum power limits of the transformer will be exceeded.

Overload energy and duration of the 2050 scenarios

As the transformer is overloaded in each of these scenarios, it may be interesting to investigate this overload more closely. The problem with overloading a transformer is usually the overheating of this component [47]. As transformers have a high thermal mass, a small and short overload peak may not cause significant wear or failure. With this in mind, the duration and energy of the overload are examined. Therefore, additional plots of the energy through the transformer above the limit (the area of apparent power above the limit) are shown in figures 6.64, 6.66 and 6.68. Next to these, the total duration of overloading of the transformer in percentages of the total simulation time is plotted in figures 6.65, 6.67 and 6.69. More plots on the overloading energy and duration of the rest of the simulation can be found in Appendix B.3 and B.4.

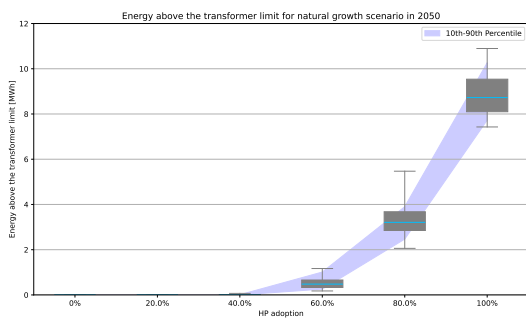


Figure 6.64: Energy above transformer limit for 100% **All-Electric ASHPs** in 2050

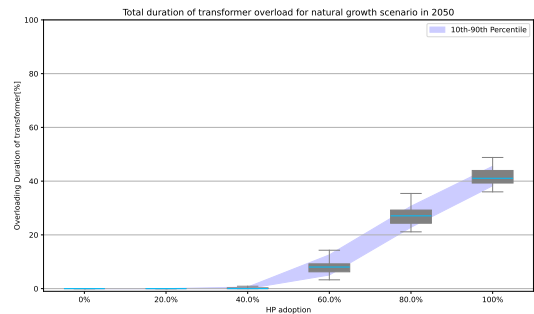


Figure 6.65: Total duration of overloading in percentage of total simulation time for 100% **All-Electric ASHPs** in 2050

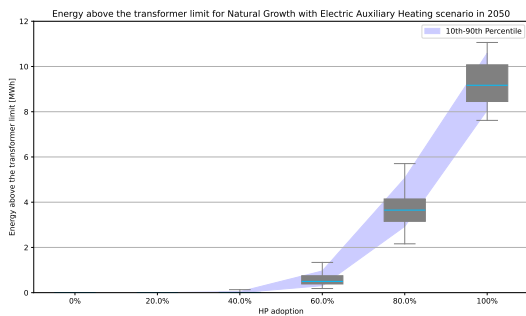


Figure 6.66: Energy above transformer limit for a mix of 65% **Electric-Resistive Hybrid ASHPs** and 35% **All-Electric ASHPs** in 2050

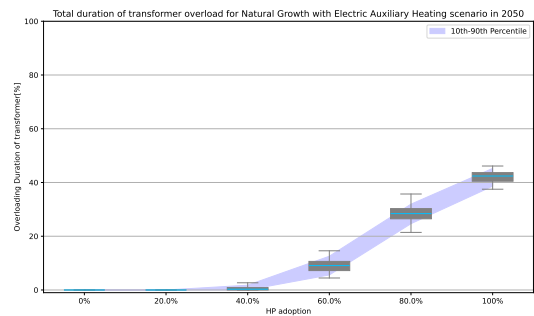


Figure 6.67: Total duration of overloading in percentage of total simulation time for a mix of 65% **Electric-Resistive Hybrid ASHPs** and 35% **All-Electric ASHPs** in 2050

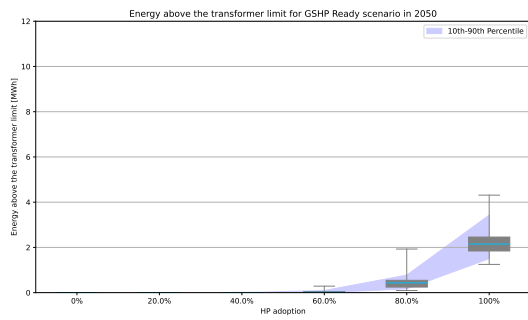


Figure 6.68: Energy above transformer limit for 100% **All-Electric GSHPs** in 2050

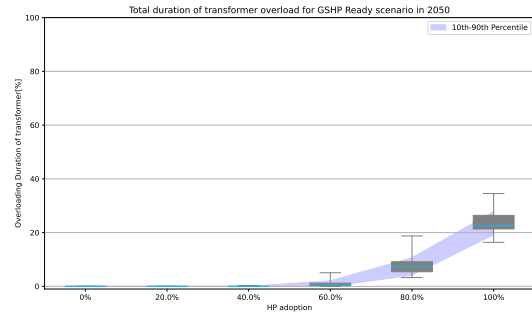


Figure 6.69: Total duration of overloading in percentage of total simulation time for 100% **All-Electric GSHPs** in 2050

These plots show that for the GSHP ready scenario, the duration of the overload for a 100% HP adoption rate is about half that of the natural growth scenarios. The energy above the transformer limit for the GSHP ready scenario is about a quarter of the natural growth scenarios for 100% adoption.

### Discussion of 2050 scenarios

In every scenario for 2050, the limits of the low-voltage grid are exceeded before the 100% penetration rate is reached. However, the overload peaks are lower and shorter for the GSHP ready than for the natural growth scenarios. The energy through the transformer above the limit is also significantly lower for the GSHP ready scenario compared to the natural growth scenarios. It may be possible that the transformer is able to cope with these smaller and shorter overload peaks in the GSHP ready scenario, especially as this maximum overload occurs at the coldest outdoor temperatures, which improves the cooling of the transformer. However, this depends on how the transformer overheats due to temporary overloading, which is outside the scope of this thesis. Therefore, it might be interesting to take this into account in a further study to see if the GSHP ready scenario is feasible without grid upgrades.

For one of the natural growth scenarios, it is recommended that this grid be upgraded to be able to handle these higher power peaks and voltage fluctuations. As this scenario is for 2050, it is likely that grid upgrades will be possible before this scenario takes place. The option to push for a GSHP ready scenario can ensure that the grid limits are reached a little later. This may provide some time for the DSOs to upgrade the grid in this neighbourhood if the upgrade capacity of these companies is not sufficient.

# 7

## Discussion

In this chapter, the results are discussed in more detail. First, the difference between power and voltage problems is discussed. The socio-economic implications are then considered, and finally, the limitations of this research are addressed.

### 7.1. Voltage problems vs power limitations

Voltage problems may not be as big a problem as power problems. Unlike the amount of power through the transformer, the voltage level can be adjusted by changing the transformer's turning ratio, thereby increasing the voltage on the LV grid. Since voltage problems during the simulated week only concern undervoltage, increasing the overall voltage in the network can reduce the time during which problematic undervoltages occur. However, changing the turning ratio to cause an increase in voltage should be a temporary solution for, say, the coldest weeks of the year, as [14] has found that overvoltage problems occur at different times of the year. Therefore, changing this ratio should be convenient enough to do it several times a year. Furthermore, a study by [53] has developed an adaptive voltage control policy for high-to-medium voltage transformers to minimise voltage limit violations on medium and low voltage grids, which proved to be effective. This improved voltage regulation reduces the need for MV/LV transformers to compensate for voltage deviations.

### 7.2. Socio-Economic Impact

In view of the heat transition that the Netherlands is currently going through, this research may have an impact on the ongoing discussion in government institutions about which alternative heating solution to natural gas should be chosen. This discussion is now often held between high- or medium-temperature district heating or air source heat pumps, and often high- or medium-temperature district heating is chosen because of the uncertainty of overloading the grid with the mass introduction of heat pumps. This research reduces this uncertainty by analysing what happens to a low-voltage grid when a neighbourhood opts for heat pumps. The results of the scenarios suggest that it may be possible to upgrade the grid in time before the grid limits are exceeded.

It also provides guidance on the options for heat pumps. More information is provided about the impact of ASHPs versus GSHPs and the effect of electric-resistive and gas hybrid heat pumps. These insights can be used to further tighten the restrictions on heat pump subsidies and to push for solutions with a lower impact on the grid.

If this uncertainty about the impact of heat pumps on the grid is reduced, government institutions may select more neighbourhoods suitable for heat pumps and fewer for high-temperature district heating. Currently, there is a negative sentiment towards district heating in the Netherlands due to the high energy and standing charges and the monopoly position of its suppliers. Therefore, a shift towards a

more individual transition to sustainable heat with a personal choice of energy supplier could convince more residents to participate in the energy transition.

If the authorities decide to use heat pumps in a neighbourhood, further (economic) research on the local situation will have to decide whether air source heat pumps, with their extra grid impact and associated costs, or ground source heat pumps, with their extra costs for wells or source networks, are best suited to a neighbourhood.

Finally, this study investigates the impact of the emergence of the dynamic electricity contract. Although it may be cheaper for consumers and the impact on the grid seems manageable at low adoption rates, its impact on the grid at high adoption rates may be more expensive in terms of collective costs in the form of grid congestion and upgrades than it saves consumers.

### 7.3. Limitations

Due to the fact that this thesis focuses on a specific grid, the limits at which the network experiences overload or voltage problems cannot be generalised to all low-voltage networks. However, the differences between the different types of heat pumps in terms of overload and voltage problems are relevant to all low-voltage networks. This also means that the scenarios simulated in this thesis may lead to different results for other low-voltage grids, where grid problems may occur earlier or later. In addition, the simulation is done only for two specific weeks in winter. This means that other effects on the grid impact, like cooling, are not taken into account here.

Furthermore, because the grid code imposes voltage problems in 10-minute resolution instead of the 1-hour resolution simulated in this thesis, it may also result in some differences in the actual problematic voltage level between the simulation and reality.

This thesis assumes that each household has the same installed capacity and production profile. In reality, however, each household's production profile will be different due to different shading effects and clouds moving across the neighbourhood. Additionally, the installed capacity will vary from household to household and is likely to increase in the coming decades as the price of solar systems falls. So, the fixed capacity assumption for the future scenarios underestimates PV electricity production.

Another aspect that is likely to influence future scenarios is dynamic tariffs. The prices used in this thesis are from 2021, when there were very few households with dynamic contracts. In the future, this amount could increase to a point where it will influence the price determination of the day-ahead market, resulting in a feedback loop. Besides this, the proportion of electricity generated by wind turbines will increase significantly in the coming decades, changing the periods of cheap electricity. These moments are now often associated with high solar production, but that does not always coincide with high wind production, so moments of cheap electricity will increasingly occur at different times of the day. This can put extra strain on the grid if, for example, these times coincide with a period of high demand, such as the beginning of the evening.

In addition, the data on charging sessions available for this thesis only included one week and was later sequenced. As a result, there is an artificial gap between weeks where, in reality, cars are plugged in, but in the simulation, they are not. Furthermore, in this research, the assumption was made that cars are to be fully charged each charging session. In reality, cars will sometimes be partially charged, especially when electricity prices are high.

Houses in the Netherlands that are heated with natural gas usually also use gas for cooking. If households stop using natural gas for heating, they will likely also switch to electricity for cooking. Therefore, there is an additional electricity load for these households, but this load is not taken into account in this study.

There is some uncertainty about the accuracy of the thermal model. Although the spread of heat loss and thermal mass reduces the importance of accuracy, the model is theoretical and not based on or validated on a real house. In addition, heat losses such as opening doors and windows, losses to the ground, and heat gains from appliances, occupants, and solar radiation are not taken into account. As a result, there could be some under- or overestimation of the thermal needs of the houses.

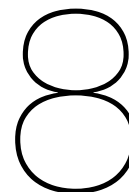
Furthermore, in reality, the control sequences are based on the measured internal temperature in combination with the return temperature of the water in the heat distribution system. The latter is not simulated in this study, so the influences of the internal heat distribution system of the house are not taken into account.

Moreover, this thesis calculates the heat loss in the houses and assumes that it is known in order to optimise the heat pump output. In reality, the heat pump does not know the exact thermal behaviour of the house and will make prediction errors, resulting in higher power consumption.

The assumption that a household will keep the set temperature of the house constant throughout the week can lead to lower concurrency than in reality. Households may lower their setpoint temperature when they are away or asleep and increase it when they return. This time of raising the setpoint can increase concurrency, as many people will come home around the same time, which can increase the peak power in the grid due to heat pumps.

To prevent the formation of legionella in the hot water tank, the water in these tanks is usually heated to at least 60°C once a week. This is called the anti-legionella cycle and is often done with an electric resistance heater. Although this process can have a high energy demand for a short period of time, it is assumed that the concurrency of this process is low and is therefore not included in this study.

Finally, the formula for calculating the COP is based on older heat pump data from up to 2019. This means that more recent improvements in technology are not included in this formula. Also, based on conversations Stedin has had with people in the industry, this particular formula overestimates the COP at lower temperatures below freezing. Therefore, the effect on overload and voltage problems may be underestimated in these simulations. More recent COP fits, such as the one used in [51], can be used to improve this limitation.



# Conclusion and Recommendations

This study aimed to analyse the impact of heat pump penetration on the low-voltage grid for future winter scenarios by looking at transformer overloading and undervoltage problems. This was done by using PowerFactory to simulate a real Dutch low-voltage grid and including loads for non-flexible consumption, public and private electric vehicle chargers, different types of heat pumps, and photovoltaic systems. The influence of dynamic energy prices and domestic hot water production on the grid impact is also investigated. This chapter will first give the conclusions of this research and then provide recommendations for further research and for distribution system operators and the government.

## 8.1. Conclusion

To answer the first research question, *What is the impact of different types of heat pumps on local grid constraints?*, the grid impact of air- and ground-source heat pumps, modulating and on-off control mechanisms and hybrid systems was analysed. It was found that air-source heat pumps have a significantly higher impact on transformer overload and voltage limit problems than ground-source heat pumps. This is caused by the higher efficiencies at lower ambient temperatures of ground-source heat pumps compared to air-source heat pumps. Furthermore, modulating heat pumps were found to cause slightly less transformer overload and voltage limit problems than on-off controlled heat pumps.

For the hybrid heat pump systems, where only air-source heat pumps are considered, this research concludes that gas-hybrid systems almost never cause transformer overload or voltage limit problems for the specific low-voltage grid simulated and the transformer loading was significantly lower than for all-electric air source heat pumps.

However, the heat pump with the electric resistive backup caused significant additional transformer overload and voltage limitation problems compared to all electric air-source heat pumps. This was due to the significant additional power demand of the resistive element, which kicked in when the ambient temperature became too low for the heat pump alone to provide all the heating. The resistive element provides heat at an efficiency much lower than that of the heat pump.

To further investigate the impact of heat pumps, three different scenarios were simulated for the years 2030 and 2050. The first scenario had a mix of all-electric and gas-hybrid heat pumps, and it was found that for 2030, no grid constraint issues are expected with the predicted heat pump penetration. However, by 2050, the grid constraints will be significantly exceeded, and grid upgrades will be required to facilitate this scenario for this specific grid.

The second scenario is also a mix of all-electric and gas hybrid heat pumps, but electric resistance backup heating is included in parts of the all-electric heat pump. This scenario has similar results to the first, with no problems expected for 2030, but the current grid infrastructure will not be sufficient for 2050.

The final scenario included a push for ground-source heat pumps, with a mix of all-electric and gas-

hybrid air source heat pumps together with all-electric ground source heat pumps in 2030. In 2030, no grid problems were expected for the predicted amount of heat pumps. In the 2050 scenario, it was assumed that every household had switched to a ground source heat pump. This resulted in grid constraints being exceeded, but to a much lesser extent than in the first two scenarios. The transformer may be able to cope with these smaller overload peaks, but this needs to be investigated in further research.

The second research question, *How do dynamic energy prices influence the impact on local grid constraints caused by heat pumps and home electric vehicle chargers?*, was answered by simulating different adoption rates of dynamic energy contracts. It was found that for the current penetration rate of heat pumps and home electric vehicle chargers, no problems are expected with the high consumer adoption of dynamic energy price contracts. However, if neighbourhoods switch completely to heat pumps, it is expected that grid constraint problems will increase significantly with more than 20% of households adopting dynamic energy contracts.

Finally, for the third research question, *How does the presence of domestic hot water production influence the impact on local grid constraints?*, it was hypothesised that the random nature of domestic hot water use could reduce the concurrency of heat pumps. However, this was not found to be the case. The transformer overload and voltage limit problems increased slightly when domestic hot water was included in the heat pump electricity demand. This was due to the extra energy required to heat this water.

## 8.2. Recommendations for future work

Although this work can give a general idea of when heat pumps will cause problems for a low voltage network, it is based only on one specific network. It is therefore recommended that future research extends this type of analysis to a variety of low-voltage networks, including other types of neighbourhoods. The simulation period can also be extended from 2 winter weeks to a full year to include other seasonal effects. For that period, cooling demand can also be implemented in the simulation.

To further improve the analysis in this study, future research can look at different solar systems and the production profiles of each system on the houses. This can make the solar production estimate more realistic. In addition, data on electric vehicle charging sessions that is longer than one week will remove the artificial appearance of limited charging during the weekend between the weeks. Furthermore, charging sessions in which some electric vehicles do not want to be fully charged also increase the realism of the simulation. As mentioned in section 7.3, limitations, the COP calculations in this thesis may be overestimated at lower temperatures. Another COP fitting formula, for example, a more recent one, can be used in future research to improve accuracy, such as the curve used in [51].

Regarding the thermal part of the simulation, the temperature of the heat distribution system could be included in the model to have a more realistic simulation of the control mechanisms. In addition, a thermal model of the houses, validated with measured data from real Dutch houses, will further improve the accuracy of the simulation. Also, heat gains from appliances, occupants, and solar radiation could be included.

Though not included in this study, the introduction of energy storage systems can further extend the analysis. Storage systems in the form of heat or electricity can make intelligent use of changing electricity prices. This can lead to a reduction in peak demand, but also to a significant increase in peak demand. With the end of the net metering ('salderingsregeling') scheme, optimising the use of self-produced solar energy will become more important. Therefore, this type of optimisation, optionally with a battery, may be interesting to include in future research.

Variable capacity tariffs do not currently exist on the Dutch grid, but may become relevant in the future. Therefore, these types of tariffs can be added to the dynamic energy price optimisation to see their impact on the grid.

In this thesis, overload problems are measured with a fixed transformer power rating. Looking at the thermal capacities of the transformer, for example, with a thermal model, one can better predict if the overload of the transformer is really problematic. Therefore, this is recommended to better estimate

whether the grid limits are actually exceeded.

Lastly, for an optimal choice of alternative heating solution in a neighbourhood, research should be done to compare the cost of upgrading the grid to make it suitable for air-source heat pumps, or subsidising the drilling of private wells, or ensuring that a source network (bronnet/ZLT-net) is built in the neighbourhood for the use of ground-source heat pumps.

### **8.3. Recommendations for distribution system operators and government**

As mentioned in the previous section, for a complete analysis of a neighbourhood's heating alternative, an economic analysis should be carried out to weigh the costs of grid upgrades for air-source heat pumps against the construction of private wells or a source network to enable ground-source heat pumps.

Besides the reduced peak power that ground-source heat pumps provide, their total energy consumption is also lower, reducing the amount of renewable energy needed for heating. In addition, ground source heat pumps have the ability to cool homes with a much lower power demand than air source heat pumps, ensuring that electricity demand in summer will be significantly lower than with their air source counterparts. Cooling with a ground source heat pump also stores heat in the well or source network for use in winter, increasing the efficiency of the heat pump during the winter season. Finally, source networks can also be used to provide a low-temperature heat sink for year-round cooling of, for example, supermarkets in the neighbourhood. In summer, they do not have to dissipate their excess heat into the warm air, but can use a relatively cold water temperature below 20°C from the source network, making their cooling more efficient.

Looking at resistive electric backup heating, this should be strongly discouraged. The extra electrical element is added to provide extra power on the coldest days, saving the need to use a heat pump with more capacity. However, these high-power elements will kick in and stay on at low temperatures when the heating demand is already high, creating an extra peak in an already heavily loaded network. Buying a heat pump with a slightly higher capacity will also provide this last bit of heating power, but with a higher COP, reducing electricity demand. Therefore, I encourage the Dutch government to consider measures to discourage these electric resistive elements, for example, by not subsidising heat pumps that use them for backup heating. Electric elements used to heat the domestic hot water tank for a short period to prevent Legionella growth will probably be much less of a problem as they are not used at the same time.

In addition, dynamic energy pricing can increase peak loads in low-voltage networks. While this is not a problem for the current adoption rates of heat pumps and home chargers for electric vehicles, dynamic energy contracts can cause significant additional overloading and voltage limitation problems as the adoption rates of heat pumps and home chargers increase. Therefore, the popularity of dynamic energy contracts should be carefully monitored to ensure that this type of contract does not become too popular.

Finally, DSOs should look at the possibility of raising the voltage during cold weather by, for example, changing the turning ratios of transformers, probably dynamically. In heat pump areas, increasing the overall voltage of the low-voltage network can reduce the number of grid code violations without causing overvoltage problems.

# Bibliography

- [1] Joel Alpízar-Castillo, Laura Ramírez-Elizondo, and Pavol Bauer. “The Effect of Non-Coordinated Heating Electrification Alternatives on a Low-Voltage Distribution Network with High PV Penetration”. In: *2023 IEEE 17th International Conference on Compatibility, Power Electronics and Power Engineering (CPE-POWERENG)*. 2023 IEEE 17th International Conference on Compatibility, Power Electronics and Power Engineering (CPE-POWERENG). Tallinn, Estonia: IEEE, June 14, 2023, pp. 1–6. ISBN: 9798350300048. DOI: [10.1109/CPE-POWERENG58103.2023.10227394](https://doi.org/10.1109/CPE-POWERENG58103.2023.10227394). URL: <https://ieeexplore.ieee.org/document/10227394/> (visited on 09/20/2024).
- [2] Joel Alpízar-Castillo, Laura M. Ramírez-Elizondo, and Pavol Bauer. “Modelling and evaluating different multi-carrier energy system configurations for a Dutch house”. In: *Applied Energy* 364 (June 2024), p. 123197. ISSN: 03062619. DOI: [10.1016/j.apenergy.2024.123197](https://doi.org/10.1016/j.apenergy.2024.123197). URL: <https://linkinghub.elsevier.com/retrieve/pii/S0306261924005804> (visited on 09/20/2024).
- [3] ANWB. *Tarieven Energiebelasting 2024 en 2025*. URL: <https://www.anwb.nl/energie/energiebelasting> (visited on 12/03/2024).
- [4] G. Bagarella, R. Lazzarin, and M. Noro. “Sizing strategy of on–off and modulating heat pump systems based on annual energy analysis”. In: *International Journal of Refrigeration* 65 (May 1, 2016), pp. 183–193. ISSN: 0140-7007. DOI: [10.1016/j.ijrefrig.2016.02.015](https://doi.org/10.1016/j.ijrefrig.2016.02.015). URL: <https://www.sciencedirect.com/science/article/pii/S0140700716000475> (visited on 04/01/2025).
- [5] Jeroen Bakker. *Actuele dynamische energie prijzen vandaag*. URL: <https://jeroen.nl/dynamische-energie/prijzen> (visited on 03/24/2025).
- [6] Jeroen Bakker. *Alles over dynamische energie contracten*. URL: <https://jeroen.nl/dynamische-energie> (visited on 01/16/2025).
- [7] Centraal Bureau voor de Statistiek. *Huishoudens; samenstelling, grootte, regio, 1 januari*. Centraal Bureau voor de Statistiek. Taken from the year 2023. June 14, 2024. URL: <https://www.cbs.nl/nl-nl/cijfers/detail/71486ned> (visited on 02/21/2025).
- [8] Centraal Bureau voor de Statistiek. *StatLine - Huishoudens; grootte, samenstelling, positie in het huishouden, 1 januari*. URL: <https://opendata.cbs.nl/statline/#/CBS/nl/dataset/82905ned/table?dl=AB545> (visited on 11/27/2024).
- [9] Centraal Bureau voor de Statistiek. *Warmtepompen; aantallen, thermisch vermogen en energiestromen*. Centraal Bureau voor de Statistiek. Last Modified: 2024-11-15T02:00:00+01:00. Nov. 15, 2024. URL: <https://www.cbs.nl/nl-nl/cijfers/detail/85523NED?q=warmtepomp> (visited on 01/08/2025).
- [10] Centraal Bureau voor de Statistiek. *Wie rijdt er elektrisch?* Centraal Bureau voor de Statistiek. Last Modified: 2023-11-24T00:00:00+01:00. Nov. 23, 2023. URL: <https://www.cbs.nl/nl-nl/longread/statistische-trends/2023/wie-rijdt-er-elektrisch-onepage=true> (visited on 02/10/2025).
- [11] Centraal Bureau voor de Statistiek. *Zonnestroom; vermogen zonnepanelen woningen, wijken en buurten, 2022*. Nov. 2024. URL: <https://opendata.cbs.nl/#/CBS/nl/dataset/86044NED/table?searchKeywords=zonnepanelen> (visited on 02/04/2025).
- [12] Ollie Creevy. *How much space is required for a ground source heat pump?* Heat Pumps UK. Jan. 27, 2022. URL: <https://heat-pumps.org.uk/how-much-space-is-required-for-a-ground-source-heat-pump/> (visited on 01/14/2025).

- [13] Nikolaos Damianakis et al. "Assessing the grid impact of Electric Vehicles, Heat Pumps & PV generation in Dutch LV distribution grids". In: *Applied Energy* 352 (Dec. 15, 2023), p. 121878. ISSN: 0306-2619. DOI: [10.1016/j.apenergy.2023.121878](https://doi.org/10.1016/j.apenergy.2023.121878). URL: <https://www.sciencedirect.com/science/article/pii/S0306261923012424> (visited on 09/20/2024).
- [14] Charlotte De Jonghe. *Effect of Dynamic Pricing on the Low-voltage Grid*. Apr. 9, 2024. URL: <https://resolver.tudelft.nl/uuid:bb5c444e-c499-4059-83e1-7b8452fbf42a> (visited on 09/30/2024).
- [15] DlgSILENT. *PowerFactory*. URL: <https://www.digsilent.de/en/powerfactory.html> (visited on 02/18/2025).
- [16] Eigen Huis. *Terugleverkosten zonnepanelen*. URL: <https://www.eigenhuis.nl/verduurzamen/energierekening/terugleverkosten-zonnepanelen> (visited on 03/24/2025).
- [17] ElaadNL. *Low-Voltage Profiles Generator*. URL: <https://platform.elaad.io/analyse/low-voltage-charging-profiles/> (visited on 03/25/2025).
- [18] ElaadNL. *Outlook dashboard*. URL: <https://platform.elaad.io/interactieve-outlook/> (visited on 03/26/2025).
- [19] Eneco. *Eneco Dynamisch: Beweeg mee met de prijzen op de energiemarkt*. URL: <https://www.eneco.nl/duurzame-energie/dynamisch-energiecontract/> (visited on 12/04/2024).
- [20] Gebouwde Omgeving Elektrificatie. *GO-e – Projectsite*. URL: <https://www.projectgo-e.nl/> (visited on 02/20/2025).
- [21] Gebouwde Omgeving Elektrificatie. *Rekenen aan flexibiliteit in distributienetten*. Apr. 17, 2023. URL: <https://www.projectgo-e.nl/rekenen-aan-flexibiliteit-in-distributienetten/> (visited on 02/14/2025).
- [22] Itho Daalderop. *Warmtepomp Voorraadvat 270L 3G*. URL: <https://www.ithodaalderop.nl/nl-NL/consument/product/03-00670> (visited on 11/28/2024).
- [23] B.M. (Bart) Kaas and S Causevic. "Definition of archetypical neighborhoods for residential flexibility analyses". In: (Feb. 8, 2024).
- [24] Kennedy, Heather E and Owen, Mark S. *ASHRAE handbook: Fundamentals*. American Society of Heating, Refrigeration, and Air-Conditioning Engineers, 2009.
- [25] Ministerie van Economische Zaken en Klimaat. *Het Akkoord - Klimaatakkoord*. Last Modified: 2021-03-18T17:26 Publisher: Ministerie van Economische Zaken en Klimaat. Aug. 6, 2019. URL: <https://www.klimaatakkoord.nl/klimaatakkoord> (visited on 02/19/2025).
- [26] Milieu Centraal. *Besparen op gas: check de tips*. URL: <https://www.milieucentraal.nl/energie-besparen/duurzaam-verwarmen-en-koelen/besparen-op-gas/> (visited on 12/10/2024).
- [27] Milieu Centraal. *Spouwmuurisolatie: dit is hoe het werkt*. URL: <https://www.milieucentraal.nl/energie-besparen/isoleren-en-besparen/spouwmuurisolatie/> (visited on 02/04/2025).
- [28] Ministerie van Algemene Zaken. *Salderingsregeling stopt in 2027 - Energie thuis - Rijksoverheid.nl*. Last Modified: 2025-02-17T10:24 Publisher: Ministerie van Algemene Zaken. Feb. 17, 2025. URL: <https://www.rijksoverheid.nl/onderwerpen/energie-thuis/salderingsregeling> (visited on 03/24/2025).
- [29] Ministerie van Algemene zaken. *Energielabel woning - Energielabel woningen en gebouwen - Rijksoverheid.nl*. Last Modified: 2024-04-23T15:16 Publisher: Ministerie van Algemene Zaken. URL: <https://www.rijksoverheid.nl/onderwerpen/energielabel-woningen-en-gebouwen/energielabel-woning> (visited on 12/11/2024).
- [30] Ministerie van Binnenlandse Zaken en Koninkrijksrelaties. *Netcode elektriciteit*. Last Modified: 2024-12-03. URL: <https://wetten.overheid.nl/BWBR0037940/2025-02-01#Hoofdstuk8> (visited on 02/18/2025).

- [31] Ministerie van Economische Zaken en Klimaat. *Klimaatakkoord - Publicatie - Klimaatakkoord*. Last Modified: 2019-08-21T09:13 Publisher: Ministerie van Economische Zaken en Klimaat. June 28, 2019. URL: <https://www.klimaatakkoord.nl/documenten/publicaties/2019/06/28/klimaatakkoord> (visited on 02/19/2025).
- [32] Nationaal Programma Lokale Warmtetransitie. “Lokale Warmtetransitie in Beeld 2024”. In: (2024).
- [33] Alejandro Navarro-Espinosa and Pierluigi Mancarella. “Probabilistic modeling and assessment of the impact of electric heat pumps on low voltage distribution networks”. In: *Applied Energy* 127 (Aug. 15, 2014), pp. 249–266. ISSN: 0306-2619. DOI: 10.1016/j.apenergy.2014.04.026. URL: <https://www.sciencedirect.com/science/article/pii/S030626191400378X> (visited on 09/20/2024).
- [34] Netbeheer Nederland. *Feiten en cijfers*. URL: <https://www.netbeheernederland.nl/feiten-en-cijfers> (visited on 02/14/2025).
- [35] Netbeheer Nederland. *Netbeheerders zien aantal huishoudens met zonnepanelen verder groeien in 2023*. Jan. 25, 2024. URL: <https://www.netbeheernederland.nl/artikelen/nieuws/netbeheerders-zien-aantal-huishoudens-met-zonnepanelen-verder-groeien-2023> (visited on 02/21/2025).
- [36] NPro. *Types of cooling and heating networks (classification)*. URL: <https://www.npro.energy/main/en/district-heating-cooling/network-types> (visited on 01/14/2025).
- [37] Rilwan O. Oliyide and Liana M. Cipcigan. “The impacts of electric vehicles and heat pumps load profiles on low voltage distribution networks in Great Britain by 2050”. In: *International Multidisciplinary Research Journal* 11 (Jan. 14, 2021), pp. 30–45. ISSN: 2231-6302. DOI: 10.25081/imrj.2021.v11.7308. URL: <http://dx.doi.org/10.25081/imrj.2021.v11.7308> (visited on 09/20/2024).
- [38] Nanda Kishor Panda, Na Li, and Simon H. Tindemans. *Aggregate Peak EV Charging Demand: The Impact of Segmented Network Tariffs*. version: 2. Apr. 2, 2024. DOI: 10.48550/arXiv.2403.12215. arXiv: 2403.12215[eess]. URL: <http://arxiv.org/abs/2403.12215> (visited on 02/20/2025).
- [39] Phase to Phase. *Gaia LV Network Design*. URL: <https://www.phasetophase.nl/producten-diensten/producten/gaia-lv-network-design/> (visited on 02/18/2025).
- [40] Planbureau Voor De Leefomgeving. *Monitor RES: snelle groei zon en wind op land, maar ‘pijplijn’ met nieuwe plannen droogt op*. Dec. 12, 2024. URL: <https://www.pbl.nl/actueel/nieuws/monitor-res-snelle-groei-zon-en-wind-op-land-maar-pijplijn-met-nieuwe-plannen-droogt-op> (visited on 03/21/2025).
- [41] Pure Energie. *De calorische waarde van gas berekenen op je jaarafrekening*. Pure Energie. URL: <https://pure-energie.nl/kennisbank/calorische-waarde-van-gas/> (visited on 03/24/2025).
- [42] Rijksdienst voor Ondernemend Nederland. “Samenvatting Nationaal Laadonderzoek 2023 - Laden van elektrische auto’s in Nederland”. In: (July 11, 2023).
- [43] Oliver Ruhnau, Lion Hirth, and Aaron Praktiknjo. “Time series of heat demand and heat pump efficiency for energy system modeling”. In: *Scientific Data* 6.1 (Oct. 1, 2019). Publisher: Nature Publishing Group, p. 189. ISSN: 2052-4463. DOI: 10.1038/s41597-019-0199-y. URL: <https://www.nature.com/articles/s41597-019-0199-y> (visited on 10/25/2024).
- [44] Shenling. *A Simple Diagram and Operation Guide of Heat Pump*. July 10, 2023. URL: <https://www.shenlingglobal.com/blog/a-simple-diagram-and-operation-guide-of-heat-pump/> (visited on 01/08/2025).
- [45] D.B. Steffelbauer, B. Hillebrand, and E.J.M. Blokker. “pySIMDEUM: An open-source stochastic water demand end-use model in Python.” In: 2nd joint Water Distribution System Analysis and Computing and Control in the Water Industry (WDSA/CCWI2022) conference. Valencia (Spain), July 18, 2022.

- [46] Judith Stute and Matthias Kühnbach. “Dynamic pricing and the flexible consumer – Investigating grid and financial implications: A case study for Germany”. In: *Energy Strategy Reviews* 45 (Jan. 1, 2023), p. 100987. ISSN: 2211-467X. DOI: [10.1016/j.esr.2022.100987](https://doi.org/10.1016/j.esr.2022.100987). URL: <https://www.sciencedirect.com/science/article/pii/S2211467X2200181X> (visited on 09/20/2024).
- [47] D. Susa and H. Nordman. “IEC 60076–7 loading guide thermal model constants estimation”. In: *International Transactions on Electrical Energy Systems* 23.7 (2013). \_eprint: <https://onlinelibrary.wiley.com/doi/pdf/10.1002/etep.1631>. pp. 946–960. ISSN: 2050-7038. DOI: [10.1002/etep.1631](https://doi.org/10.1002/etep.1631). URL: <https://onlinelibrary.wiley.com/doi/abs/10.1002/etep.1631> (visited on 04/03/2025).
- [48] Rokas Valancius et al. “A Review of Heat Pump Systems and Applications in Cold Climates: Evidence from Lithuania”. In: *Energies* 12.22 (Jan. 2019). Number: 22 Publisher: Multidisciplinary Digital Publishing Institute, p. 4331. ISSN: 1996-1073. DOI: [10.3390/en12224331](https://doi.org/10.3390/en12224331). URL: <https://www.mdpi.com/1996-1073/12/22/4331> (visited on 01/08/2025).
- [49] Celine Van der Veen. “Analysing Thermal Energy Storage in Residential Buildings: Towards Decarbonization of the Heating Sector”. In: (Oct. 2022).
- [50] Vattenfall. *Energie uit de bodem met de bodem-water warmtepomp*. URL: <https://www.vattenfall.nl/warmtepomp/bodemwarmtepomp/> (visited on 01/14/2025).
- [51] Gijs Verhoeven, Bart Van der Holst, and Sjoerd C. Doumen. “Modeling a Domestic All-Electric Air-Water Heat-Pump System for Discrete-Time Simulations”. In: *2022 57th International Universities Power Engineering Conference (UPEC)*. 2022 57th International Universities Power Engineering Conference (UPEC). Aug. 2022, pp. 1–6. DOI: [10.1109/UPEC55022.2022.9917983](https://doi.org/10.1109/UPEC55022.2022.9917983). URL: <https://ieeexplore.ieee.org/document/9917983> (visited on 02/20/2025).
- [52] Jan de Wit. *Nationaal Warmtepomp Trendrapport 24/25*. Dutch New Energy Research, Nov. 13, 2024. URL: <https://www.dutchnewenergy.nl/nationaal-warmtepomp-trendrapport/>.
- [53] C. B. J. Zevenbergen. “Development of a Universal Adaptive Voltage Control Policy for Power Distribution Networks”. In: (2024). URL: <https://repository.tudelft.nl/record/uuid:d53aaf91-0e06-44b1-89cf-a31cc4022936> (visited on 03/12/2025).
- [54] Zonneplan. *Soorten energiecontracten: vast, variabel of dynamisch contract?* Zonneplan. Oct. 24, 2024. URL: <https://www.zonneplan.nl/energie/soorten-energiecontracten> (visited on 12/05/2024).

# Appendix

## A.1 Thermal house model parameters

Here, the parameters used for the thermal house model are depicted as used in the model and taken from [49].

Table 1: House parameters considering the walls.

Variable	Value	Unit
House length	15	m
House width	8	m
House height	2.6	m
Thickness of wall	0.25	m
Density of concrete	2400	kg/m <sup>3</sup>
Specific heat of concrete	750	J/kgK
Thermal conductivity of concrete	0.14	W/mK
Convective heat transfer coefficient from indoor to wall	0.9 <sup>1</sup>	W/m <sup>2</sup> K
Convective heat transfer coefficient from wall to outdoor	0.9 <sup>1</sup>	W/m <sup>2</sup> K

<sup>1</sup> This value is not realistic, as it was scaled to reach an overall heat transfer coefficient of 2.14 m<sup>2</sup>K/W. This is an average value for a residential building with energy label C.

Table 2: House parameters considering the windows.

Variable	Value	Unit
Number of windows in room 1	3	-
Number of windows in room 2	2	-
Number of windows in room 3	2	-
Number of windows in room 4	1	-
Height of windows	1	m
Width of windows	1	m
Thickness of single window pane	0.004	m
Thickness of cavity between panes	0.014	m
Density of glass	2500	kg/m <sup>3</sup>
Specific heat of glass	840	J/kgK
Thermal conductivity of glass	0.8	W/mK
Convective heat transfer coefficient from indoor to glass	25	W/m <sup>2</sup> K
Convective heat transfer coefficient from glass to outdoor	32	W/m <sup>2</sup> K

Table 3: House parameters considering the roof.

Variable	Value	Unit
Pitch of roof	40	°
Thickness of roof	0.2	m
Density of glass wool	12 <sup>1</sup>	kg/m <sup>3</sup>
Specific heat of glass fiber	835	J/kgK
Thermal conductivity of glass fiber	0.04	W/mK
Convective heat transfer coefficient from indoor to roof	12	W/m <sup>2</sup> K
Convective heat transfer coefficient from roof to outdoor	38	W/m <sup>2</sup> K

<sup>1</sup> This value is changed from 2440kg/m<sup>3</sup> in [49], because the original value resembled the density of pure glass fibre, not that of glass wool.

### B.1 Power profiles

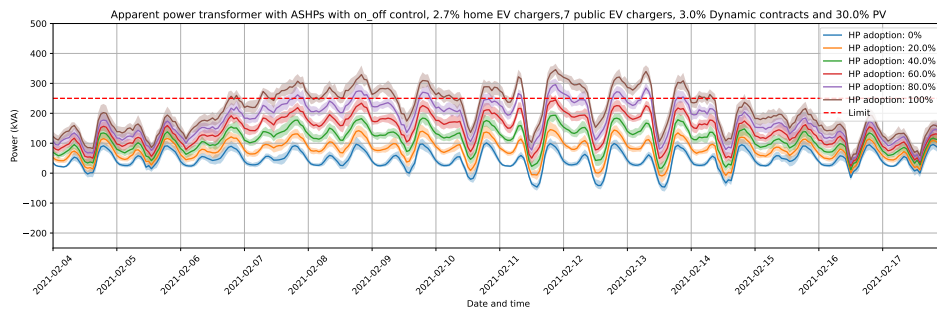


Figure 1: Apparent power through the transformer during the simulation period for **ASHPs with on-off control**

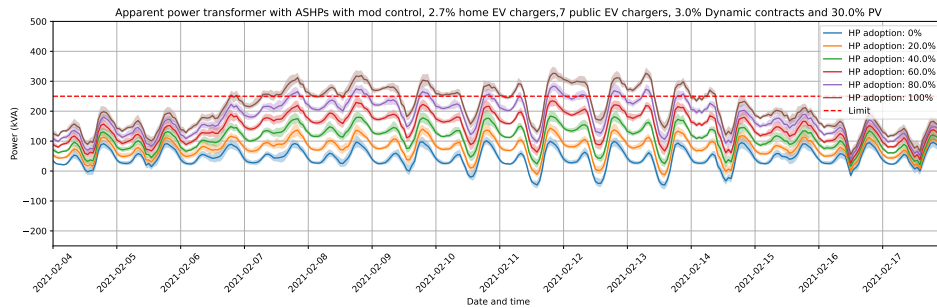


Figure 2: Apparent power through the transformer during the simulation period for **ASHPs with modulating control**

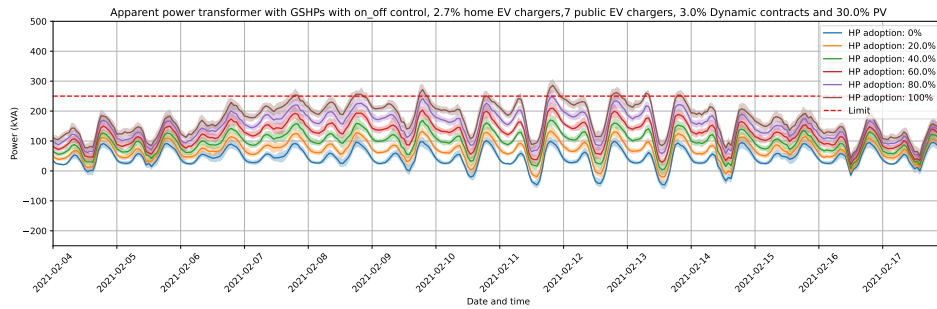


Figure 3: Apparent power through the transformer during the simulation period for **GSHPs with on-off control**

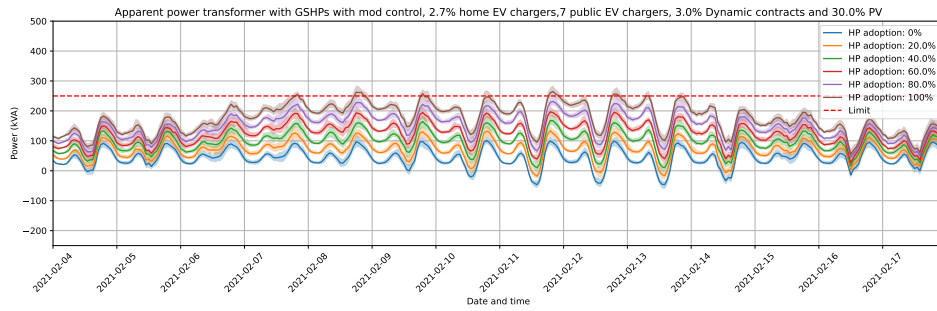


Figure 4: Apparent power through the transformer during the simulation period for **GSHPs with modulating control**

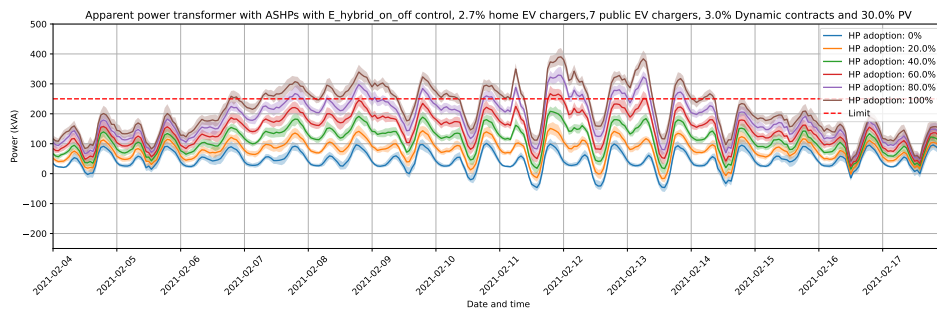


Figure 5: Apparent power through the transformer during the simulation period for **ASHPs with on-off control and resistive electric auxiliary heaters**.

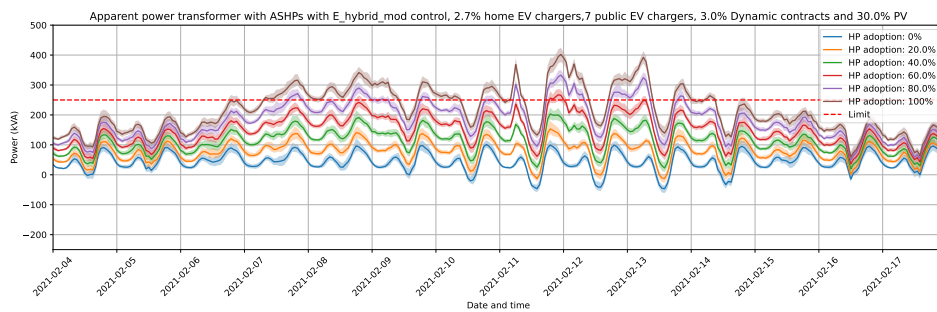


Figure 6: Apparent power through the transformer during the simulation period for **ASHPs with modulating control and resistive electric auxiliary heaters**.

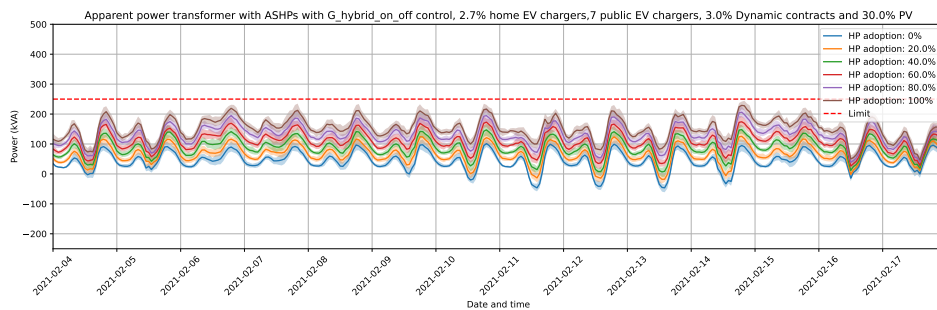


Figure 7: Apparent power through the transformer during the simulation period for **ASHPs with on-off control and a natural gas auxiliary heater**.

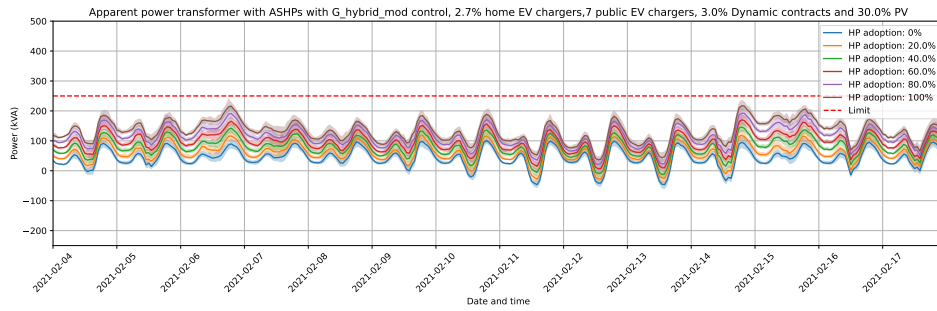


Figure 8: Apparent power through the transformer during the simulation period for **ASHPs with modulating control and a natural gas auxiliary heater.**

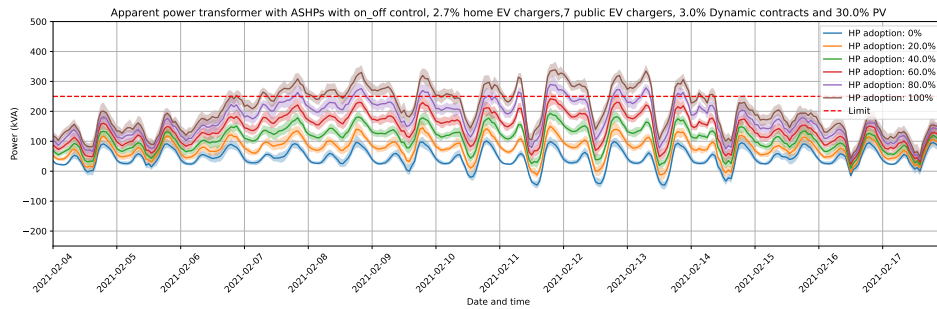


Figure 9: Apparent power through the transformer during the simulation period for **ASHPs with on-off control without DHW production**

## B.2 Voltage profiles

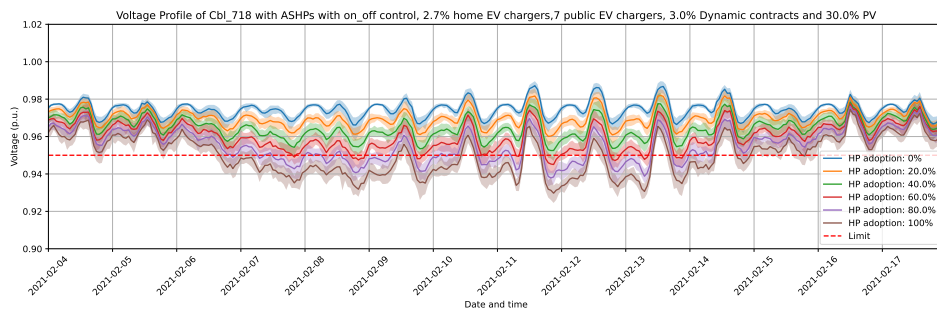


Figure 10: Voltage profile at CBL\_718 for **ASHPs with on-off control**

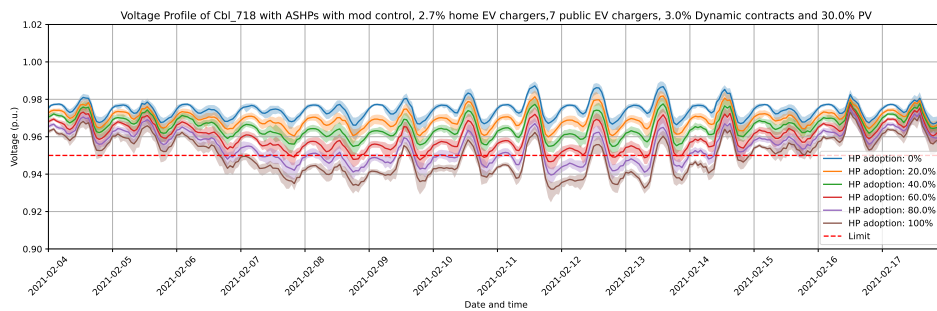


Figure 11: Voltage profile at CBL\_718 for **ASHPs with modulating control**

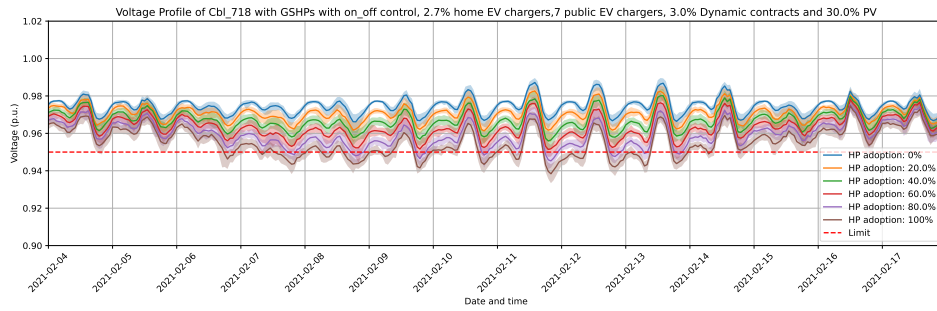


Figure 12: Voltage profile at CBL\_718 for GSHPs with on-off control

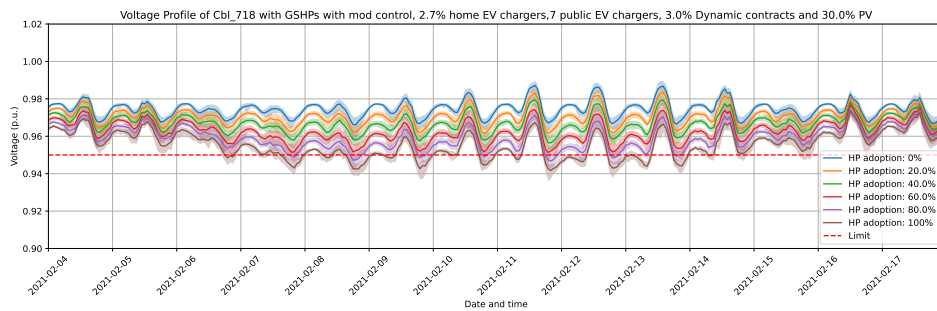


Figure 13: Voltage profile at CBL\_718 for GSHPs with modulating control

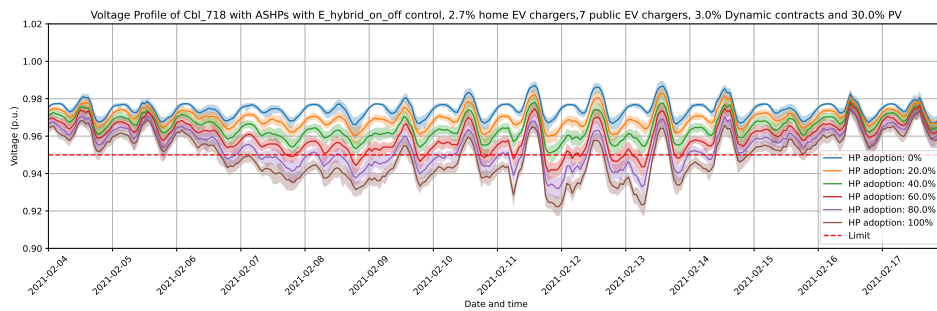


Figure 14: Voltage profile at CBL\_718 for ASHPs with on-off control and resistive electric auxiliary heaters

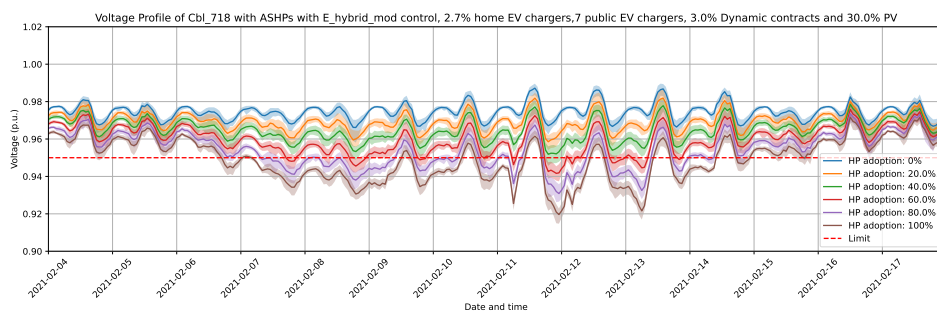


Figure 15: Voltage profile at CBL\_718 for ASHPs with modulating control and resistive electric auxiliary heaters

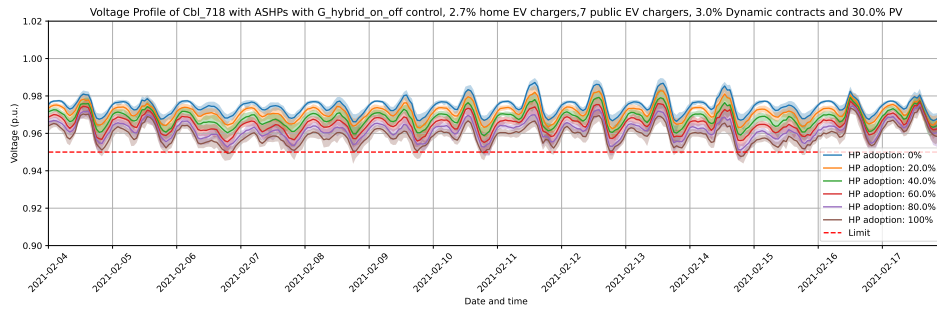


Figure 16: Voltage profile at CBL\_718 for ASHPs with on-off control and natural gas auxiliary heaters

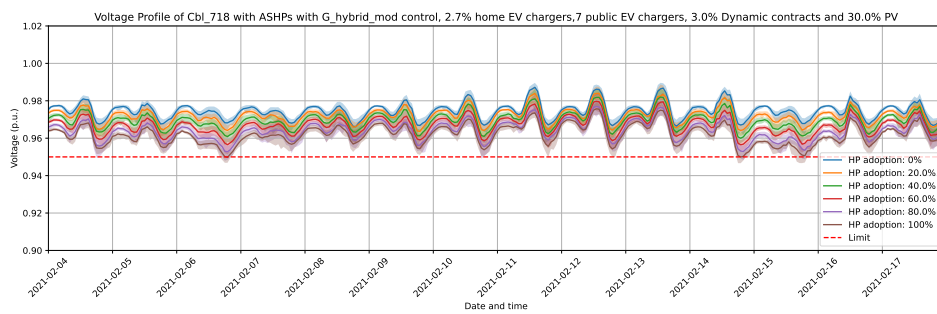


Figure 17: Voltage profile at CBL\_718 for ASHPs with modulating control and natural gas auxiliary heaters

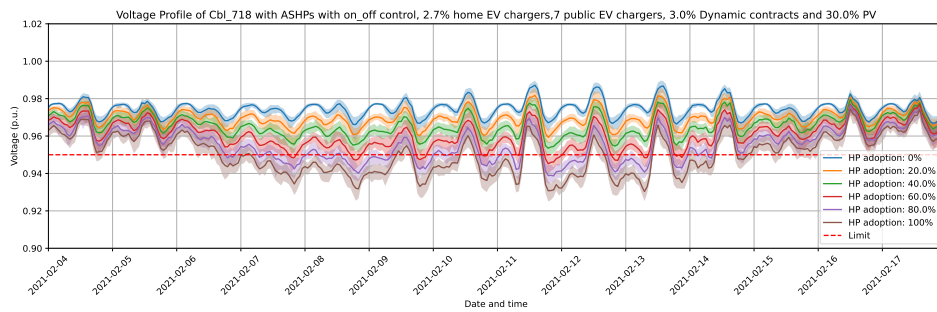


Figure 18: Voltage profile at CBL\_718 for ASHPs with on-off control without DHW

### B.3 Overload energy plots

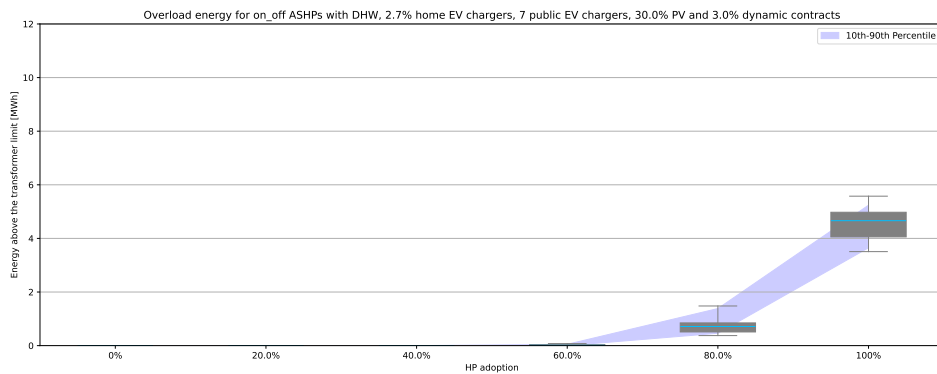


Figure 19: Energy above transformer limit for ASHPs with on-off control

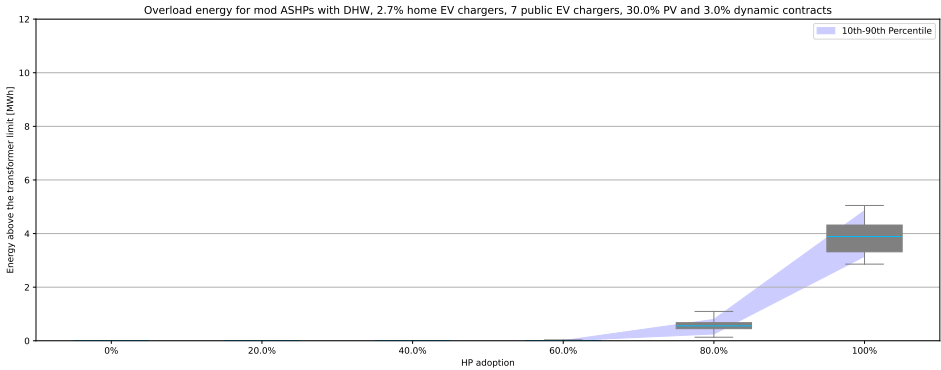


Figure 20: Energy above transformer limit for ASHPs with modulating control

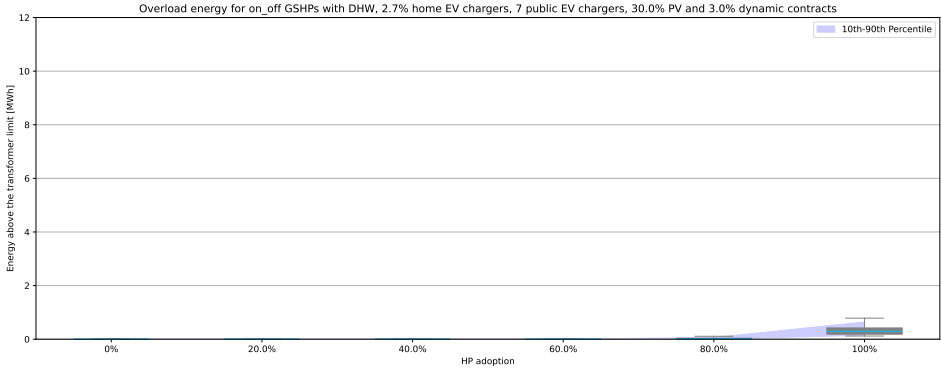


Figure 21: Energy above transformer limit for GSHPs with on-off control

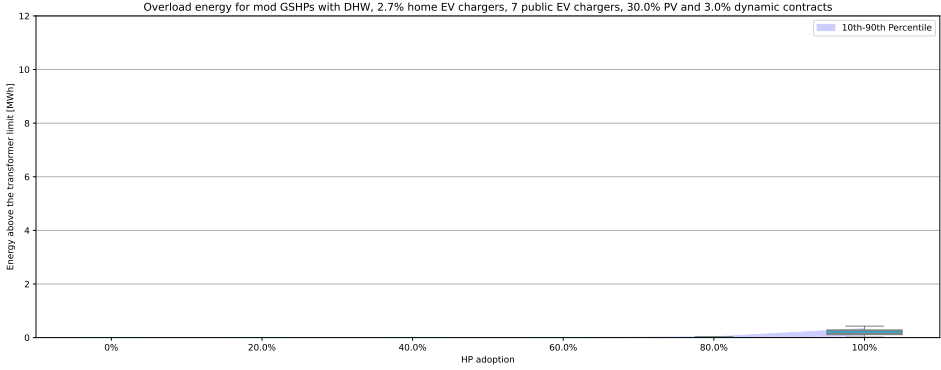


Figure 22: Energy above transformer limit for GSHPs with modulating control

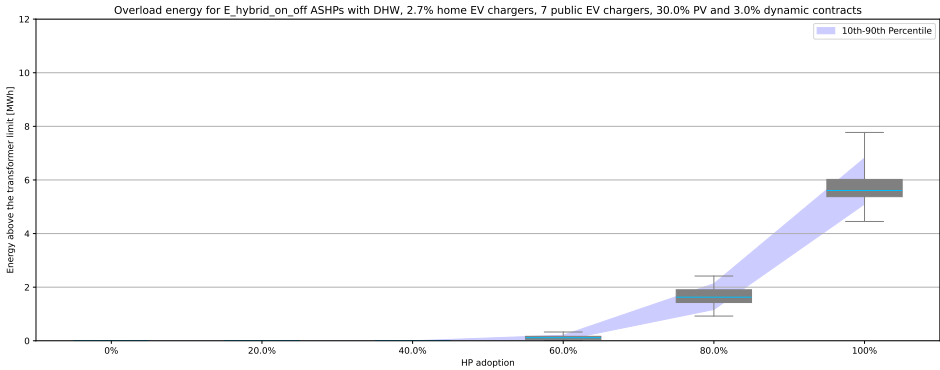


Figure 23: Energy above transformer limit for ASHPs with on-off control and resistive electric auxiliary heaters

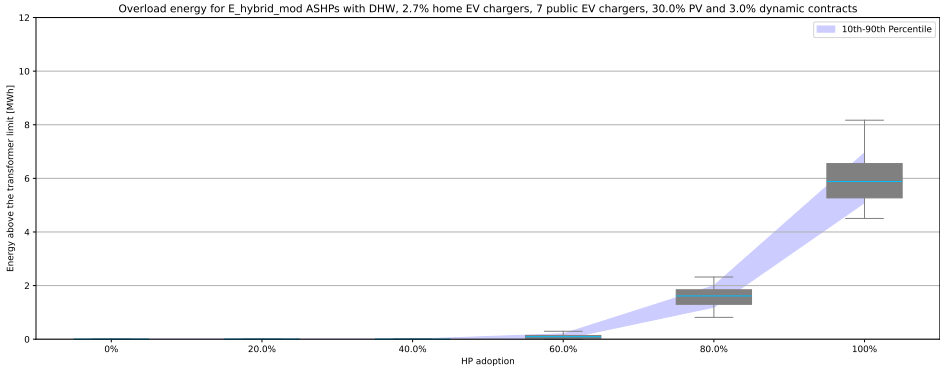


Figure 24: Energy above transformer limit for ASHPs with modulating control and resistive electric auxiliary heaters

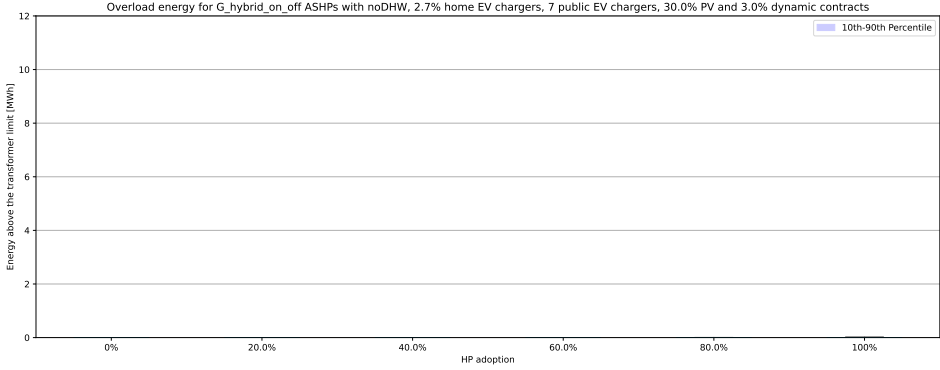


Figure 25: Energy above transformer limit for ASHPs with on-off control and natural gas auxiliary heaters, no overload took place

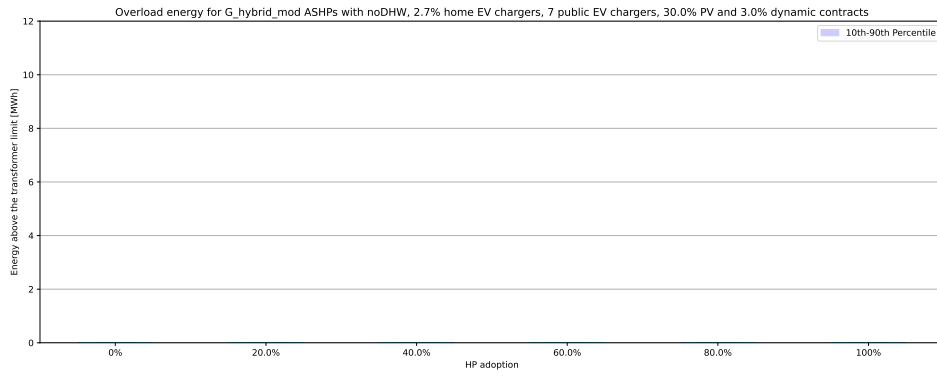


Figure 26: Energy above transformer limit for **ASHPs with modulating control and natural gas auxiliary heaters**, no overload took place

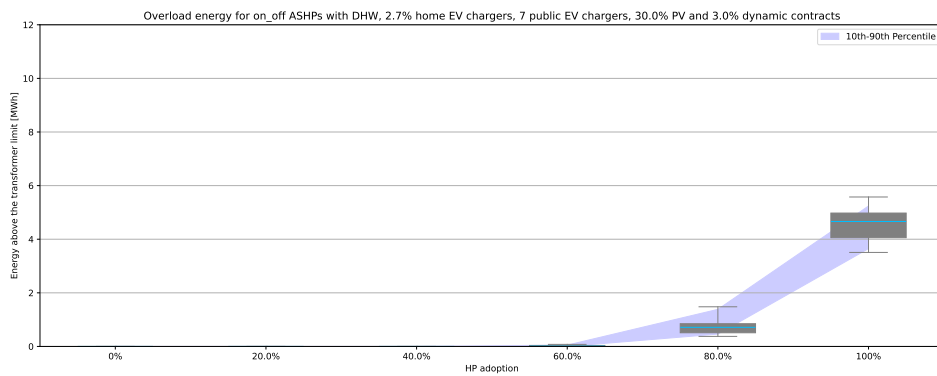


Figure 27: Energy above transformer limit for **ASHPs with on-off control** without DHW

## B.4 Overload duration plots

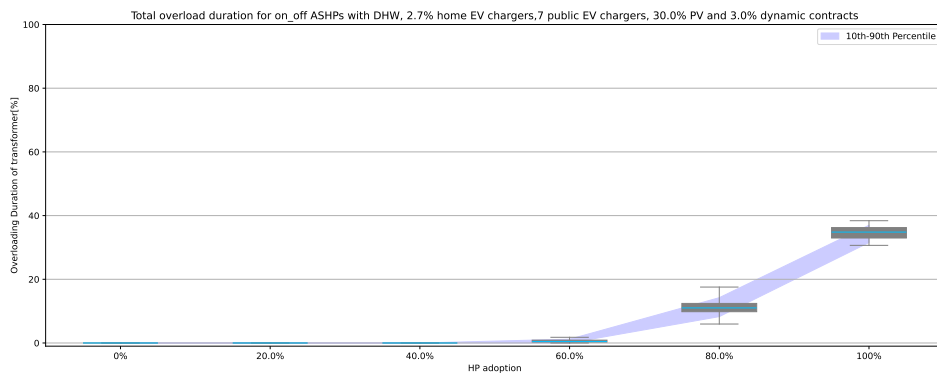


Figure 28: Energy above transformer limit for **ASHPs with on-off control**

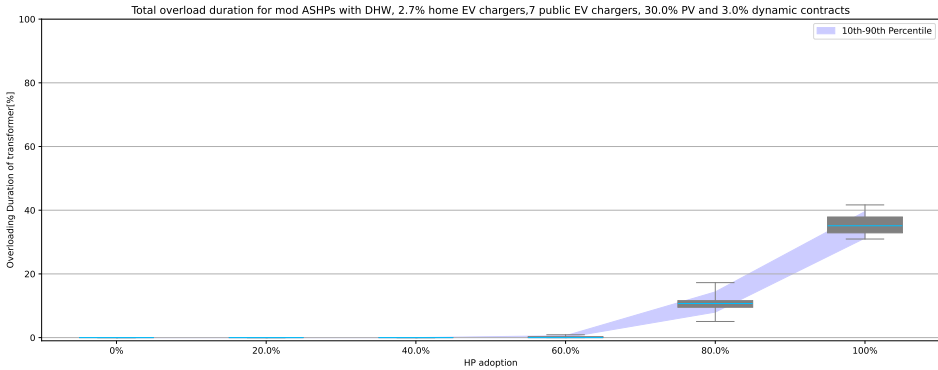


Figure 29: Energy above transformer limit for ASHPs with modulating control

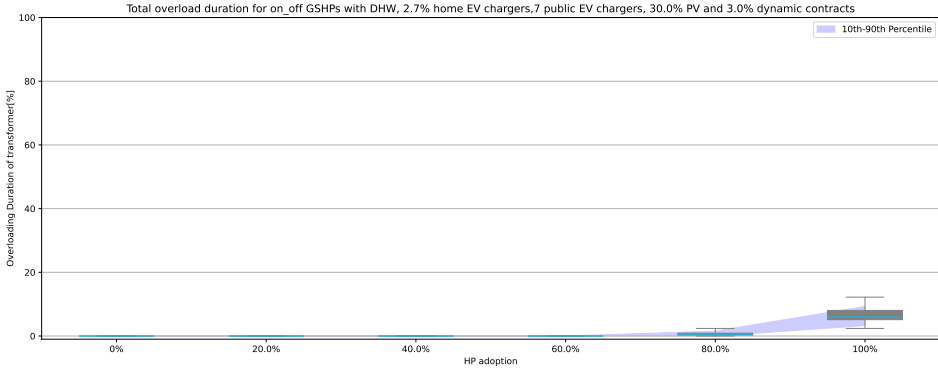


Figure 30: Energy above transformer limit for GSHPs with on-off control

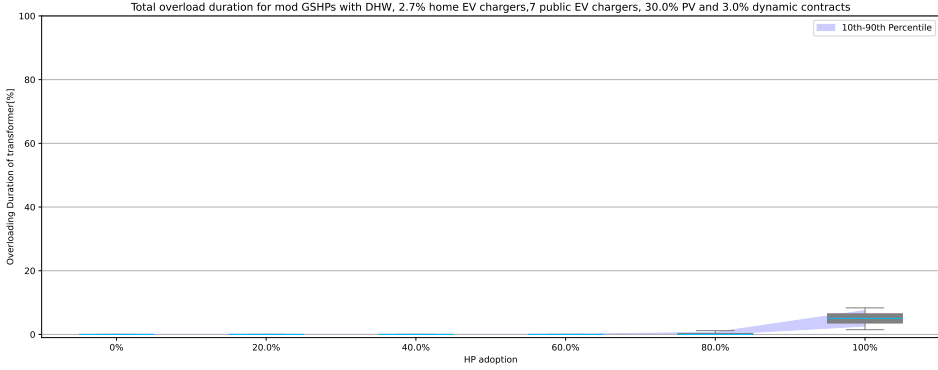


Figure 31: Energy above transformer limit for GSHPs with modulating control

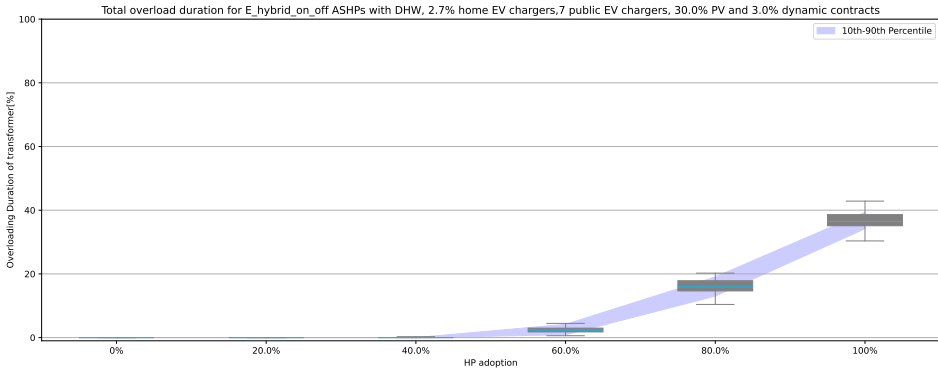


Figure 32: Energy above transformer limit for ASHPs with on-off control and resistive electric auxiliary heaters

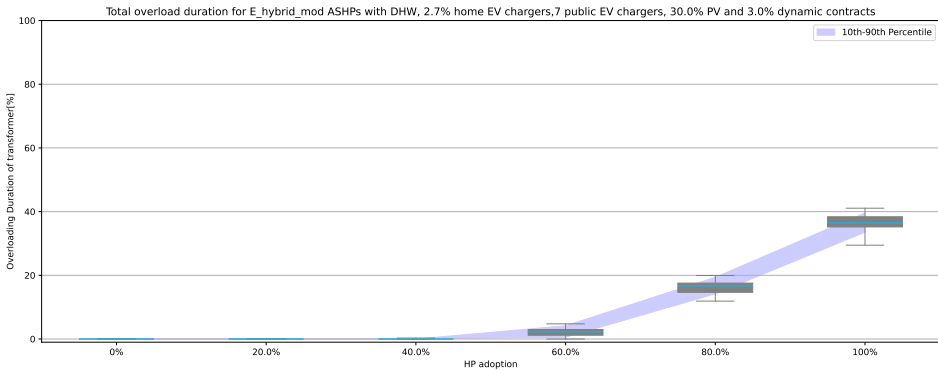


Figure 33: Energy above transformer limit for ASHPs with modulating control and resistive electric auxiliary heaters

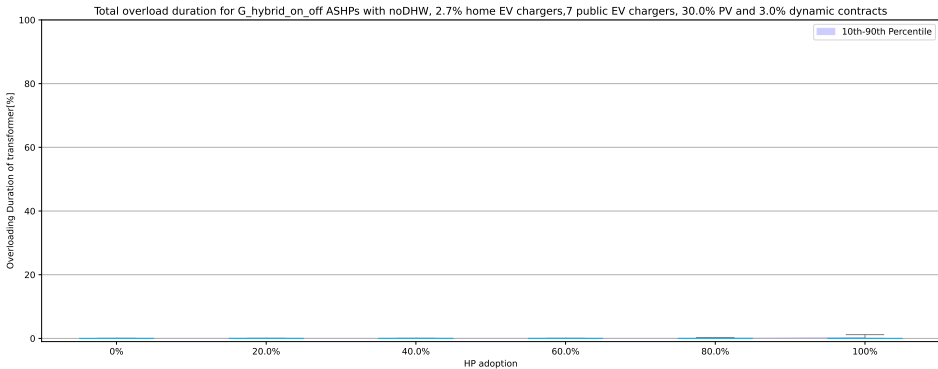


Figure 34: Energy above transformer limit for ASHPs with on-off control and natural gas auxiliary heaters, no overload took place

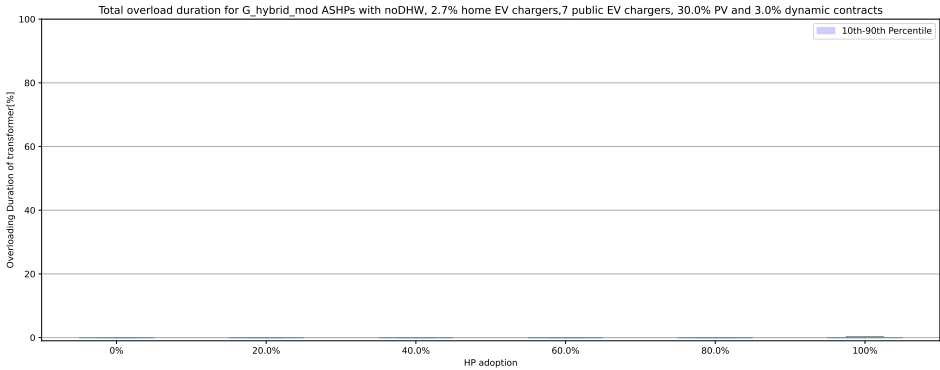


Figure 35: Energy above transformer limit for **ASHPs with modulating control and natural gas auxiliary heaters**, no overload took place

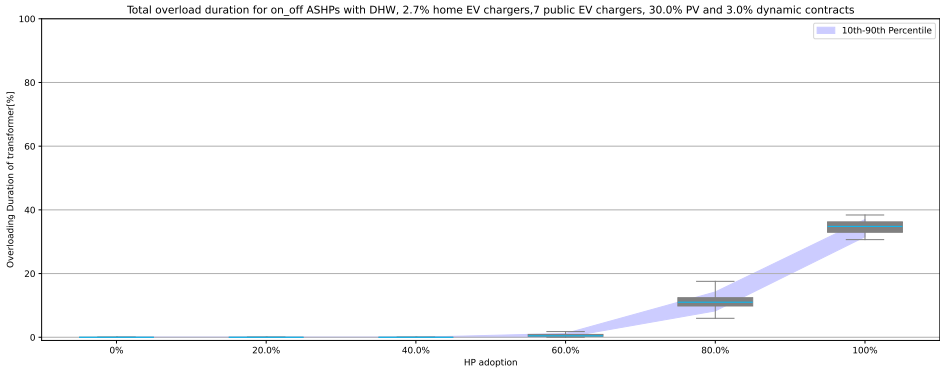


Figure 36: Energy above transformer limit for **ASHPs with on-off control** without DHW